ASSESSING THE IMPACT OF LAND USE ON WATER AND NUTRIENT FLUXES IN THE SOUTH-WEST MAU, KENYA

SUZANNE ROBIN JACOBS

A dissertation submitted by M.Sc. Suzanne Robin Jacobs to the Institute of Natural Sciences at the Department of Landscape, Water and Biogeochemical Cycles of the Justus Liebig University Giessen for the degree of
Doctor of Natural Sciences (Dr. rer. nat.)

Referees:

Prof. Dr. Lutz Breuer	Justus Liebig University Giessen
Prof. Dr. Jan Siemens	Justus Liebig University Giessen
Prof. Dr. Andreas Gattinger	Justus Liebig University Giessen
Prof. Dr. Christoph Müller	Justus Liebig University Giessen

Submitted: 28 February 2018

Abstract

Although tropical montane forests are considered to provide important water-related ecosystem services, such as the supply of clean fresh water, these forests are under significant threat of conversion to agriculture, because of their suitable climate and fertile soils. However, there is little scientific evidence on how land use change affects water and nutrient fluxes in this important ecosystem, especially in Africa. To assess the effect of land use on water provenance, flow paths and nutrient dynamics in the Mau Forest Complex, Kenya, three sub-catchments (27–36 km²) with different land use (i.e. natural forest, smallholder agriculture and commercial tea plantations) were selected within a 1,021 km² catchment. Spatial sampling campaigns showed that land use had a significant effect on nitrate and total dissolved nitrogen concentrations during baseflow, while dissolved organic carbon and nitrogen were more influenced by the hydrological regime and catchment characteristics, such as catchment area. A 2-year high-resolution (10-minute interval) dataset recorded by automatic measurement stations located at the outlet of the sub-catchments showed highest nitrate concentrations in the tea plantation sub-catchment, followed by the smallholder agriculture sub-catchment, caused by leaching of fertilizer to the groundwater. In the natural forest, nitrate entered the stream through shallow sub-surface flow during rainfall events, while surface runoff resulted in dilution of nitrate concentrations in the agricultural sub-catchments. A tracer-based study estimated a mean transit time of ~4 years and showed an increased contribution of groundwater sources to streamflow during high flow in all sub-catchments, emphasising the importance of groundwater in this area. The majority of stream water in the tea plantation sub-catchment originated from springs, while precipitation dominated in the forest and smallholder agriculture sub-catchments. The results clearly show that land use influences water and nutrient dynamics, which could have a detrimental effect on water supply and quality in tropical montane areas and downstream regions.

Table of content

List of tables

List of figures

1 Extended summary

1.1 Introduction

The perceived role of forests as a source of clean water has put this ecosystem high on the international research agenda. Although forest hydrology has been studied for more than a century, the relationship between forests and water first received global attention after the International Expert Meeting on Forests and Water in Shiga, Japan and the subsequent Shiga Declaration on Forest and Water in 2002. One of the key issues identified during this meeting was the need to improve "our understanding of the bio-physical interactions between forests and water" (FAO, 2013), especially in the form of long-term ecohydrological monitoring. The need for further research is highlighted by the debate on whether forests indeed provide the water-related ecosystem services they are associated with, such as flow regulation, flood reduction and maintaining water quality (Calder, 2002). This knowledge is important to be able to meet growing domestic, agricultural, industrial and ecological demands for clean fresh water. Forests are under significant pressure of agricultural expansion due to the world's increasing population and subsequent need for food production. Especially in the tropics, conversion of forest to large- and small-scale agricultural land and industry occurs at high rates (Malhi et al., 2014; Weng et al., 2013). As long as the consequences of land use change for water quality and quantity remain uncertain, planning and sustainable management of land use and water resources will be very challenging.

Tropical montane forests, one of the ecosystems under threat of conversion to agricultural land, have not received much attention in hydrological research so far. These forests occur in the high elevation tropics, where the average minimum temperature drops below 18°C (Bruijnzeel, 2005). They are characterised by smaller trees than in tropical lowland forest

and high abundance of epiphytes and mosses. Tropical montane forests are well-known for their rich biodiversity with a high degree of endemism (Burgess et al., 2007; Gradstein et al., 2008; Martínez et al., 2009), but are also recognised as an important carbon store (Spracklen and Righelato, 2014) and regulator of the regional and sub-continental hydrological cycle (Célleri and Feyen, 2009; Martínez et al., 2009). Yet, the hydrological functioning of tropical montane forests has only been studied in few areas, mainly in the Neotropics (e.g. Ataroff and Rada, 2000; Boy et al., 2008; Célleri and Feyen, 2009; Muñoz-Villers and McDonnell, 2012; Ponette-González et al., 2014; Windhorst et al., 2014), while African tropical montane forests have received much less attention (Bjørndalen, 1992; Munishi and Shear, 2005). Furthermore, little is known about the effect of land use change on this important ecosystem (Bruijnzeel, 2001).

Reviews of the numerous studies on the effect of deforestation on water yield (e.g. Bosch and Hewlett, 1982; Brown et al., 2005; Bruijnzeel, 2004, 1990; Sahin and Hall, 1996). show that, although there seems to be a general increase in annual water yield with decreasing forest cover, there is considerable variation in the response of catchments to deforestation due to differences in climate, hydrogeology, soil and topography. On regional and continental scale, forest cover is argued to increase precipitation through increased water recycling as consequence of the generally higher evapotranspiration rate of forests compared to other land use types (Ellison et al., 2012). Deforestation in the Amazon basin is, for example, likely to result in a significant decrease in precipitation in the region (Spracklen et al., 2012). However, the effect of deforestation on precipitation is variable and depends, amongst other factors, on deforestation extent and the characteristics of the replacing land cover (Lawrence and Vandecar, 2015; van der Ent et al., 2012). Furthermore, this is mainly relevant for regions that receive the majority of their precipitation from areas where recycling of rainfall is important.

Not only changes in vegetation cover, but also land use change can influence streamflow. Land use change often results in changes in soil hydraulic properties, which could lead to changes in hydrological flow paths, i.e. the pathway along which incoming precipitation eventually reaches the stream. In forested catchments, water is usually transported to the stream through sub-surface flow paths (Bonell, 1998; McGuire and McDonnell, 2006). Conversion of forest to pasture led to a 17-fold increase in stormflow volume, caused by soil compaction and decreased hydraulic conductivity in the south-western Amazon

(Germer et al., 2010). Lower infiltration rates in agricultural land use types than in forested land use types were observed in the Mau Forest Complex, Kenya (Owuor et al., 2018) and the Amazon (Zimmermann et al., 2006). Although the differences in soil hydraulic properties between land use types in both studies were not significant at greater depth (Owuor et al., 2018; Zimmermann et al., 2006), such changes can still affect runoff generation processes, resulting in increased occurrence of surface runoff (Chaves et al., 2008; Giertz et al., 2005; Neill et al., 2011). A shift of sub-surface flow to surface runoff could lead to faster transport of water through the catchment and thus shorter transit times (Chaves et al., 2008). Flow paths and transit times do not only influence streamflow response to rainfall (Rodgers et al., 2005a), but also water quality, because solutes undergo biogeochemical processes along these flow paths, such as adsorption, decomposition or uptake by micro-organisms. The contact time of incoming precipitation, soil water and groundwater with soils and bedrock will therefore affect the chemical composition of water entering the stream (McGuire and McDonnell, 2006).

Water quality changes are often observed after conversion of forest to other land use types: deforested catchments are often associated with increased nitrate loss (Williams et al., 1997), turbidity and nutrient loads (Figueiredo et al., 2010; Gücker et al., 2016) or suspended sediment and total nitrogen loads (Hunter and Walton, 2008). High turbidity and sediment loads are a consequence of increased erosion caused by surface runoff (Glendell and Brazier, 2014) or bank erosion, while increased nutrient concentrations and loads, particularly of nitrate and total dissolved nitrogen, are often related to fertilizer inputs (Mitchell et al., 2009) or wetlands, due to their high biogeochemical activity. Furthermore, changes in soil moisture, temperature, pH, organic matter content, and carbon and nitrogen stocks through soil and land management practices can also affect biogeochemical processes in the soil and thus mobility and availability of nutrients for export (Zhang et al., 2016).

Despite the availability of evidence supporting the presumed water-related ecosystem services provided by forests, the observed effects of land use change on streamflow and water quality remain variable and site-specific. This emphasises the need for local or regional studies on hydrological processes and how they are affected by land use. The highlands of Kenya are home to five tropical montane forests, of which the Mau Forest Complex is the largest with a surface area of over 400,000 ha. The Mau Forest Complex

is considered an important 'water tower', providing approximately 5 million people with fresh water from rivers originating in the forest (Kenya Water Towers Agency, 2015). Despite its widely recognised significance as water source, the Mau Forest Complex is under risk of conversion to agriculture due to its fertile soils and suitable climate: more than 25% of the forest was lost to agriculture and settlements over the past decades (Government of Kenya, 2009). Several modelling studies conducted in the Mau Forest Complex concluded that these changes resulted in higher surface runoff and a decrease in groundwater recharge (Baker and Miller, 2013), reduced dry season flow and increased stormflow (Mango et al., 2011), increased erosion (Defersha and Melesse, 2012) and increased annual runoff (Baldyga et al., 2004; Mwangi et al., 2016). Furthermore, differences in water quality and macro-invertebrate assemblages in parts of the Mau Forest Complex have been attributed to land use (Kilonzo et al., 2014; Masese et al., 2017). However, most of these studies are based on limited field data, while solid evidence from long-term field observations and thorough understanding of the driving processes behind flow regimes, i.e. rainfall-runoff processes and water storage, are missing. Yet, these data and knowledge are essential to assess the effect of land use change on tropical montane forests and the ecosystem services they provide.

This dissertation aims to reduce this knowledge gap using a combination of spatial sampling campaigns, high-resolution field measurements and stable water isotopes (δ^2H and δ^{18}O) studies in catchments with contrasting land use in the Mau Forest Complex. The insights obtained from this dissertation will increase our understanding of hydro-geochemical processes and their relationship to land use in an African montane region. Together with the results from other studies on drivers of deforestation (Bewernick, 2016), land use change (Swart, 2016), greenhouse gas fluxes (Arias-Navarro et al., 2017b, 2017a; Wanyama et al., 2018) and soil hydraulic properties (Owuor et al., 2018), this dissertation will contribute to building a more complete picture of land use, water and nutrient dynamics in the Mau Forest Complex. Furthermore, the long-term dataset can be used as a basis for upscaling, modelling land use change scenarios and validation of low-costs, sustainable water quality and quantity monitoring methods to support and improve monitoring and management activities of the local water resources management authority (Weeser et al., in review).

1.2 Objectives

The main aim of this dissertation is:

> *To assess the effect of land use on water and nutrient fluxes in the South-West Mau, Kenya, based on long-term field measurements.*

This can be subdivided in three objectives, which will be addressed in separate chapters in this dissertation:

1. To estimate and explain the influence of land use and catchment characteristics, such as elevation, drainage density and catchment area, on spatial patterns in dissolved organic carbon and dissolved nitrogen concentrations (Chapter 2);
2. To identify and compare processes driving temporal discharge and nitrate concentration patterns in sub-catchments with contrasting land use, i.e. natural forest, smallholder agriculture and commercial tea and tree plantations, and assess how these patterns are reflected downstream (Chapter 3); and
3. To estimate the mean transit time of water and the relative contribution of different water sources to streamflow in the three sub-catchments as well as to assess the influence of land use on hydrological flow paths (Chapter 4).

In addition to addressing the scientific knowledge gap in hydrological processes and nutrient fluxes in this tropical montane ecosystem, the knowledge gained from this study can also contribute to sustainable water resources management and land use planning.

1.3 Study area

1.3.1 Land use

The study area is located in a headwater catchment of the Sondu basin in western Kenya (Figure 1.1). The Sondu River is one of the twelve major rivers originating in the Mau Forest Complex and its headwater area covers the majority of the South-West Mau block of the Mau Forest Complex. The area is characterised by three land use types: (a) indigenous Afromontane mixed forest (Kinyanjui, 2011), (b) smallholder agriculture with farms of less than 2 ha, and (c) commercial tea and tree plantations (Figure 1.2).

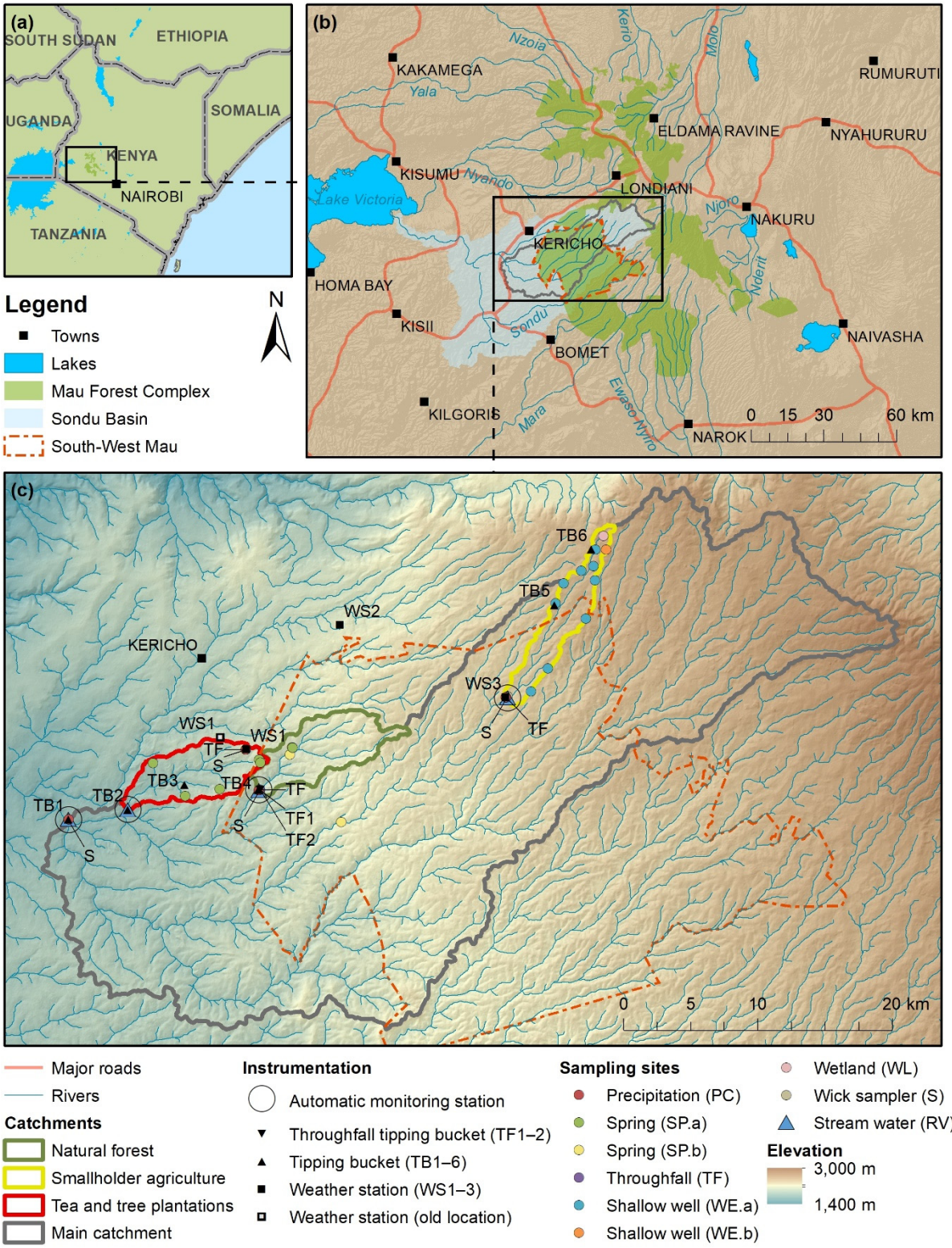

Figure 1.1 Maps of the study area: (a) location of the study area within Kenya, (b) major rivers originating in the Mau Forest Complex and location of the Sondu basin, and (c) selected study catchments, instrumentation, location of end member sampling sites and elevation (USGS, 2000) in the South-West Mau, Kenya.

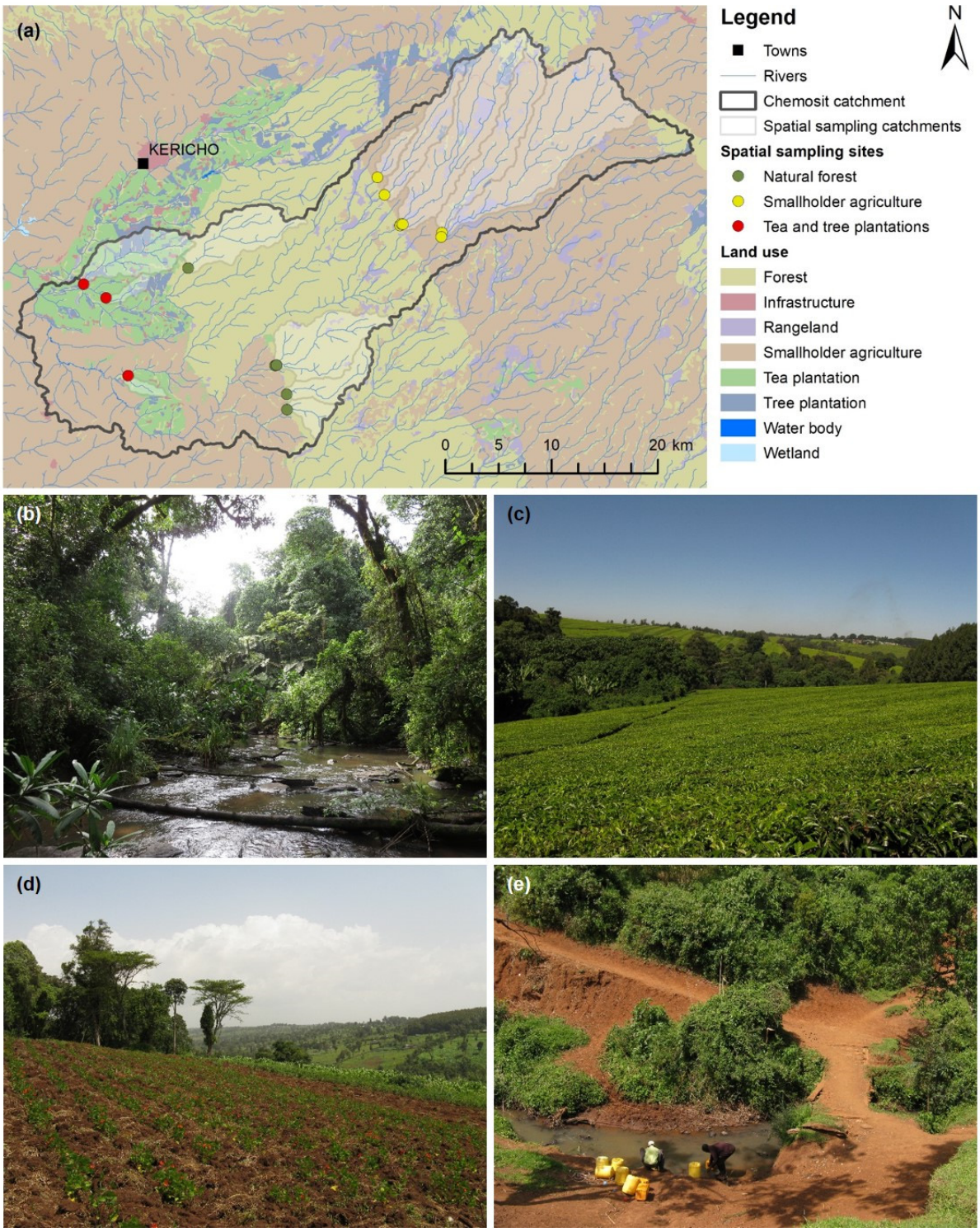

Figure 1.2 (a) Map of the study area showing the spatial sampling sites and land use (Swart, 2016), and characteristics of the dominant land use types in the South-West Mau: (b) indigenous Afromontane forest, (c) commercial tea plantations alternated with Eucalyptus plantations and native vegetation along the rivers, (d) smallholder agriculture with crop fields, grazing land and small woodlots, and (e) erosion along river banks in the smallholder agriculture area.

The natural forest vegetation in the South-West Mau extends from an elevation of 1,950 m a.s.l. upwards, transitioning from evergreen montane forest (Figure 1.2b) to bamboo forest at around 2,300 m a.s.l. (Blackie, 1972). In addition to its supposed role as water source, the South-West Mau, as well as other parts of the Mau Forest Complex, is rich in biodiversity and home to dwindling numbers of African elephants (*Loxodonta africana*) and the critically endangered Eastern or Mountain Bongo (*Tragelaphus eurycerus* ssp. *isaaci*). Little forest is left above 2,400 m a.s.l. due to deforestation. In total, 25% of the forest cover in the South-West Mau was lost between 1973 and 2013, mainly through conversion to smallholder agriculture (Swart, 2016). The forest adjacent to areas with smallholder farms is degraded through encroachment of farmland, grazing of sheep and cattle, charcoal burning, extraction of firewood and timber harvesting (Bewernick, 2016). Along the eastern and western forest boundary, a buffer zone of governmental tea plantations has been established to prevent encroachment and access to the forest by the local community (Nyayo Tea Zones Development Corporation, 2016). Other conservation and forest restoration measures, such as tree planting and fencing, are considered to further reduce the potential impact of human activities on the forest (Butynski and De Jong, 2016).

The commercial tea plantations are located on the western side of the forest close to the town of Kericho (0°22'08" S, 35°17'10" E) and cover an area of approximately 20,000 ha. The first tea plantations were established in 1912 and expanded until mid to late 1900s. The landscape consists of a patchwork of tea fields and Eucalyptus plantations (Figure 1.2c), with an average surface area ratio of 3:1 tea–Eucalyptus. Eucalyptus is mainly used as fuelwood for tea processing. Remnants of native vegetation, such as *Macaranga kilimandscharica*, *Polyscias kikuyuensis*, *Olea hochstetteri* and *Casearia battiscombei* are found along rivers and act as riparian buffer zones with a maximum width of 30 m (Ekirapa and Shitakha, 1996). Although the current extent of the commercial tea plantations is quite stable, land use change occurs within the tea estates when tea fields are converted to Eucalyptus plantations and vice versa.

The remaining part of the study area is dominated by smallholder agriculture (Figure 1.2d). At higher elevation, subsistence farmers mainly grow maize, beans, potatoes and cabbage, while tea is grown as an additional source of income at lower elevation. Crop fields are interspersed with grazing areas and small woodlots of Eucalyptus, Cypress and

Pine. Along large stretches of the rivers, native riparian vegetation is replaced by crops, grazing areas or small tree plantations, and severe bank erosion is visible in places that are frequently accessed by humans and livestock (Figure 1.2e). The majority of the population in this area depends on springs, streams and shallow wells for their domestic water use.

1.3.2 Climate

Precipitation in the study area is characterised by a bi-modal rainfall pattern, influenced by the shift of the intertropical convergence zone (ITCZ) from the southern to the northern hemisphere and back (Camberlin et al., 2009). Highest rainfall occurs in the months April and May and August and September during the 'long rains' and 'short rains', respectively (Figure 1.3). January and February are considered the dry season. Long-term (1905–2014) average annual precipitation recorded in a commercial tea estate at 2,100 m a.s.l. is 1,988±328 mm (Jacobs et al., 2017). Minimum daily temperatures vary little throughout the year, fluctuating around 11°C. There is more variation in the maximum daily temperature, with highest temperatures (> 25°C) observed during the dry season, especially in February. June and July are usually the coldest months with maxima around 22°C.

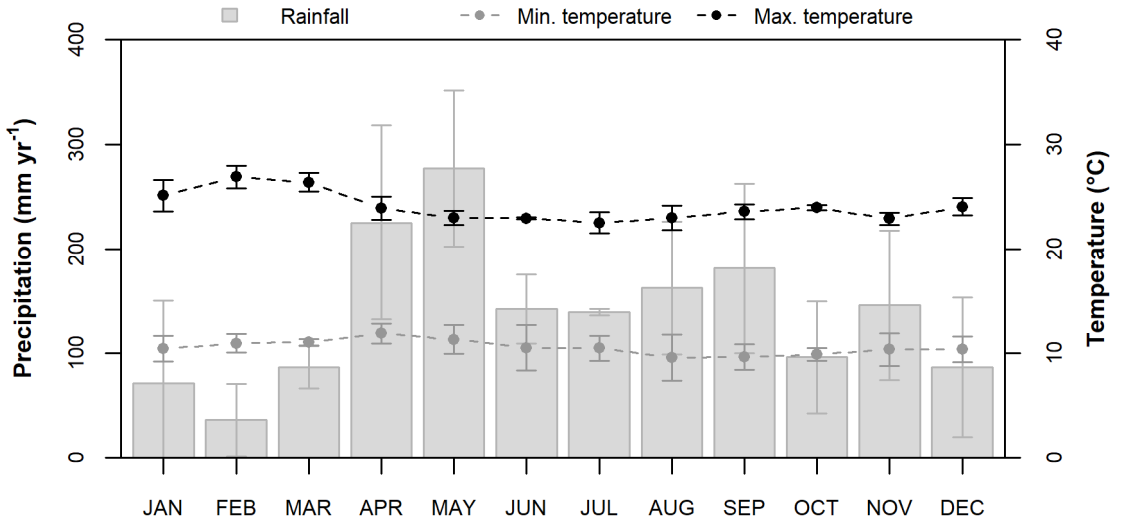

Figure 1.3 Mean±SD monthly rainfall in the Chemosit catchment (South-West Mau, Kenya) and daily minimum/maximum temperature recorded at WS1 at 2,100 m a.s.l. between November 2014 and January 2018.

1.3.3 Study catchments

This study was carried out in the catchment of the Chemosit River, referred to as the 'main catchment' in this dissertation, which is a 1,021 km² sub-catchment of the Sondu basin (Figure 1.1). To assess the effect of individual land use types, three sub-catchments (27–36 km²) dominated by either natural forest, smallholder agriculture or commercial tea and tree plantations, were selected within the main catchment. While the main criteria for site selection were land use and comparability of the geological substrate, security of field equipment and accessibility of the site during the rainy season were also taken into account. The geology of the three sub-catchments is characterised by phonolites, although phonolitic nephelinites with a variety of Tertiary tuffs occur in the upper part of the smallholder agriculture sub-catchment (Jennings, 1971). Soils are up to 6 m deep and well-drained, and are classified as humic Nitisols (Ekirapa and Shitakha, 1996).

1.3.4 Instrumentation and sampling

The three sub-catchments were instrumented in October 2014 and the main catchment in April 2015. Each site was equipped with an automatic measurement system (Figure 1.4a–b), consisting of a radar-based water level sensor (VEGAPULS WL61, VEGA Grieshaber KG, Schiltach, Germany), a UV/Vis spectrometer probe for nitrate (NO_3-N), total and dissolved organic carbon (TOC, DOC) and turbidity (spectro::lyser, s::can Messtechnik GmbH, Vienna, Austria), and an electrical conductivity (EC) probe, which also measured stream temperature (condu::lyser, s::can Messtechnik GmbH, Vienna, Austria). All sites were fenced and had 24-hour security to avoid interference with measurements or equipment, vandalism and theft. The four stations were visited on a weekly basis for sampling and maintenance. Weekly to bi-weekly grab samples were obtained for the comparison of nitrate (NO_3-N) values from the laboratory with *in situ* measurements (Jacobs et al., 2018). Discharge measurements were taken regularly for rating curve development using the slug injection salt dilution method (Moore, 2004), an Acoustic Doppler Velocimeter (ADV; FlowTracker, SonTek, San Diego CA, USA) or an Acoustic Doppler Current Profiler (ADCP; RiverSurveyor S5, SonTek, San Diego CA, USA), depending on discharge. In January 2016 three of the four automatic systems were connected to a server at Justus Liebig University Giessen and since then data has been automatically imported to an online database (http://fb09-pasig.umwelt.uni-giessen.de:8050/). No GPRS network was available at the fourth site (outlet of the natural forest sub-catchment) and data has been uploaded manually.

Figure 1.4 Instrumentation of the study catchments: (a) automatic measurement station with water level sensor, water quality sensors and data logger, (b) water quality sensor for nitrate, total and dissolved organic carbon and turbidity (left) and electrical conductivity and stream temperature (right), (c) throughfall tipping bucket, (d) tipping bucket, (e) weather station, (f) precipitation sampler, (g) wick sampler plate and (h) tubes leading to sample collection bottles for the wick sampler.

Weather data was collected at several sites in the main catchment throughout the study period (Figure 1.1c): throughfall and air temperature data from two throughfall tipping buckets located close to the outlet of the natural forest catchment (Figure 1.4c;

Umweltanalytische Produkte GmbH, Ibbenbüren, Germany), rainfall data from six tipping buckets (Figure 1.4d; Theodor Friedrichs, Schenefeld, Germany) and weather data from two weather stations (Figure 1.4e). A third weather station (WS2; Figure 1.1c) was installed in an area northwest of the study catchment for a study on greenhouse gas emissions from forest soils and soils from adjacent land use types. Weather station WS1 had to be relocated in September 2015 due to construction work on its original site. The weather stations recorded wind speed and direction (Davis cup anemometer), relative humidity and air temperature (VP-3 humidity/temperature sensor), photosynthetically active radiation (QSO-S PAR photon flux sensor) and soil volumetric water content, temperature and conductivity at 10–15 cm depth (GS3 soil moisture sensor) in addition to rainfall (ECRN-100 high resolution rain gauge). WS1 was equipped with additional soil moisture sensors at 30, 45, 60 and 85 cm depth. All sensors were manufactured by Decagon Devices, Pullman WA, USA.

Low-cost samplers to collect precipitation and throughfall samples for stable water isotope (δ^2H and δ^{18}O) analysis were installed in the three sub-catchments. The main catchment was only equipped with a precipitation sampler. The samplers consisted of a funnel to collect the rainfall and a glass bottle covered with aluminium foil (Figure 1.4f). A table tennis ball was placed inside the funnel to avoid sample modification through evaporative enrichment (Prechsl et al., 2014; Windhorst et al., 2013). All sites were equipped with a passive capillary wick sampler to collect mobile soil water at 15, 30 and 50 cm depth (Brown et al., 1989; Landon et al., 1999). These samplers were constructed from PE plates of 30 by 30 cm, inserted in the soil at the appropriate depth with as little soil disturbance as possible (Figure 1.4g). An unravelled part of a fibreglass wick was draped on top of the plate and the remaining part of the wick was led through a tube to glass bottles placed at 1 to 1.5 m depth in the ground (Figure 1.4h). Samples from stream water, precipitation, throughfall and soil water were collected on a weekly basis since October 2015. Concurrently, weekly stream water samples for trace element analysis were collected at the outlet of the three sub-catchments and the main catchment for the identification of stream water sources between October 2015 and October 2016. Potential water sources or ‘end members’ were sampled irregularly over the same period.

To complement the water quality data from the automatic stations and to get a better understanding of factors influencing spatial variation in stream water quality, five spatial

sampling campaigns were carried out, covering 16 sites within the main catchment (Figure 1.2a). Each site represented a sub-catchment (4–103 km²) characterised by either natural forest, smallholder agriculture or commercial tea and tree plantations as dominant land use. Three 2-day spatial sampling campaigns were carried out during the dry season in 2015, whereby 13 sites were sampled. Three sites were added in 2016 to increase the range of catchment areas. All sites were sampled again during two additional campaigns in the dry season of 2016. Such 'snapshot sampling' campaigns carried out in a short time during stable flow allow for comparison of water quality data obtained from different sites at a specific point in time (Grayson et al., 1997). At each site, filtered water samples were collected for analysis for dissolved organic carbon (DOC), total dissolved nitrogen (TDN) and nitrate (NO_3-N). Dissolved organic nitrogen (DON) was estimated as the difference between TDN and dissolved inorganic nitrogen. As ammonium (NH_4-N) and nitrite (NO_2-N) were only found in very low concentrations down to the detection limit, NO_3-N was assumed to represent the dissolved inorganic nitrogen fraction (Jacobs et al., 2017). Discharge was measured using the salt dilution method (Moore, 2004) and converted to specific discharge, i.e. discharge per unit area. Stream water temperature was recorded as well.

1.4 Summary of results

1.4.1 Objective 1: Spatial patterns in water quality

To assess the influence of land use and catchment characteristics on spatial variation in water quality, five spatial sampling campaigns were carried out during baseflow in the dry season of 2015 and 2016 (Chapter 2). Data on dissolved organic carbon (DOC), total dissolved nitrogen (TDN), nitrate (NO_3-N) and dissolved organic nitrogen (DON) obtained during the spatial sampling campaigns were related to stream temperature, precipitation in the six weeks leading up to the sampling campaigns, percent tree cover and the catchment characteristics elevation, catchment area, drainage density and topographical wetness index (TWI) obtained from a 30 m resolution digital elevation model (USGS, 2000). Percent tree cover within the catchment was used as proxy for land use, because the three land use types had significantly different tree cover ($p < 0.05$). Stepwise forward linear regression was used to quantify the effect of each of the selected variables on DOC, TDN, NO_3-N and DON concentrations. Variables were only included when significant at $p < 0.01$ to avoid overfitting of the model and if the variance inflation

factor (VIF) was less than 10 to avoid inclusion of highly collinear variables (O'Brien, 2007).

Although DOC concentrations were significantly lower in the commercial tea and tree plantation catchments (1.00±0.25 mg C l^{-1}) than in the smallholder agriculture (2.09±0.65 mg C l^{-1}) and natural forest catchments (1.53±0.43 mg C l^{-1}; $p < 0.001$), there was no clear effect of land use on DOC concentrations. The multiple regression model identified catchment area as variable explaining most of the variation in DOC (41.1%), followed by specific discharge (18.5%). Additionally, a minor effect of precipitation, drainage density and TWI (3.4%, 4.3% and 5.0%, respectively) was observed. The strong positive effect of catchment area, supported by the negative effect of drainage density, suggests that a larger catchment with longer transport pathways to the stream could act as greater source of DOC, thus resulting in higher stream water DOC concentrations. TWI was included in the analysis as index to predict soil wetness patterns within a catchment (Beven and Kirkby, 1979). Although wetter areas are potential sources of organic carbon and nitrogen (Chapman et al., 2001; Kalbitz et al., 2000), this was not observed in this study. However, low connectivity between wet areas and streams during the dry season potentially reduced the DOC supply from wetlands to the stream. The positive effect of precipitation in the six weeks preceding the sampling campaigns, as indicator of antecedent wetness conditions in the catchment, also suggests that stream water DOC concentrations increase when soils are wetter.

In contrast to DOC, TDN and NO_3-N were both strongly influenced by land use, with highest concentrations in the tea plantation catchments (1.80±0.50 and 1.62±0.60 mg N l^{-1}, respectively) and lowest in the natural forest catchments (0.55±0.15 and 0.30±0.08 mg N l^{-1}, respectively). This was reflected in the multiple linear regression model, where tree cover explained 64.4% and 47.3% of the variation in stream water TDN and NO_3-N concentrations, respectively. Since land use was stratified by elevation, with the tea plantation catchments located at lower elevation, the observed negative effect of elevation could also be attributed to land use. The effect of land use effect is most likely caused by differences in fertilizer application between the three land use types: commercial tea plantations receive 150–250 kg N ha^{-1} yr^{-1}, which is almost ten times the amount applied annually on smallholder farms (< 20 kg N ha^{-1} yr^{-1}). Increased TDN and NO_3-N concentrations are commonly observed in agricultural catchments when compared to

forested catchments (Biggs et al., 2004; Li et al., 2016; Martínez et al., 2009). Stream water DON concentrations, on the other hand, did not differ significantly between the three land use types and most of the variation was explained by precipitation (46.7%) and specific discharge (4.8%). The lack of significant differences in DON concentrations between catchments with contrasting land use was also found in other studies from the tropics (Gücker et al., 2016b; Neill et al., 2001; Recha et al., 2013). The results of this study show that different processes influenced dissolved organic carbon and nitrogen versus TDN and NO_3-N concentrations in the South-West Mau. The latter two solutes were strongly related to anthropogenic nitrogen (fertilizer) inputs, while the organic fractions were more controlled by the hydrological regime and, in the case of DOC, also catchment characteristics.

1.4.2 Objective 2: Land use effect on temporal nitrate dynamics

To assess whether land use affects NO_3-N sources, transport pathways and biogeochemical processes, a 2-year high-resolution dataset (10-minute resolution, sampling period January 2015–December 2016) of water level and stream water NO_3-N concentrations, collected by the four automatic measurement systems, was investigated for temporal NO_3-N patterns and responses to rainfall events in the three sub-catchments with different land use and at the outlet of the main catchment (Chapter 3). The raw data from the automatic measurement systems was processed to exclude unreliable data points, such as faulty measurements and implausible outliers. To estimate discharge from the water level time series, a second order polynomial rating curve was developed with discharge measurements over a range of water levels. NO_3-N laboratory values from grab samples were used to establish a linear relationship between field and lab measurements, which was then applied to the NO_3-N dataset for site-specific calibration. NO_3-N loads were calculated using the estimated discharge and calibrated NO_3-N concentration data. A 95% confidence interval was determined for the rating curve and the calibration model to estimate uncertainty. The final dataset, consisting of specific discharge, NO_3-N concentrations and NO_3-N loads, was assessed for seasonal patterns, the relationship between NO_3-N concentration and discharge, and 'hot moments', i.e. short periods of enhanced biogeochemical activity (McClain et al., 2003). Additionally, ten rainfall events from different seasons in both years were selected for hysteresis analysis, whereby observed changes in discharge and NO_3-N concentrations during the events were interpreted to identify sources of stormflow and solutes (Evans and Davies, 1998).

In accordance with the results of the spatial sampling campaigns (Chapter 2), the tea and tree plantation sub-catchment (TTP) had the highest flow-weighted mean NO_3-N concentrations (2.14±0.19 mg N l^{-1}) and annual specific loads (12.0–16.3 kg N ha^{-1} yr^{-1}), followed by the smallholder agriculture sub-catchment (SHA; 1.10±0.11 mg N l^{-1} and 4.9–6.0 kg N ha^{-1} yr^{-1}) and the main catchment (OUT; 0.89±0.10 mg N l^{-1} and 4.56 kg N ha^{-1} yr^{-1}). The natural forest sub-catchment (NF) had the lowest concentrations and loads (0.44±0.043 mg N l^{-1} and 2.6–3.2 kg N ha^{-1} yr^{-1}). As discussed in Section 1.4.1, the magnitude of NO_3-N concentrations is commonly influenced by anthropogenic N inputs, such as fertilizers (Poor and McDonnell, 2007). Therefore, higher loads from agricultural catchments are commonly observed (Gücker et al., 2016b; Recha et al., 2013; Riskin et al., 2017). Extrapolation of specific loads based on percentage land use in the main catchment resulted in an estimated 27.6% contribution of tea and tree plantations, which cover 11.1% of the main catchment, to the annual NO_3-N export of the OUT, while natural forest (covering 37% of the main catchment) only contributed 20%.

The specific discharge time series exhibited strong seasonality in all catchments, closely following the bi-modal precipitation pattern described in Section 1.3.2. This seasonality was also observed in NO_3-N concentrations in SHA, TTP and OUT, with increased concentrations during periods of high discharge, whereas NO_3-N concentrations in NF remained fairly constant throughout the year. Consequently, there was no relationship between NO_3-N concentrations and discharge in NF (R^2 = 0.070). OUT showed a weak log-linear relationship (R^2 = 0.217), while the log-linear relationships in TTP and SHA were quite strong (R^2 = 0.725 and R^2 = 0.630, respectively). The differences in the concentration–discharge relationships suggest different sources and/or mobilization processes of NO_3-N in SHA and TTP compared to NF.

Based on the results obtained from this study, a conceptual model of nitrogen fluxes was developed for the three sub-catchments with different land use (Figure 1.5). Leaching of NO_3-N from fertilizer inputs to groundwater during the rainy season could have contributed to the increased NO_3-N concentrations in SHA and TTP during the rainy season (Figure 1.5). This could be enhanced by the well-drained soils with relatively high soil organic carbon content (56.9–81.1 g kg^{-1}) (Owuor et al., 2018), which reduce NO_3-N retention (Lohse and Matson, 2005; Soares et al., 2005). Also discharge originating from soil layers with high inorganic N content could increase NO_3-N inputs to the stream

during the rainy season, while this NO_3-N source is most likely disconnected from the stream during the dry season (Musolff et al., 2016). These results suggest that groundwater is the major source of NO_3-N in SHA and TTP, as in many agricultural catchments (Durand et al., 2011).

NF does not receive any fertilizer and therefore leaching is limited (Figure 1.5), despite the potential accumulation of NO_3-N in the topsoil during the dry season due to nitrification (Kiese et al., 2003). Furthermore, NO_3-N concentrations could be reduced along the vertical flow path from the topsoil to groundwater due to uptake by deep-rooted vegetation, denitrification and abiotic N retention in deeper soil layers, as has been observed in a tropical forest in the Amazon (Chaves et al., 2009) and a tropical montane forest in Peru (Saunders et al., 2006). The differences in vegetation type, rooting depth and tree cover, especially in the riparian zone, between the sub-catchments could further influence the amount of NO_3-N in groundwater that enters the stream.

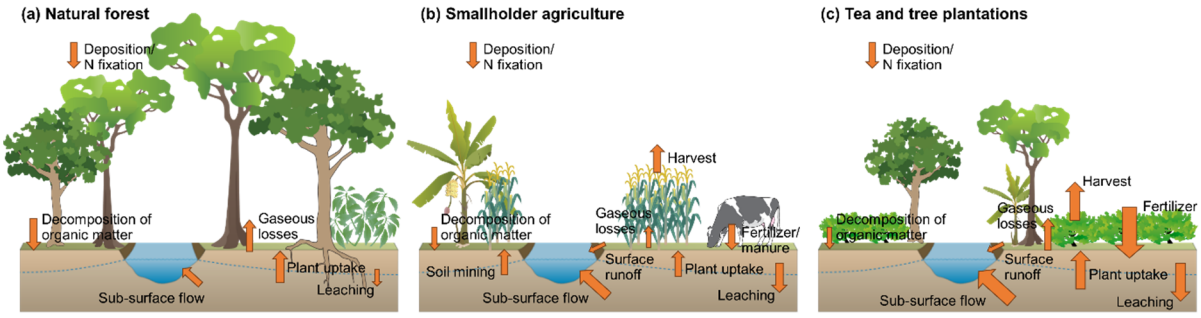

Figure 1.5 Conceptual model of nitrogen (N) fluxes in the (a) natural forest, (b) smallholder agriculture, and (c) tea and tree plantations based on the interpretation of a 2-year time series (January 2015 to December 2016) of stream water nitrate (NO_3-N) concentration and discharge data from the South-West Mau, Kenya. Difference in arrow size represents the relative difference in magnitude of N flux between the three land use types.

The hysteresis analysis of ten rainfall events showed that NO_3-N enters the stream in NF through shallow sub-surface flow paths. The shape of most hysteresis loops in NF suggested inflow of NO_3-N rich soil water to the stream through shallow sub-surface flow caused by rainfall (Evans and Davies, 1998), resulting in an increase in the NO_3-N concentration during rainfall events. Conversely, the majority of the rainfall events led to dilution in SHA, TTP and OUT. This supports our previous finding that groundwater is the major source of NO_3-N, because inflow of NO_3-N rich groundwater is diluted with rainwater with low NO_3-N concentrations during rainfall events (Bartsch et al., 2013). The dilution effect furthermore implies an increased contribution of surface runoff to

streamflow, suggesting that conversion of natural forest to agricultural land would result in a shift from sub-surface flow to surface runoff during rainfall events. This could be caused by reduced infiltration rates in grasslands, croplands and tea plantations (13.8–43.3 cm h^{-1}) compared to tree plantations and natural forest (60.2–76.1 cm h^{-1}) (Owuor et al., 2018). These results also demonstrate that hysteresis loops are potentially good indicators for land use change impacts on hydro-biogeochemical fluxes.

The high-resolution dataset revealed 'hot moments' of increased NO_3-N concentrations during rainfall events at the end of the dry season in 2015 in NF and TTP, whereas no such peaks were observed after the dry season in 2016. Such a peak in NO_3-N concentrations is a common phenomenon in soils and is related to rapid mineralization of organic matter and a more active microbial community after rewetting of dry soil (Birch, 1964) or accumulation of NO_3-N in the topsoil during the dry season (Kiese et al., 2003; Wong and Nortcliff, 1995). The absence of similar hot moments in 2016 is most likely related to the relatively high rainfall during the dry season, while very little precipitation fell during the dry season of 2015.

1.4.3 Objective 3: Hydrological flow paths

Although the time series analysis described in Section 1.4.2 already provided some insight into hydrological flow paths in the three sub-catchments with different land use, further evidence to support these findings was sought with the help of stable water isotopes (δ^2H and δ^{18}O) and trace element data (Chapter 4). Samples from precipitation, stream and soil water from NF, SHA, TTP and OUT were analysed for stable isotopes and used to estimate the mean transit time (MTT) of stream and soil water. The results from this analysis were complemented by an end member mixing analysis (EMMA), whereby trace element signatures of different water sources, the so-called 'end members' (precipitation, throughfall, springs, wetlands and shallow wells), were used to identify stream water provenance.

The MTTs of stream water and soil water in the three sub-catchments and main catchment were estimated with the gamma model (GM) and the exponential piston flow model (EPM), which have been successfully used for MTT estimation in the past (Hrachowitz et al., 2010; McGuire and McDonnell, 2006; Timbe et al., 2014). Generalised likelihood uncertainty estimation (GLUE) was used to assess the uncertainty in MTT estimates. GM performed best for stream water data, although the modelling efficiency (Nash-Sutcliffe

efficiency, NSE) was generally low (0.05–0.33) due to the low variation in the isotopic signal of stream water compared to precipitation. The MTTs of NF and SHA were estimated at 4.0 (3.3–4.6) years and 3.8 (3.1–4.5) years, respectively. OUT had a much shorter estimated MTT of 2.5 (1.8–3.4) years, which could be caused by different geology in part of the catchment (Capell et al., 2012; Timbe et al., 2017). However, not enough information on soils and soil properties was available to confirm this. TTP had an estimated MTT of 3.3 (2.8–4.3) years, but the result was discarded because of the low NSE of 0.05. The highly damped stream water isotopic signal suggests that the sub-catchment most likely has a MTT of more than 4 years, which requires the use other tracers, such as tritium (^{3}H) (Cartwright et al., 2017). The fairly long MTTs are more comparable with tropical montane catchments with similar deep soils, such as in Mexico (Muñoz-Villers and McDonnell, 2012), than with Andean tropical montane catchments with steep slopes and shallow soils, which have much shorter MTTs (< 1 year) (Crespo et al., 2012). Long MTTs also indicate a considerable contribution of 'old water' or groundwater to streamflow. Both models performed reasonably well for soil water (NSE = 0.46–0.79), but MTTs could only be estimated for NF at 15 cm depth and for OUT at 15 and 50 cm depth due to the limited number of samples. The estimated MTT at 15 cm depth was shorter in NF (3.2–3.3 weeks) than in OUT (4.5–7.5 weeks). This was probably caused by the lower hydraulic conductivity in pasture soils compared to native forest soils (Owuor et al., 2018). Soil water at 50 cm depth in OUT had the longest MTT of 10.4–10.8 weeks.

Based on the EMMA and supported by evidence from the analysis of the high-resolution discharge and NO_3-N data, it was possible to develop a conceptual model of rainfall-runoff processes under low and high flow conditions (Figure 1.6). Despite the lack of difference in MTT between the three land use types, end member selection and behaviour was different for the three sub-catchments according to the EMMA using seven conservative trace elements (Li, Na, Mg, K, Rb, Sr and Ba). The higher contribution of the groundwater-related end members, i.e. the wetland in SHA (51%) and springs in NF (22%) and TTP (65%), to streamflow during high flow than during low flow (1%, 18% and 48%, respectively; Figure 1.6) corresponds to the findings of the time series analysis (Section 1.4.2), which suggested that inflow of NO_3-N rich groundwater increased during the rainy season in SHA and TTP. In SHA, a different groundwater source, represented by samples from one specific shallow well, was identified as important end member

during low flows (14%), although its contribution was still low compared to precipitation (84%; Figure 1.6).

The contribution of precipitation to streamflow was highest in SHA (59%), suggesting that a significant amount of surface runoff occurs during rainfall events, which is commonly observed in tropical montane catchments that have been converted to pasture (Chaves et al., 2008; Neill et al., 2011). However, precipitation (45%) and throughfall (31%) were also the main sources of streamflow in NF according to the EMMA. Although surface runoff has been observed in tropical montane forest catchments (de Moraes et al., 2006; Johnson et al., 2006a), it is more likely that these water sources contributed through fast sub-surface flow paths in NF (Boy et al., 2008; Muñoz-Villers and McDonnell, 2012; Saunders et al., 2006) or shallow flow from the saturated riparian zone (Mosquera et al., 2015; von Freyberg et al., 2014). This corresponds to the hydrological processes inferred from hysteresis analysis of nitrate concentrations during storm events (Chapter 3). The majority of streamflow in TTP originated from springs (59%). However, the mixing model was unable to capture all stream water samples in the mixing space enclosed by the three selected end members, resulting in a large overestimation of end member contributions (up to 853%). Although this could be related to uncertainty in laboratory measurements and temporal variation in the chemical composition of the selected end members, it is very likely that an important end member is missing (Barthold et al., 2011). There was also considerable over- and underestimation of end member contributions in SHA and OUT. This could be improved by sampling additional end members, which, for example, better represent groundwater and surface runoff, and sampling end members on a regular basis to better capture the temporal variation in end member composition.

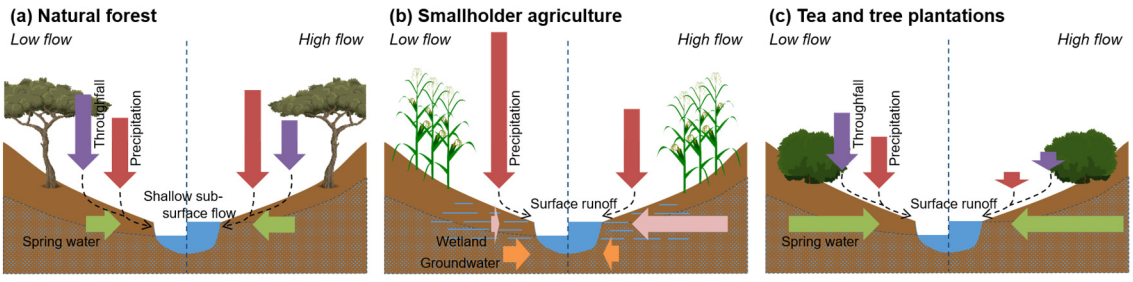

Figure 1.6 Dominant water sources and their relative contribution, represented by arrow length, to streamflow during low and high flows in (a) the natural forest, (b) smallholder agriculture, and (c) tea and tree plantation sub-catchments based on the end member mixing analysis using data collected between October 2015 and October 2016 in the South-West Mau, Kenya.

1.5 Implications of findings and recommendations for further research

The studies on temporal and spatial variation in nitrate (NO_3-N) concentrations both indicated an effect of land use on NO_3-N concentrations, which is strongly related to fertilizer application. Furthermore, the spatial sampling study showed that this effect was reflected in total dissolved nitrogen (TDN) concentrations. High concentrations in streams draining areas with commercial tea and tree plantations were reduced downstream by mixing with stream water with lower concentrations, suggesting that the magnitude of NO_3-N concentrations in stream water is related to the overall fertilizer input within a catchment. Consequently, future conversion of natural forest to agricultural land or intensification of agricultural practices will likely result in a further increase in NO_3-N concentrations and export. Deforestation rates in the tropics are high, with an annual forest loss of 600,000 ha between 2000 and 2015 (FAO, 2016), and the demand for food continues to increase due to population growth, thus posing a significant threat for surface water quality and river ecology, also in downstream regions. Eutrophication is, for example, already considered a major issue in Lake Victoria (Juma et al., 2014), and a further increase in N-loading could aggravate the problem.

Since leaching of fertilizer to the groundwater was identified as the major source of NO_3-N inputs to the stream in the smallholder agriculture and commercial tea plantation sub-catchments, careful consideration of the timing and rate of fertilizer application is required to maximise food production while minimizing the risk of nutrient losses. However, there are still large gaps in our knowledge of nutrient flows in food production systems, especially in sub-Saharan Africa (Masso et al., 2017; Rufino et al., 2014). This provides an opportunity for future research to quantify nutrient flows in East African agricultural systems and develop methodologies that can be applied by smallholder farmers and large scale agricultural producers to optimise nutrient use and productivity.

In addition to the role of groundwater as NO_3-N source, it as also an important source of stream water, which highlights the importance of sufficient groundwater recharge to maintain streamflow throughout the year. The increased occurrence of surface runoff in the smallholder agriculture and tea plantation sub-catchments, as inferred from the hysteresis analysis of rainfall events, suggest that a smaller part of the precipitation infiltrates during rainfall events. Therefore, agricultural areas could benefit from the

implementation of methods to promote infiltration of rainwater. This would also reduce the risk of soil erosion and degradation, and reduce sediment loads in rivers. High sediment loads could affect the ecological functioning of streams through increased turbidity, decreased primary productivity and alterations of the food web (Dudgeon et al., 2006; Kemp et al., 2011), but could also cause siltation of dams and hydropower installations. Erosion and sediment loads are a major concern in the Sondu basin, especially since many people in rural areas depend on the rivers as water source for domestic use. A significant decrease in Secchi transparency, i.e. clarity of the water, has already been observed in the Winam Gulf of Lake Victoria, into which the Sondu River discharges (Juma et al., 2014). Increased turbidity was also reported at sites disturbed by anthropogenic disturbance in the Upper Mara basin, bordering the Sondu basin to the south (Kilonzo et al., 2014) and modelling studies suggest strong increase in sediment yield from managed land use types in the same basin (Defersha et al., 2012; Defersha and Melesse, 2012). Turbidity data from the four automatic stations show significant increases in turbidity during storm events, specifically in the agricultural sub-catchments and at the main outlet. Using a site-specific relationship between turbidity and sediment concentrations, sediment export could be estimated for each land use based on the available turbidity data. Furthermore, methods such as sediment fingerprinting could identify main sources of sediment (Dutton et al., 2013; Mukundan et al., 2010), which could help to identify land use related sediment losses and target areas where soil conservation measures would be most effective and appropriate. The analysis of sediment for carbon and nitrogen content, especially during storm events, could provide further insights in to nutrient export. Little data is available on particulate carbon and nitrogen export from tropical catchments (e.g. Lewis et al., 1999; Zuijdgeest et al., 2015), yet this could contribute significantly to the total annual nutrient load.

Although the high-resolution dataset has already provided significant insights into water and nutrient fluxes in the South-West Mau, the dataset has not yet been exploited to its full potential. Maximum overlap discrete wavelet transform (MODWT) is a mathematical tool for time series analysis in various time resolutions. Applications of this tool or other wavelet analysis methods in hydrological research have been rather limited so far (e.g. Cauvy-Fraunié et al., 2013; Kang and Lin, 2007; Koirala et al., 2011; Labat et al., 2005), but its properties could make it a very suitable means to investigate temporal patterns in high-resolution time series. The application of MODWT to the high-resolution NO_3-N

time series led to the discovery of diurnal patterns in NO_3-N concentrations at all sites. Diurnal patterns are daily recurring patterns, directly or indirectly related to fluctuations in light availability and temperature caused by the rotation of the Earth. For NO_3-N, diurnal variations are attributed to transformation processes such as nitrification, denitrification, metabolic uptake and release of nutrients (Nimick et al., 2011). Because of the differences in diurnal patterns between the three sub-catchments, it could be argued that different processes drive the diurnal changes in NO_3-N concentrations. If this hypothesis is true, it would provide further evidence that land use change causes changes in nutrient cycling. In combination with recorded data on photosynthetically active radiation, precipitation, stream water and air temperature, water level and soil moisture, further analysis could reveal which parameters control the occurrence of diurnal patterns and therefore which factors drive nutrient metabolism and cycling in tropical montane streams under different land use. However, the observed patterns could also be artefacts created by diurnal changes in temperature or sunlight that affect the performance of the *in situ* sensors. Therefore, a careful investigation of potential external influences on NO_3-N measurements by the UV/Vis sensors should be conducted before interpreting the observed differences and shifts in diurnal patterns.

Besides changes in land use, climate change could also affect water and nutrient fluxes. Biogeochemical processes are often linked to climate-related factors such as soil moisture, temperature and precipitation, as illustrated by the distinct peaks or 'hot moments' in NO_3-N concentrations observed during rainfall events at the end of the dry season of 2015. Furthermore, annual NO_3-N loads in all sub-catchments were lower in the drier year 2016 than in 2015, suggesting that changes in annual precipitation affect the nitrogen budget as well. Although no significant changes in annual precipitation were observed in the last decades (Ongoma et al., 2018b), several studies suggest that the timing of rainfall will change in the future, resulting in less rainfall during the long rainy season and more rainfall during the short rainy season (Cook and Vizy, 2013; Schmocker et al., 2016; Shongwe et al., 2010). Furthermore, the number of extremes in rainfall amount and intensity is also likely to increase (Ongoma et al., 2018a; Schmocker et al., 2016). Investigation of the influence of extreme events, both droughts and storms, on biogeochemical processes and nutrient fluxes would help to predict the consequences of future climate change in the Mau Forest Complex.

2 Land use affects total dissolved nitrogen and nitrate concentrations in tropical montane streams in Kenya

This chapter is published in *Science of the Total Environment* as:

Jacobs, S. R., Breuer, L., Butterbach-Bahl, K., Pelster, D. E. and Rufino, M. C., 2017. Land use affects total dissolved nitrogen and nitrate concentrations in tropical montane streams in Kenya. Science of the Total Environment, 603–604:519–532, doi:10.1016/j.scitotenv.2017.06.100.

2.1 Introduction

Forests are widely recognised as playing an important role in regulating streamflow and water quality (Calder, 2002). However, the magnitude and direction of these effects are not well understood, because other factors contribute to solute concentrations in stream water. These factors include geomorphological catchment characteristics like geology, soil type and topography (Varanka et al., 2015), but also processes such as mixing of water of different geographical and hydrological sources (Bustillo et al., 2011), and inputs from precipitation (Billett and Cresser, 1996; Caine and Thurman, 1990). Hydrological flow paths (Boy et al., 2008; Hagedorn et al., 2000) and the transit time of water through a catchment regulate the chemical composition of water that enters the stream through sub-surface flow (Burns et al., 2003; Yamashita et al., 2014). During baseflow, stream water often originates from groundwater or deeper layers in the soil profile. The composition of water entering the stream will therefore most likely be determined by conditions in the soil, such as organic matter or inorganic nitrogen (N) contents, composition of the decomposer community, soil pH, moisture, temperature and the contact time between water and soil (Kalbitz et al., 2000). Furthermore, in-stream biogeochemical processes, such as N mineralisation and nitrification, respiration of

organic material and uptake during (micro)biological processes further alter stream water chemistry (Neill et al., 2006).

In addition to the aforementioned natural factors, human activities may also have a large impact on water quality. Stream water chemistry can be altered directly through the addition of nutrients and pollutants to soils and water bodies, but also indirectly through land management practices that alter primary productivity, infiltration rates, flow paths, erosion of land surfaces, sediment deposition in streams or biogeochemical processes. Human activities can therefore have a detrimental effect on nutrient cycling and water quality, but also on stream ecological functioning (e.g. Kilonzo et al., 2014; Maloney and Weller, 2011).

Most of the research on stream water chemistry has been carried out in temperate zones, whereas much less is known about tropical regions, especially Africa. However, due to climatic and pedological differences, findings from temperate areas cannot simply be extrapolated to Africa. Moreover, in large parts of Africa land use and agricultural management practices, which are often characterised by low fertilizer use, differ markedly from temperate regions (Ometo et al., 2000). A particular ecosystem that has received less attention in hydrological research is the tropical montane forest (Bruijnzeel, 2001). Forests in this ecosystem are recognised for their high biodiversity and provision of ecosystem services such as clean drinking water (Martínez et al., 2009), and as important carbon sinks (Spracklen and Righelato, 2014). The geographical distribution of the tropical montane forest ecosystem is delimited by climate and elevation. Tropical montane forests are under threat through conversion to agriculture, as the generally cool and wet climate and fertile soils make such areas very attractive for agriculture. In spite of the regional importance of this ecosystem, the consequences of land use changes in tropical montane areas are still poorly understood.

The carbon (C) and nitrogen (N) cycles are closely linked to the hydrological cycle with stream water DOC concentrations strongly related to discharge patterns (Goller et al., 2006; Hope et al., 1994; Raymond and Oh, 2007) and flow paths (Boy et al., 2008; Wilson and Xenopoulos, 2008). The transport and export of nitrogen is similarly controlled by hydrology (Mitchell, 2001). Because land use change can alter hydrological processes, e.g. through reduction in mean transit time after conversion from forest to grassland (Roa-García and Weiler, 2010), or changes in soil hydrological properties such as infiltration

(Owuor et al., 2016) which might result in an increased contribution of overland flow to streamflow (Chaves et al., 2008; Neill et al., 2011), land use changes can increase nutrient export or reduce concentrations through dilution.

Deforestation and land use change are considered important human drivers of changes in stream water chemistry with significant alterations observed after conversion from forest to agriculture or pastures in the Central Amazon, including elevated nitrate (NO_3-N) loads (Williams et al., 1997; Williams and Melack, 1997) or increased turbidity as a consequence of accelerated soil erosion in the Eastern Amazon (Figueiredo et al., 2010) and India (Singh and Mishra, 2014). Other evidence suggests that large-scale (> 66–75%) deforestation causes higher total dissolved nitrogen (TDN) concentrations in the dry season in the Amazon due to loss of nutrient retention capacity of the soil and direct inputs from cattle and humans, especially around urban areas (Biggs et al., 2004). A 1-year field study in a tropical rain forest in western Kenya found that dissolved organic carbon (DOC) exports rose by 153% after conversion to agriculture due to mobilization of organic C originally stored in the forest topsoil (Recha et al., 2013). Studies, mainly conducted in the northern hemisphere, confirm that streams from catchments with a high percentage of agricultural land or wetlands have higher DOC concentrations than streams from forested catchments (e.g. Glendell and Brazier, 2014; Graeber et al., 2012b; Singh et al., 2015).

Despite the evidence that land use plays a role in regulating concentrations of dissolved C and N, there is no agreement on the importance of land use compared to other catchment characteristics such as topography. Oni et al. (2014) observed very different patterns in DOC concentrations and loadings in two similar catchments, indicating complex interactions of seasonality and land use on DOC concentrations. Neff et al. (2013) demonstrated that elevation and topography influences NO_3-N concentrations in the Great Smoky Mountains, USA, through increased rates of acid deposition, precipitation, base cation leaching and increased occurrence of steeper slopes with less well-developed soils at higher elevation (Neff et al., 2013). Elevation changes are also linked to changes in temperature, which can affect the composition and activity of the soil microbial community and rates of mineralisation and primary productivity (Monteith et al., 2015; Nottingham et al., 2015). In addition, soil types play an important role in controlling concentrations of N and DOC (Wohlfart et al., 2012). Many studies conclude that there

is no single controlling variable and in most cases stream water chemistry is a result of a combination of factors such as topography, land cover, geochemical reactivity, climate and catchment area (Chuman et al., 2013; Rothwell et al., 2010).

This study focuses on the Mau Forest Complex, which is the largest remaining indigenous tropical montane forest area in Kenya. The forest is classified as Afromontane mixed forest dominated by a *Tabernaemontana–Allophylus–Drypetes* forest formation at lower altitude (Kinyanjui, 2011), changing into montane bamboo forest above 2,300 m elevation (Edwards and Blackie, 1979). The Mau Forest Complex is the headwater area for twelve major rivers in western Kenya and is an important source of freshwater for approximately 5 million people living downstream (UNEP et al., 2008). The area is also highly suitable for agriculture due to the high annual rainfall and well-drained deep soils (Krhoda, 1988). Consequently, 25% of the forest was converted to agriculture between 1973 and 2013 (Swart, 2016) and it is believed to have led to significant decrease in water quality through increased nutrient and sediment loads (Kilonzo et al., 2014; Nyairo et al., 2015), but thorough scientific evidence is lacking. Therefore, this study aims to estimate and explain the influence of land use, physicochemical and physical catchment characteristics, such as elevation, drainage density and topographical wetness index (TWI) on stream water chemistry in the Mau Forest Complex.

2.2 Methods

2.2.1 Study area

The study was located in the headwater area of the Sondu River, which originates in the South-West block of the Mau Forest Complex and drains into Lake Victoria. The South-West Mau is under human pressure through forest excisions, encroachment of smallholder farms into the forest, illegal logging, charcoal burning and poaching (Government of Kenya, 2009; Olang and Kundu, 2011). Large parts of the forest have been converted to smallholder agriculture in the past decades (Baldyga et al., 2008), while commercial tea plantations were established in the area in the first half of the 20th century (Binge, 1962). The sampling sites selected for this study fall within the Chemosit River basin with an area of 1,023 km², a sub-basin of the Sondu basin (Figure 2.1a). Elevation ranges from 2,932 m on top of the Mau Escarpment to 1,717 m at the outlet of the catchment. The geology in the area originates from the early Miocene (Edwards and Blackie, 1979), with phonolites dominating in the lower part of the catchment, and

phonolitic nephelinites in the upper part (Binge, 1962; Woolley, 2001). A variety of Tertiary tuffs are found on the highest part of the Mau Escarpment (Jennings, 1971).

The temperature in the study area is relatively constant throughout the year with a mean of 15.7 °C at 2,081 m elevation between 1990 and 1996 (Ekirapa and Shitakha, 1996). Daily minimum temperatures lie between 8 and 9 °C throughout the year, while the daily maximum temperature ranges from 21 °C in July to 25 °C in March (Stephens et al., 1992). The area experiences a bi-modal rainfall pattern, with the long rains occurring from April to July and the short rains from October to December. Mean annual precipitation between 1905 and 2014 was 1,988±328 mm, with highest rainfall generally occurring in April and May during the long rains (> 250 mm per month) and lowest in January and February during the dry season (< 75 mm per month).

The Chemosit basin is dominated by three land use types: (a) natural forest (NF), (b) smallholder agriculture (SHA) and (c) commercial tea and tree plantations (TTP; Figure 2.1b). The natural forest is located between 1,930 and 2,470 m elevation. The eastern part of the forest, bordering an area of smallholder agriculture, is degraded through human encroachment. In total, more than 25% of the forest cover in the South-West Mau was lost since the 1990s (Kinyanjui, 2011), although forest cover is slowly increasing after eviction of settlers from this area in 2005 and 2006 (Chacha, 2015). However, illegal activities such as logging, charcoal burning and grazing are still ongoing. The area of the forest neighbouring the tea plantations in the west is less degraded (Bewernick, 2016), although the mentioned human activities also affect the forest on that side.

On the north eastern side of the forest, smallholder agriculture is prevalent, mainly consisting of small farms of up to 2 ha. People practice subsistence farming, growing maize, beans, cabbage and potatoes, interspersed with grazing areas and *Eucalyptus* spp. or *Cupressus* spp. woodlots. Farmers apply up to 50 kg N ha^{-1}, depending on the crops they grow, although this can increase to 100–120 kg N ha^{-1} at smallholder farms where tea is grown. Riparian zones are often severely degraded, due to cultivation up to the river bank and access to the river for fetching water, washing clothes and bathing as well as watering livestock, predominantly cattle. In several places the natural bamboo vegetation in the riparian zone is replaced by small Eucalyptus plantations.

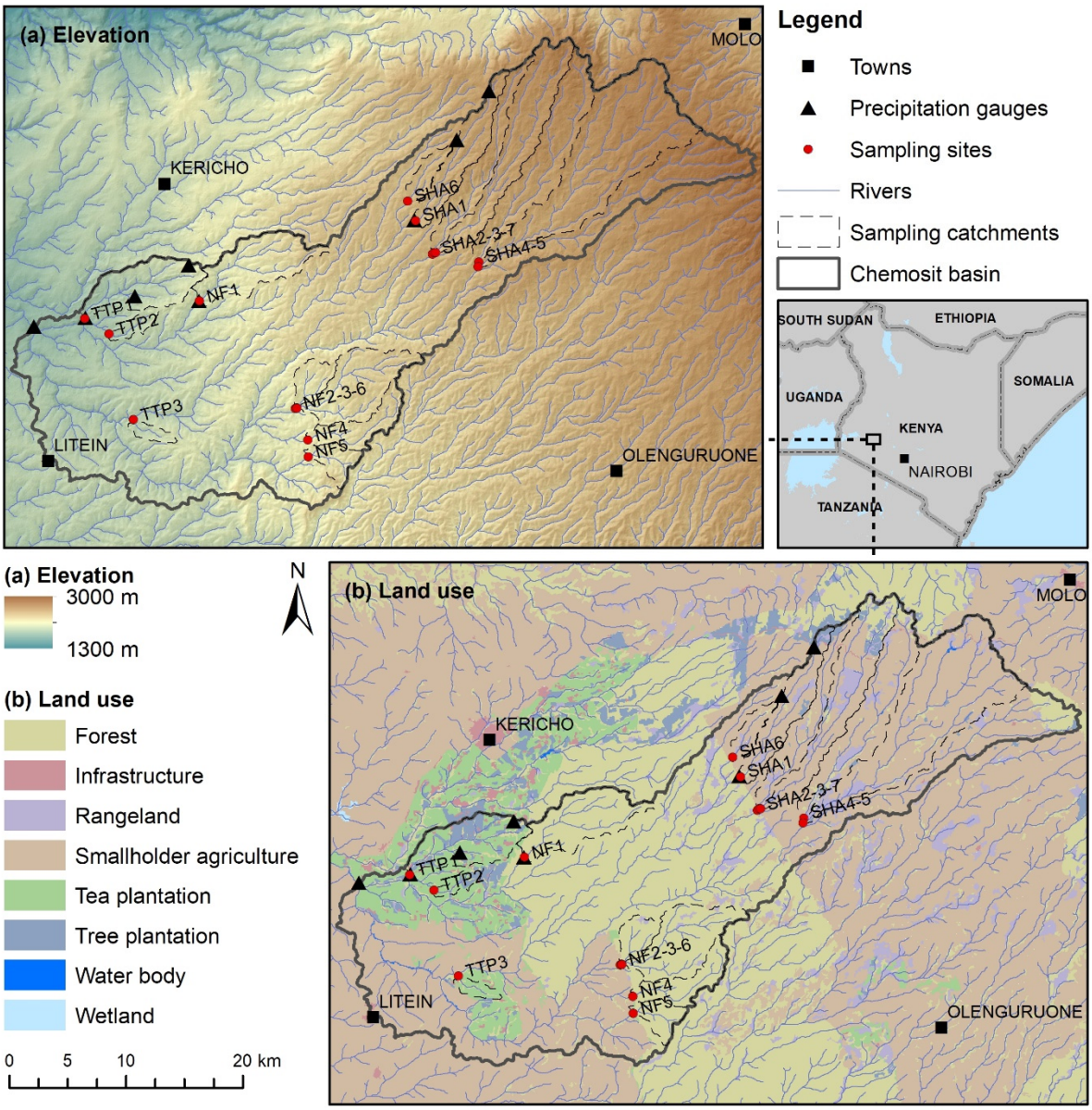

Figure 2.1 Maps of the study area in the South-West Mau, Kenya, showing (a) elevation (SRTM digital elevation model 30 m resolution; USGS, 2000), and (b) land use classification based on LandSat imagery from 2013 (Swart, 2016). Precipitation gauges, sampling sites and catchments within the Chemosit basin are indicated on both maps. Labels refer to the sampling site and corresponding land use: NF = natural forest, SHA = smallholder agriculture and TTP = tea and tree plantations.

At a low altitude (< 2,100 m), an area of approx. 20,000 ha is covered by commercial tea plantations, some of which fall within the study catchment. Within this area, the commercial tea fields are alternated with Eucalyptus and Cypress plantations with an average ratio of 3:1 (tea–tree plantation). Riparian zones of up to 30 m distance from the river are maintained within the tea estates and consist of native vegetation. Aerial

application of fertilizer in pellet form is carried out two to three times per year, with annual application rates of 150–250 kg N ha^{-1} depending on the soil fertility status of individual tea fields. Manure is applied manually on fields within the commercial estates where certified-organic tea is grown. Land use change occurs within commercial tea plantations, whereby tea fields are replaced by Eucalyptus and vice versa, depending on soil conditions. The area of commercial tea production is surrounded by smallholder farms, where tea is grown on small fields of < 1 ha in addition to the common food crops.

2.2.2 Sites selection and sampling campaigns

Sampling sites were selected based on land use and accessibility. Initially thirteen sites were selected: five in the smallholder area (SHA1–5), five in the natural forest (NF1–5) and three within the commercial tea and tree plantations (TTP1–3; Figure 2.1), covering a broad range of catchment sizes (4–103 km^2). Three sites were added in 2016: SHA2 and SHA3 were combined to form SHA7 after the confluence of the streams draining SHA2 and SHA3, and NF2 and NF3 to form NF6 to increase the number of sites with a catchment size > 40 km^2. SHA6 was selected to include a smallholder catchment with size < 10 km. No additional suitable and accessible TTP catchments could be identified within the study area.

In total five snapshot sampling campaigns were conducted during periods of baseflow, which coincided with the dry season: on 9–10, 12–13 and 23–24 February 2015, 16–17 February 2016 and 5–6 March 2016, with each campaign taking two days. Opportunities for sampling were limited, because a period of stable flow is required for the sampling (Grayson et al., 1997). Daily and highly localised rainfall hinders sampling in periods other than the dry season, because it could result in sampling during rising or falling limbs of the hydrograph, reducing the comparability of the samples. Rainfall events were more frequent in the dry season of 2016 than in the dry season of 2015, further limiting the number of sampling campaigns. In February 2015, the 13 initially selected sites were sampled, while in 2016 all 16 sites were sampled. The route along sampling sites differed between 2015 and 2016 to avoid bias of sampling time. However, in both years all TTP catchments were sampled during the afternoon, whereas NF and SHA catchments were sampled in the morning and afternoon.

During all sampling campaigns, discharge was measured using the salt dilution method, whereby a known quantity of table salt (NaCl) mixed in a bucket with stream water was

instantaneously released in the river (Moore, 2004). Electrical conductivity (EC) was measured downstream at a 1-second interval, using a handheld data logger (Multi 3420, WTW Wissenschaftlich-Technische Werkstätten GmbH, Weilheim, Germany) equipped with an EC probe (TetraCon 925-3, WTW Wissenschaftlich-Technische Werkstätten GmbH, Weilheim, Germany). The sensor also measured stream water temperature. The resulting time-concentration curve was used to calculate discharge (Moore, 2004). The quantity of salt and distance between salt release and EC measurement (20–100 m) was determined on site based on visually estimated discharge to ensure proper mixing of the salt with stream water. Specific discharge was calculated using the equation:

$$Q_s = \frac{Q_m}{A} * 864 \quad (2.1)$$

where Q_s is specific discharge in $m^3\ ha^{-1}\ day^{-1}$, Q_m is the measured discharge in $m^3\ s^{-1}$ and A is the catchment area in km^2. A factor of 864 was included to convert the units from $m^3\ km^{-2}\ s^{-1}$ to $m^3\ ha^{-1}\ day^{-1}$.

Stream water samples were filtered using a syringe and 0.45 µm polypropylene filter (Whatman Puradisc 25 syringe filter, GE Healthcare, Little Chalfont, UK or KX syringe filter, Kinesis Ltd., St. Neods, UK) and stored in clean 125 ml HDPE bottles with screw cap. The samples were immediately stored in a cooler box with ice and frozen on return from the field. All samples were analysed in the lab of Justus Liebig University Giessen, Germany for DOC and TDN (TOC cube, Elementar Analysensysteme GmbH, Hanau, Germany), as well as NO_3-N (ICS-2000, Dionex, Sunnyvale CA, USA). Dissolved organic nitrogen (DON) was estimated by subtracting NO_3-N from TDN, assuming that NO_3-N was the dominant form of dissolved inorganic N. Four sites were sampled four times during baseflow and samples were analysed for both ammonium (NH_4-N) and NO_3-N. NH_4-N concentrations were found to be negligible, probably due to missing point source pollution or any intensive farming activities. In 4 out of 77 samples, measured NO_3-N values exceeded the TDN values, which is a common problem with this method of DON estimation when the DIN:TDN ratio is high (Graeber et al., 2012a). In these cases, DON concentrations were set to zero. In addition, two values for NO_3-N were discarded based on improbability of the values compared to other results and identification as outliers by Grubbs' test ($p < 0.05$). For NF6 and SHA7, which are both combinations of two smaller catchments, parameters for campaigns 1–3 were estimated

by combining the data from NF2 and NF3, and SHA2 and SHA3, respectively. The data obtained during campaigns 4–5 confirmed that this is a reasonable estimate.

2.2.3 Explanatory variables

Data on stream water temperature and specific discharge were collected during the field campaigns as described above. Precipitation in the six weeks before each sampling campaign was calculated using precipitation data recorded at 10-minute intervals using six tipping buckets (Theodor Friedrichs, Schenefeld, Germany) and two weather stations (Decagon Devices, Meter Group, Pullman WA, USA) within the Chemosit basin (Figure 2.1). Total precipitation for each catchment was estimated by weighing the data from each station using Thiessen polygons.

Data on catchment characteristics (Table 2.1) were collected from GIS sources. The categorical variable *land use* was obtained from a land use classification analysis for the Mau Forest complex, using LandSat imagery from 2013 (Swart, 2016). Tree cover was calculated from a raster dataset on forest cover in the area in 2016 and includes primary and secondary forest, shady forest in mountain ridges and tree plantations (Bewernick, 2016). The 30 m resolution of the LandSat imagery was not sufficient to map single trees or small woodlots on farms.

All data on topography and drainage network were derived from a 30 m SRTM digital elevation model (USGS, 2000). Elevation data was obtained directly from the SRTM DEM. Catchments were delineated using the Spatial Analyst toolbox in ArcMap 10.2 (Environmental Systems Research Institute, Inc. (ESRI), Redlands, California, USA). These were used to calculate catchment area and drainage density for each catchment. SAGA GIS (Conrad et al., 2015) was used to delineate the stream network and to calculate topographical wetness index (TWI). TWI is an index developed for the prediction of wetness patterns within a catchment, based on upslope contributing area α and slope tan β derived from commercially available topographic data (Beven and Kirkby, 1979; Rodhe and Seibert, 1999):

$$TWI = \frac{\alpha}{\tan(\beta)} \tag{2.2}$$

Both α and tan(β) were derived directly from the DEM and used to calculated TWI with the Topographical Wetness Index module in SAGA GIS. The results were then normalised to range from 0 to 1.

Table 2.1 Characteristics of the 16 snapshot sampling catchments in the South-West Mau, Kenya. Dominant land use and percentage tree cover were derived from 2013 and 2016 LandSat imagery, respectively. Mean elevation, area, drainage density and topographical wetness index were calculated from SRTM DEM with 30 m resolution (USGS, 2000).

Site	Coordinates[a]		Land use[b]	Tree cover	Mean elevation	Area	Drainage density	Topographical wetness index
	Longitude	*Latitude*		*%*	*m*	*km²*	*km km⁻²*	
NF1	35°18'32.939" E	0°27'48.286" S	NF	99.00	2,177	35.9	1.652	0.176
NF2	35°23'2.220" E	0°32'45.474" S	NF	95.23	2,200	9.7	1.515	0.181
NF3	35°23'2.374" E	0°32'46.352" S	NF	97.76	2,269	36.2	1.793	0.181
NF4	35°23'33.598" E	0°34'15.531" S	NF	98.89	2,254	17.8	1.657	0.177
NF5	35°23'34.575" E	0°35'2.451" S	NF	97.80	2,222	9.5	1.737	0.166
NF6	35°22'57.998" E	0°32'47.376" S	NF	97.13	2,254	46.0	1.772	0.181
SHA1	35°28'31.454" E	0°24'3.797" S	SHA	9.29	2,524	27.2	1.467	0.194
SHA2	35°29'22.864" E	0°25'32.442" S	SHA	5.26	2,536	26.7	1.640	0.200
SHA3	35°29'26.687" E	0°25'33.112" S	SHA	2.69	2,602	48.7	1.577	0.199
SHA4	35°31'26.721" E	0°25'58.857" S	SHA	3.98	2,606	49.9	1.583	0.197
SHA5	35°31'24.400" E	0°26'12.150" S	SHA	1.68	2,651	103.7	1.645	0.209
SHA6	35°28'9.278" E	0°23'9.573" S	SHA	4.77	2,445	7.7	1.429	0.194
SHA7	35°29'17.812" E	0°25'37.110" S	SHA	3.73	2,574	77.8	1.639	0.199
TTP1	35°13'15.216" E	0°28'37.699" S	TTP	34.10	1,953	33.3	1.667	0.196
TTP2	35°14'23.210" E	0°29'19.548" S	TTP	34.20	1,949	5.3	1.679	0.197
TTP3	35°15'30.753" E	0°33'18.911" S	TTP	17.28	1,992	4.3	1.605	0.189

[a] WGS 1984 UTM Zone 36S; [b] NF = natural forest, SHA = smallholder agriculture, TTP = tea and tree plantations

2.2.4 Statistical analysis

All variables were tested for normality using Q-Q plots and the Shapiro-Wilk test ($p < 0.05$). DOC, TDN, NO_3-N concentrations, specific discharge, precipitation and tree cover showed a significant deviation and were therefore log-transformed.

ANOVA and Tukey's HSD test were applied to test for significant differences ($p < 0.05$) in stream water concentrations for catchments with different land use. SHA3–5 were excluded from the analysis because of the different underlying geology. Pearson's correlation coefficients were calculated to identify the strength and direction of significant relationships ($p < 0.05$) between the dependent and explanatory variables.

Stepwise-forward linear regression was used to quantify the effect of all continuous explanatory variables on water quality. Tree cover (%) was included in the analysis as a proxy for the categorical variable *land use*. To avoid overfitting the model, variables with $p > 0.01$ were excluded from the model as having no significant influence on the water quality parameter. The variance inflation factor (VIF) was used to assess multicollinearity between variables included in the model. A variable was considered highly collinear if the VIF > 10 (O'Brien, 2007) and consequently excluded from the model. We report adjusted R^2 as a measure of explanatory power of each model. All statistics were carried out with R 3.2.1 (R Core Team, 2015).

2.3 Results

2.3.1 Stream water chemistry across catchments

Highest stream water electrical conductivity (EC) values were observed in the catchments dominated by smallholder agriculture (SHA), followed by commercial tea and tree plantations (TTP) and the natural forest (NF; Table 2.2; $p < 0.01$). Stream temperature varied between 12.0 and 21.7 °C, with the lowest temperatures recorded in the morning around 7 a.m. and a highest around 2 p.m. Stream water temperatures in the NF catchments were significantly lower ($p < 0.01$) than in the TTP catchments. However, temperatures in NF and SHA as well as in SHA and TTP did not differ significantly ($p = 0.219$ and $p = 0.354$, respectively). Specific discharge was lower for SHA catchments than for NF and TTP catchments ($p < 0.001$). Overall, baseflow specific discharge values were lower during the campaigns of 2015, with a mean of 2.07±1.15 $m^3\ ha^{-1}\ day^{-1}$ in 2015 compared to 5.84±4.50 $m^3\ ha^{-1}\ day^{-1}$ in 2016. This is most likely due to more rainfall in the period preceding the samplings campaigns in 2016.

The TTP catchments were characterised by the highest stream water TDN and NO_3-N concentrations (Figure 2.2). Minimum values in the three TTP catchments were up to 4 times higher than the maximum values in all other catchments (Table 2.2). NF catchments showed the lowest stream water TDN and NO_3-N concentrations. Concentrations of both solutes also differed between catchments dominated by the three different land uses ($p < 0.001$). Conversely, DOC concentrations in the TTP catchments were significantly lower ($p < 0.001$) than in NF and SHA catchments (Figure 2.2; Table 2.2). DON concentrations were similar across all catchments ($p = 0.738$).

Table 2.2 Stream water chemistry for all sites sampled in February 2015 and February/March 2016 (n = 5 for all sites, except SHA6 with n = 2) in the South-West Mau, Kenya. Range is presented for concentrations of dissolved organic carbon (DOC), total dissolved nitrogen (TDN), nitrate (NO_3-N), dissolved organic nitrogen (DON), electrical conductivity (EC), stream temperature and specific discharge. Mean±SD of these variables is given in parentheses for all sampling sites of the same land use. Different superscripts for the means of each parameter indicate significant differences ($p < 0.05$) between sites grouped by land use (NF = natural forest, SHA = smallholder agriculture, TTP = tea and tree plantations). The total amount of precipitation was calculated for a period of six weeks preceding each sampling campaign (1–5).

Site	DOC	TDN	NO_3-N	DON	EC	Stream temp.	Specific discharge	Precipitation				
	mg C l^{-1}	*mg N l^{-1}*	*mg N l^{-1}*	*mg N l^{-1}*	*µS cm^{-1}*	*°C*	*m^3 ha^{-1} day^{-1}*	*mm*				
								1	2	3	4	5
NF1	1.66-3.21	0.50-0.90	0.36-0.40	0.11-0.52	30.1-44.0	13.1-21.7	2.41-8.20	6.2	5.8	56.6	297.5	79.6
NF2	1.29-1.72	0.51-0.81	0.29-0.43	0.10-0.50	25.6-37.8	12.0-17.2	2.04-12.72	6.4	6.0	58.2	278.2	73.2
NF3	0.82-1.51	0.32-0.64	0.18-0.26	0.06-0.46	28.7-45.2	12.9-17.1	2.53-10.37	4.3	3.7	41.1	214.6	54.1
NF4	1.12-1.60	0.35-0.47	0.21-0.31	0.07-0.25	26.1-35.3	13.0-16.6	2.00-11.55	4.8	4.3	45.2	229.9	58.7
NF5	1.34-1.84	0.47-0.58	0.27-0.43	0.11-0.29	28.1-41.3	12.9-18.6	1.35-11.67	7.6	6.9	70.5	278.2	73.2
NF6	1.00-1.75	0.37-0.68	0.21-0.31	0.09-0.46	28.2-43.7	12.7-15.7	2.52-11.07	3.6	3.3	32.4	228.1	58.1
NF	(1.53±0.43)^{a}	(0.55±0.15)^{a}	(0.30±0.08)^{a}	(0.26±0.16)^{a}	(34.7±5.7)^{a}	(15.1±2.4)^{a}	(4.81±3.41)^{a}					
SHA1	1.44-1.86	0.76-0.98	0.39-0.87	0.10-0.42	51.6-72.4	12.5-18.2	1.52-4.60	3.3	3.1	12.6	146.1	38.7
SHA2	1.44-2.05	0.76-0.96	0.54-0.79	0.04-0.42	55.8-66.9	15.1-19.5	0.93-2.73	2.8	2.6	13.6	150.3	39.9
SHA3	1.42-2.54	0.74-1.10	0.44-0.67	0.08-0.50	64.9-96.2	16.6-18.6	0.65-1.51	1.8	1.8	8.8	152.9	43.3
SHA4	1.77-3.06	0.74-0.98	0.36-0.92	0.06-0.38	66.9-83.8	14.3-19.9	0.36-1.11	2.2	2.1	8.7	150.2	42.3
SHA5	2.94-3.72	0.54-0.67	0.19-0.55	0.12-0.37	98.6-135.8	12.3-21.5	0.41-0.84	1.5	1.5	6.5	153.1	44.5
SHA6	1.26-1.44	0.69-0.79	0.58-0.73	0.06-0.11	36.5-37.7	12.1-12.6	3.51-5.78	3.6	3.3	18.6	149.4	37.1
SHA7	1.50-2.77	0.80-1.04	0.57-0.71	0.16-0.46	60.5-84.6	14.5-20.2	0.75-1.98	2.2	2.1	11.0	152.6	42.1
SHA	(2.09±0.65)^{a}	(0.82±0.13)^{b}	(0.57±0.17)^{b}	(0.24±0.14)^{a}	(76.1±24.4)^{b}	(16.6±2.6)^{ab}	(1.41±1.25)^{b}					
TTP1	0.73-1.02	1.48-1.74	1.14-1.71	0.00-0.35	38.2-41.7	16.3-17.3	3.38-16.56	4.0	3.9	43.8	275.6	93.9
TTP2	0.80-1.58	1.17-1.74	0.94-1.74	0.00-0.32	37.3-39.5	12.2-18.0	3.01-15.06	4.3	4.3	29.3	254.4	97.5
TTP3	0.80-1.48	1.97-2.91	1.66-3.07	0.00-0.34	46.3-48.9	18.0-20.4	2.26-9.66	10.2	10.1	39.8	201.8	86.0
TTP	(1.00±0.25)^{b}	(1.80±0.50)^{c}	(1.62±0.60)^{c}	(0.20±0.15)^{a}	(41.8±4.4)^{c}	(17.4±1.8)^{b}	(6.04±4.47)^{a}					

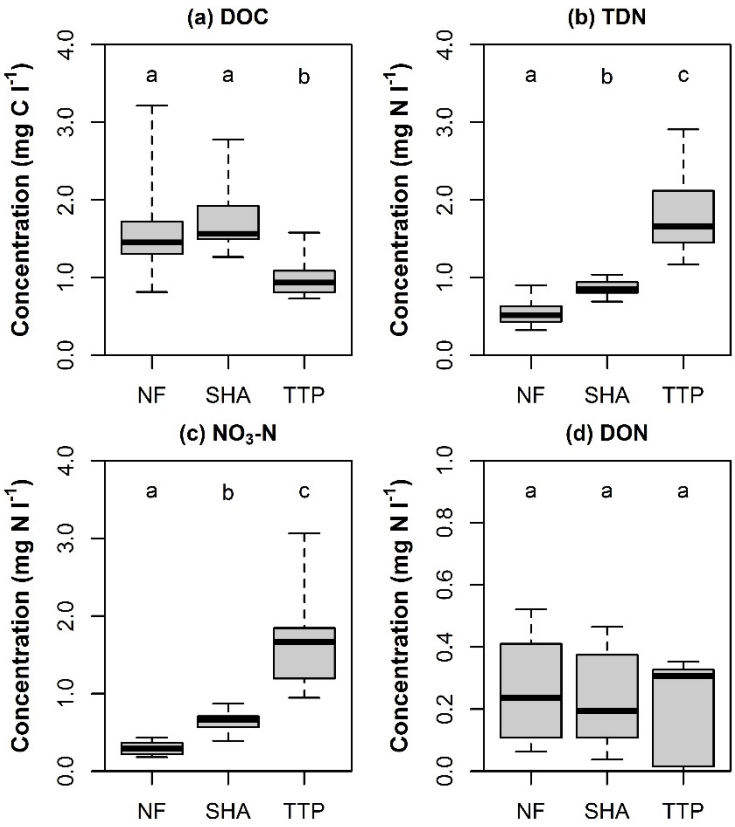

Figure 2.2 Comparison of (a) dissolved organic carbon (DOC), (b) total dissolved nitrogen (TDN), (c) nitrate (NO_3-N) and (d) dissolved organic nitrogen (DON) concentrations between the three land use types (NF = natural forest, SHA = smallholder agriculture, TTP = tea and tree plantations) based on data collected in the South-West Mau, Kenya, in February 2015 and February/March 2016. The thick line represents the median and the box the inter quartile range, while whiskers show the minimum and maximum values. Different letters above the land uses in the box plot indicate a significantly different mean ($p < 0.05$).

2.3.2 Correlation between variables

DOC concentrations showed a negative correlation with specific discharge and tree cover (%) (Table 2.3), a strong positive correlation with elevation and area, and a weak positive correlation with TWI. Significant correlations between the explanatory variables and TDN and NO_3-N were similar in direction and magnitude, except for catchment area, which was correlated only with NO_3-N. This similarity can be explained by the high correlation between TDN and NO_3-N ($r = 0.894$; $p < 0.001$). The strongest correlation was found between TWI and both TDN and NO_3-N. DON was only significantly correlated to specific discharge and precipitation.

Table 2.3 Significant Pearson's correlation coefficients ($p < 0.05$) for relationships between dissolved organic carbon (DOC), total dissolved nitrogen (TDN), nitrate (NO_3-N) and dissolved organic nitrogen (DON) and the explanatory variables included in the analysis for all samples taken at the 16 sampling sites in the South-West Mau, Kenya, in February 2015 and February/March 2016.

	n	Stream temp.	Specific discharge	Precipitation	Elevation	Area	Drainage density	Topographical wetness index	Tree cover
DOC	77	n.s.	-0.589^{***}	n.s.	0.727^{***}	0.641^{***}	n.s.	0.263^{*}	-0.496^{***}
TDN	77	0.341^{**}	n.s.	n.s.	-0.359^{**}	n.s.	-0.275^{*}	0.433^{***}	-0.284^{*}
NO_3-N	75	0.419^{***}	n.s.	n.s.	-0.343^{**}	-0.287^{*}	-0.301^{**}	0.414^{***}	-0.296^{*}
DON	75	n.s.	-0.389^{**}	-0.684^{***}	n.s.	n.s.	n.s.	n.s.	n.s.

* $p < 0.05$; ** $p < 0.01$; *** $p < 0.001$; n.s. = not significant ($p \geq 0.05$).

2.3.3 Explaining stream water chemistry

A model including area, precipitation in the six weeks before the sampling campaign, specific discharge, TWI and drainage density explained 70.3% of the variation in DOC concentrations ($p < 0.001$; Table 2.4). The most important variables were catchment area and specific discharge, which together explained 59.1% of the variance (Figure 2.3).

Elevation and tree cover were both included in the models predicting TDN and NO_3-N concentrations in stream water. Whereas these are the only selected variables for TDN, explaining 78.2% of TDN variation ($p < 0.001$), stream water temperature, area and specific discharge were also included in the model for NO_3-N. However, elevation and tree cover were also the most important variables for NO_3-N, explaining 12.5 and 47.3% of the variation, respectively. Precipitation, specific discharge and tree cover explained 53.1% of variation in DON concentrations ($p < 0.001$), but the contributions of tree cover (3.6%) and specific discharge (4.8%) are very small compared to precipitation (46.7%).

Table 2.4 Coefficients and standardised beta coefficients (in parentheses) of significant variables ($p < 0.01$) included the multiple linear regression models for dissolved organic carbon (DOC), total dissolved nitrogen (TDN), nitrate (NO_3-N) and dissolved organic nitrogen (DON) concentrations in stream water, based on data collected in the South-West Mau, Kenya, during five sampling campaigns in February 2015 and February/March 2016.

Variable	ln DOC	ln TDN	ln NO_3-N	DON
Stream temperature			0.050^{***}	
			(0.181)	
ln Specific discharge	-0.246^{***}		0.293^{***}	-0.059^{**}
	(−0.629)		(0.326)	(−0.389)
ln Precipitation	0.103^{***}			-0.048^{***}
	(0.459)			(−0.563)
Elevation		-0.002^{***}	-0.002^{***}	
		(−1.221)	(−0.826)	
Area	0.008^{***}		-0.008^{***}	
	(0.607)		(−0.291)	
Drainage density	-1.130^{***}			
	(−0.274)			
Topographical wetness index	-12.987^{***}			
	(−0.396)			
ln Tree cover		-0.380^{***}	-0.579^{***}	0.041^{***}
		(−1.178)	(−1.245)	(0.438)
Constant	4.353^{***}	6.686^{***}	5.903^{***}	0.323^{***}
Adj. R^2	0.703	0.766	0.869	0.531
Overall model p	< 0.001	< 0.001	< 0.001	< 0.001
n	77	77	75	75

** $p < 0.01$; *** $p < 0.001$

2.4 Discussion

2.4.1 Variation in DOC

The DOC concentrations in our natural forest (NF) and smallholder (SHA) catchments are similar to those found in the tropical montane forests in the Aberdare Mountains in central Kenya (Bouillon et al., 2009), the forest and agricultural areas in the Transmara block of the Mau Forest Complex (Masese et al., 2017), and in the tropical rain forest and catchments dominated by maize cultivation in western Kenya (Recha et al., 2013; Table 2.5).

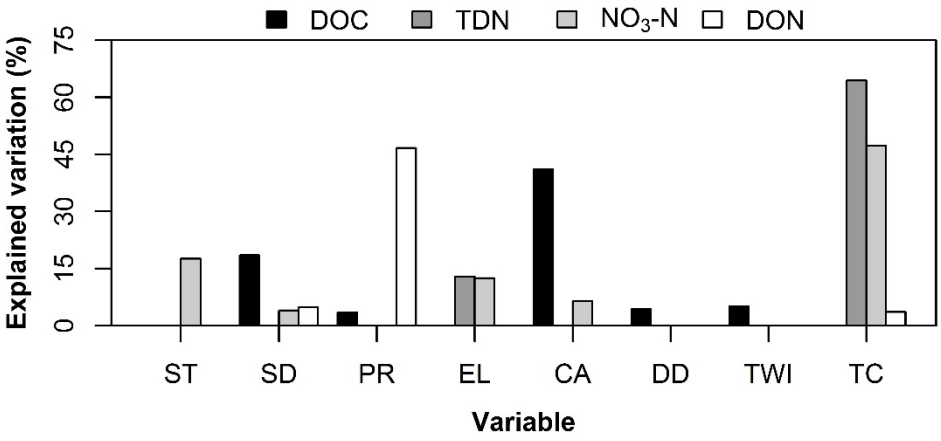

Figure 2.3 Percentage of variation in dissolved organic carbon (DOC), total dissolved nitrogen (TDN), nitrate (NO_3-N) and dissolved organic nitrogen (DON) explained by the different variables included in the multiple regression models, based on partial R^2. ST = stream temperature, SD = specific discharge, PR = precipitation, EL = elevation, CA = catchment area, DD = drainage density, TWI = topographical wetness index and TC = tree cover.

Despite the similarity with values found in other Kenyan case studies, DOC concentrations in our forest catchments (1.53±0.43 mg l^{-1}) were lower than those measured in small headwater catchments in a tropical montane forest in Ecuador (Goller et al., 2006), and in Peru (Saunders et al., 2006; Table 2.5). This difference could be related to sampling conditions, since our values represent baseflow, while the concentrations reported by Goller et al. (2006) and by Saunders et al. (2006) represented different flow conditions throughout the year. Similar to our study, Goller et al. (2006) found that stream water DOC concentrations were positively related to rainfall, potentially through flushing of soluble organic compounds from the organic layer, which can explain the higher values found in their study. Furthermore, the catchments in our study were on average > 10 times larger, suggesting a longer transit time and therefore a higher possibility for sorption of DOC to soil particles before reaching the stream, resulting in lower stream concentrations. However, this contradicts the results of our multiple regression analysis, which showed a strong positive effect of catchment area.

The negative effect of discharge on DOC in our study cannot be attributed to dilution by rainfall, because sampling was carried out during baseflow. The effect observed here most likely reflects land use, because the lowest specific discharge was found in the SHA catchments, which exhibit the highest DOC concentrations, whereas higher specific discharge and lower DOC concentrations were found in the TTP catchments. Reduced

infiltration rates were observed in croplands (40.5±21.5 cm h^{-1}), pastures (13.8±14.6 cm h^{-1}) as well as commercial tea plantations (43.3±29.2 cm h^{-1}) compared to natural forest (76.1±50.0 cm h^{-1}) in our study area (Owuor et al., 2018), which could result in lower specific discharge during baseflow, due to decreased replenishment of groundwater during the wet season. Furthermore, the SHA catchments received on average 52.9±15.7% and 57.0±11.7% less precipitation in the six weeks before each sampling campaign than NF and TTP catchments, respectively.

Despite the significant negative correlation between DOC concentrations and tree cover, only the commercial tea and tree plantation (TTP) catchments had significantly lower DOC concentrations ($p < 0.05$). Most of the biomass produced in the TTP catchments is harvested (both tea and timber) and is therefore not available for decomposition and eventual export as DOC in the streams, which could explain lower DOC concentrations in the TTP catchments. However, a catchment dominated by an agro-forestry cacao plantation in northeast Brazil showed higher DOC concentrations (4.1 mg l^{-1}) compared to tropical sub-montane forest (2.6 mg l^{-1}) during baseflow (Da Costa et al., 2017). Also Brazilian catchments dominated by sugar cane production exhibited higher DOC concentrations (2.23–3.44 mg l^{-1}) than catchments with natural Cerrado savannah or Eucalyptus plantations (1.38–1.71 mg l^{-1}) (Da Silva et al., 2007). This could be due to soil management practices such as ploughing or harvesting that stimulate mobilization of the organic C pool in the soil (Nosrati et al., 2012). Less shading of streams in the SHA catchments due to degraded riparian vegetation could lead to increased in-stream productivity as an effect of higher light-availability for primary producers. Furthermore, the SHA catchments receive manure inputs due to livestock watering, whereas this is not the case in the NF and TTP catchments. Direct inputs from livestock drinking from the streams or disturbance of river banks and stream bed sediment through human and animal activity could have resulted in higher DOC concentrations in the SHA catchments during baseflow.

Table 2.5 Studies reporting concentrations for dissolved organic carbon (DOC), total dissolved nitrogen (TDN), nitrate (NO_3-N) and dissolved organic nitrogen (DON) in Kenyan headwater streams, tropical montane forest streams and selected tropical lowland forest streams (and paired catchments with different land use) worldwide. Values represent reported mean (±SD when available) concentrations. When means for several catchments with the same land use were reported, the range of means for that particular land use is given instead.

Source	Location	Study period	Coordinates	Land use	Elevation *m*	Area *km²*	*n*	DOC *mg C l⁻¹*	TDN *mg N l⁻¹*	NO_3-N *mg N l⁻¹*	DON *mg N l⁻¹*
Current study	Sondu Basin, South-West Mau, Kenya	Feb 2015, Feb/Mar 2016	0°32' S, 35°22' E	Montane forest	2177–2269	9.5–46.0	30	1.53±0.43*	0.55±0.15*	0.30±0.08*	0.26±0.16*
			0°25' S, 35°29' E	Agriculture	2445–2651	7.7–103.7	32	2.09±0.65*	0.82±0.13*	0.57±0.17*	0.24±0.14*
			0°30' S, 35°14' E	Tea and tree plantation	1949–1992	4.3–33.2	15	1.00±0.25*	1.80±0.50*	1.62±0.60*	0.20±0.15*
Headwater catchments in Kenya											
Bouillon et al. (2009)	Aberdare Mountains, Tana River Basin, Kenya	Feb 2008	n.a.	Montane forest	2010–3020	n.a.	4	0.67–2.48*	n.a.	0.02–0.19*	n.a.
	Mount Kenya, Tana River Basin, Kenya		n.a.	Agriculture	1350–1590	n.a.	5	0.29–1.21*	n.a.	0.08–0.80*	n.a.
Kilonzo et al. (2014)	Upper Mara Basin, Mau Forest, Kenya	Feb–Apr 2011	1°2'15.2" S, 35°14'31.7" E	Montane forest and agriculture	1800–3000	n.a.	16	n.a.	n.a.	0.21–2.7	n.a.
Maghanga et al. (2012)	Nandi Hills, western Kenya	2004–2006	n.a.	Tea plantation	1600–2000	n.a.	90	n.a.	n.a.	0.8–2.3	n.a.
Masese et al. (2014)	Mara River Basin, Mau Forest, Kenya	Jan–Feb 2011	n.a.	Agriculture	1900–2300	n.a.	7	3.6±0.9*	1.1±0.3*	1.2±0.3*	n.a.
							7	8.1±0.92°	1.3±0.4°	1.2±0.3°	n.a
				Montane forest	1900–2300	n.a.	10	2.7±0.4*	0.3±0.2*	0.3±0.1*	n.a.
							10	3.5±0.6°	1.0±0.4°	0.3±0.1°	n.a.
				Mixed	1900–2300	n.a.	7	3.9±0.3*	1.2±0.3*	1.2±0.4*	n.a.
							7	4.2±1.23°	2.8±0.5°	1.2±0.4°	n.a.
Masese et al. (2017)	Mara River Basin, Mau Forest, Kenya	Dec 2011–Jan 2012	n.a.	Montane forest	1900–2300	2.02–59.85	19	1.7±0.4	1.2±0.5	1.0±0.4	0.2±0.1
				Mixed	1900–2300	2.02–59.85	14	1.1±0.4	1.7±1.2	1.5±1.1	0.2±0.2
				Agriculture	1900–2300	2.02–59.85	17	1.4±0.7	6.6±2.6	6.1±6.1	0.5±0.2
Mokaya et al. (2004)	Njoro River, Mau Forest, Kenya	May–Aug 2000	0°22'32" S, 35°56'18" E	Agriculture	2255	n.a.	6	n.a.	n.a.	0.36±0.06	n.a.

Source	Location	Study period	Coordinates	Land use	Elevation *m*	Area *km²*	*n*	DOC *mg C l⁻¹*	TDN *mg N l⁻¹*	NO_3-N *mg N l⁻¹*	DON *mg N l⁻¹*
Nyairo et al. (2015)	Nyangores River, Mara River Basin, Mau Forest, Kenya	n.a.	0°40'–1°02' S, 35°14'–35°28' E	Agriculture and settlement	1665–2105	n.a.	n.a.	n.a.	n.a.	0.101–0.26*	n.a.
							n.a.	n.a.	n.a.	0.147–0.274°	n.a.
	Amala River, Mara River Basin, Mau Forest, Kenya		0°45'–1°02' S, 35°14'–35°38' E	Agriculture and settlement	1665–2096	n.a.	n.a.	n.a.	n.a.	0.080–0.21*	n.a.
							n.a.	n.a.	n.a.	0.221–0.443°	n.a.
Recha et al. (2013)	Kapchorwa, Nandi County, Kenya	2006	0°10'0" N, 35°0'0" E	Rainforest	1800	0.128	12	1.31	0.49	0.4	0.1
				Maize 5 years	1800	0.144	12	1.48	0.67	0.58	0.09
				Maize 10 years	1800	0.091	12	1.47	4.83	4.71	0.1
				Maize 50 years	1800	0.100	12	1.52	4.64	4.52	0.12
Tamooh et al. (2012)	Aberdare Mountains, Tana River Basin, Kenya	Nov 2009, Jun–Jul 2010	0°21'–0°31' S, 36°40'–36°53' E	Montane forest	1991–3003	n.a.	7	1.1–3.5	n.a.	n.a	n.a.
	Mount Kenya, Tana River Basin, Kenya		0°09'–0°23' S, 37°18'–37°26' E	Montane forest	1461–2964	n.a.	5	0.6–4.1	n.a.	n.a	n.a.
Tropical montane forests and selected studies in tropical lowland forests											
Boy et al. (2008)	San Francisco catchment, Andes, Ecuador	Apr 1998–Apr 2003	4°00' S, 79°05' W	Montane forest	1900–2200	0.08–0.13	302	n.a.	n.a.	0.02–0.10*	0.10–0.17
							487	n.a.	n.a.	0.03–0.22°	0.09–0.42
Bücker et al. (2011)	San Francisco catchment, Andes, Ecuador	Apr 2007–May 2008	3°58'30" S, 79°4'25" W	Montane forest	1800–3140	1.3–4.5	n.a.	n.a.	n.a.	0.54–0.69	n.a.
				Mixed	1800–3140	0.7–76	n.a.	n.a.	n.a.	0.55–0.62	n.a.
Da Costa et al. (2017)	Northeast Brazil	21 weeks in 2012–2013	14°27'27.7" S, 39°04'17.6" W	Sub-montane forest	n.a.	0.36	16	2.6*	n.a.	n.a.	n.a.
								3.1	n.a.	n.a.	n.a.
			16°46'16.2" S, 40°01'21.2" W	Cacao plantation	n.a.	0.73	17	4.06*	n.a.	n.a.	n.a.
								13.1	n.a.	n.a.	n.a.
Da Silva et al. (2007)	Paulicéia, Santa Rita do Passa Quatro, Brazil	Jun 2005–May 2006	21°38'85" S, 47°38'09" W	Savannah	660–730	11.5	12	1.47±1.52	n.a.	0.04±0.013	n.a.
			21°39'47" S, 47°37'56" W	Savannah and Eucalyptus	660–730	17.5	12	1.71±2.02	n.a.	0.11±0.010	n.a.
	Água Santa, Santa Rita do Passa Quatro, Brazil		21°40'11" S, 47°36'87" W	Sugar cane	660–730	2.87	12	2.23±1.61	n.a.	0.55±0.16	n.a.
			22°69'55" S, 47°01'87" W	Sugar cane	660–730	12.0	12	3.44±1.30	n.a.	0.45±0.085	n.a.
	Cara Prata, Santa Rita do Passa Quatro, Brazil		21°36'51" S, 47°34'43" W	Eucalyptus	660–730	4.23	12	1.38±1.42	n.a.	0.47±0.11	n.a.

Source	Location	Study period	Coordinates	Land use	Elevation *m*	Area *km²*	*n*	DOC *mg C l⁻¹*	TDN *mg N l⁻¹*	NO_3-N *mg N l⁻¹*	DON *mg N l⁻¹*
Goller et al. (2006)	San Francisco catchment, Andes, Ecuador	May 1999–Apr 2002	4°00' S, 79°05' W	Montane forest	1900–2200	0.08–0.13	156	4.6–5.6	0.34–0.39	0.08–0.16	0.1–0.21
Gücker et al. (2016a)	20 sites on Rio das Mortas, Brazil	Mar, May, Sep, Dec 2012	n.a.	Atlantic forest	n.a.	0.08–11.9	20	0.9–4.3	n.a.	n.a.	0.065–0.23
				Pasture	n.a.	0.08–11.9	20	0.6–0.9	n.a.	n.a.	0.073–0.11
				Urban	n.a.	0.08–11.9	20	9.9–14.6	n.a.	n.a.	0.32–1.70
				Agriculture	n.a.	0.08–11.9	20	0.7–2.0	n.a.	n.a.	0.063–0.35
Martínez et al. (2009)	La Antigua, Mexico	Jul 2005–May 2006	19°05'–19°34' N, 96°06'–97°16' W	Montane forest	480–4200	n.a.	22	n.a.	n.a.	1.4±0.94	n.a.
				Coffee plantation	480–4200	n.a.	33	n.a.	n.a.	3.7±2.8	n.a.
				Grassland	480–4200	n.a.	33	n.a.	n.a.	0.3±0.19	n.a.
McDowell and Asbury (1994)	Rio Icacos, Luquillo Experimental Forest, Puerto Rico	Jun 1983–May 1986	18°15' N, 65°50' W	Rainforest	n.a.	0.162–3.26	352–477	1.36–2.13	n.a.	0.062–0.066	0.11–0.15
Neill et al. (2001)	Fazenda Nova Vida, Rondônia, Brazil	1994–1998	10°30' S, 62°30' W	Evergreen forest	200–500	n.a.	24–30	n.a.	n.a.	0.13–0.15*	0.02–0.26*
							36–40	n.a.	n.a.	0.03–0.10°	0.16–0.18°
				Pasture	200–500	n.a.	25–32	n.a.	n.a.	0.011–0.02*	0.42–0.50*
							36–44	n.a.	n.a.	0.011–0.020°	0.18–0.23°
Saunders et al. (2006)	Yanachaga-Chemillen National Park, Peru	Mar 2002–Mar 2003	10°32'45.9" S, 75°31'28.4" W	Montane forest	2414	n.a.	20	3.13±1.55*	n.a.	0.011±0.034*	0.12±0.084*
							27	n.a.	n.a.	0.024±0.020°	n.a.
Wilcke et al. (2001)	San Francisco catchment, Andes, Ecuador	Mar 1998–Apr 1999	4°00' S, 79°05' W	Montane forest	1900–2200	0.08–0.13	174	n.a.	n.a.	0.047–0.081	n.a.
Wilcke et al. (2013)	San Francisco catchment, Andes, Ecuador	Apr 1998–Dec 2010	4°00' S, 79°05' W	Montane forest	1850–2200	0.091	108	n.a.	n.a.	0.08	0.12
Yamashita et al. (2014)	Baru experimental catchment, Sabah, Borneo	Apr 2008–Dec 2011	5°01' N, 117°48.75' E	Rainforest	171–255	0.441	90	3.1	n.a.	0.12	0.11

* Concentrations measured during baseflow. ° Concentrations measured during stormflow. n.a. = Data not provided.

TWI was negatively correlated to DOC concentrations. High TWI values are indicative of shallow groundwater table and higher soil moisture (Rodhe and Seibert, 1999). Therefore, areas with high TWI can represent wetland areas that can act as source of DOC, since waterlogged or poorly drained soils are usually rich in DOC (Kalbitz et al., 2000). However, the negative relationship between TWI and DOC found here, contradicts the common finding that wetland areas significantly increase DOC concentrations in streams (Chapman et al., 2001; Monteith et al., 2015). The range of TWI values for all catchments was very narrow, which could also explain why the expected positive correlation was not found. Moreover, as water samples were taken during dry season, the effect of wetlands was potentially limited due to a lack of hydrological connectivity.

Because TWI is strongly negatively correlated to slope ($r = -0.959$, $p < 0.05$), it is also possible that the significant effect is caused by a positive effect of slope rather than a negative effect of TWI itself. Steeper slopes often promote overland flow, especially in managed catchments, which could be an important source of DOC in stream water. However, the range of mean slope values was small (7.43%–13.5%) and such effect would not be visible during baseflow.

Soil type and texture have been found to be relevant predictors of in-stream DOC concentrations. Billett et al. (2006) identified, for example, that soil C stocks are related to DOC concentrations in stream water, though the relationship is complex and does not hold in small catchments. Since stocks of soil organic carbon (SOC) were higher in forest soils compared to agricultural soils in neighbouring part of the Mau Forest (Were et al., 2016), this could explain the higher DOC concentrations in streams in the NF catchments than in TTP catchments. We also noticed that catchments with mollic Andosols as dominant soil type (SHA3−5) showed significantly higher DOC concentrations ($p < 0.001$) than the catchments dominated by humic Nitisols when controlling for land use. Both soil types, but especially Andosols, are characterised by high organic matter content. These soils also contain iron ($Fe^{2+/3+}$) or aluminium (Al^{3+}), which strongly bind organic matter, making the organic matter difficult to mobilise. However, increased mobilization and loss of soil organic carbon from forest soils converted to agriculture is commonly found in Andosols (Covaleda et al., 2011; Were et al., 2013), which could lead to increased DOC concentrations in stream water. This implies a potential role of soil type or geology on stream water DOC concentrations. More data on soil organic matter

content, C and N stocks is required to confirm this hypothesis, but this data was not available for our study area.

2.4.2 Variation in dissolved nitrogen fractions

Total dissolved nitrogen (TDN) concentrations in the NF catchments were higher than found in tropical montane forest in Kenya (Masese et al., 2014) and Ecuador (Goller et al., 2006), whereas the values found in SHA and TTP catchments were lower than in agricultural areas in the Mara Basin, Kenya (Masese et al., 2017, 2014; Table 2.5). Conversely, nitrate (NO_3-N) concentrations in smallholder areas in the Eastern Mau (Mokaya et al., 2004) and Mara River Basin, Kenya (Kilonzo et al., 2014; Nyairo et al., 2015) were slightly lower than in our SHA catchments. The mean NO_3-N concentration in the TTP catchments was in the range of values found in stream water of a catchment dominated by commercial tea plantations in Nandi, Kenya (Maghanga et al., 2012). NO_3-N concentrations in the natural forest were high compared to values observed in tropical montane forests elsewhere, whereas dissolved organic nitrogen (DON) concentrations were similar (Table 2.5).

Dissolved organic N has been neglected in water quality research for a long time, the focus being on inorganic N forms such as ammonium and particularly NO_3-N, which usually dominate N exports from temperate areas in the Northern Hemisphere (Breuer et al., 2015; Perakis and Hedin, 2002; van Breemen, 2002). Similar to our results, many studies show higher contributions of DON to TDN in natural catchments compared to managed catchments, e.g. 16.7% in natural forest compared to 7.6% in smallholder catchments in the Mara Basin, Kenya (Masese et al., 2017) and 20.4% in tropical rainforest versus 2.1–13.4% in maize cultivated catchments in western Kenya (Recha et al., 2013).

Our study found that elevation and tree cover explained 78.2% and 59.8% of the variance in TDN and NO_3-N concentrations in stream water, respectively. Elevation probably indicates an effect of land use, since the land use types in the studied catchments were highly stratified by elevation. The inclusion of tree cover is also a strong indicator that land use plays a major role in determining stream water TDN and NO_3-N concentrations, since the three land uses studied here have distinctively different mean tree cover (NF = 97.6±1.4%, SHA = 4.5±2.4% and TTP = 28.5±9.7%, $p < 0.001$). Furthermore, areas under high tree cover receive less or no fertilizer compared to crops and tea plantations.

Commercial tea fields receive 4–10 times more N ha^{-1} than smallholder agriculture, although the difference is less (1–3 times) for smallholder farms where tea is grown, and the natural forest does not receive any fertilizer inputs. This is likely to result in differences in N inputs to surface water and thus higher TDN and NO_3-N concentrations.

The land use effect observed in this study agrees with findings of a study in southwest China, where catchments dominated by rubber plantations depicted higher TDN and NO_3-N concentrations compared to rainforest catchments (Li et al., 2016). Furthermore, Biggs et al. (2004) found up to 4 times higher TDN concentrations in deforested catchments in the Brazilian Amazon, with the effect being strongest in catchments with > 66–75% deforestation. Conversion of montane forest to coffee plantations increased NO_3-N concentrations from 1.4 to 3.7 mg N l^{-1} (Martínez et al., 2009). An exception to this is conversion of forest to pasture, which often leads to a reduction in NO_3-N concentrations in stream water (Martínez et al., 2009; Neill et al., 2001).

Despite a significant difference ($p < 0.005$) in DON contribution to TDN in stream water between land use types, with contributions up to 72% in the NF catchments, DON concentrations were similar in all three land use types. This agrees with findings by Gücker et al. (2016b) in a transition zone between the Brazilian Cerrado savannah and the Atlantic rain forest in Brazil, Neill et al. (2001) in the Brazilian Amazon and Recha et al. (2013) in Kenya. Nevertheless, the stepwise linear regression model included percent tree cover as significant variable, although it only explains 3.6% of the variation in DON concentrations. Tree cover could affect DON concentrations through differences in quantity, quality and composition of organic material in the litter layer and soil compared to tea and crop cover, which would influence the availability of DON for export in stream water.

We found a positive relationship between NO_3-N concentrations and specific discharge, which is most likely related to land use, as was suggested in Section 2.4.1 for DOC concentrations. However, specific discharge negatively affected DON concentrations. Due to the lack of difference in DON concentrations between the three land uses, it is unlikely that this reflects a land use effect. Furthermore, 46.7% of the variance in DON concentrations was explained by precipitation in the six weeks preceding the sampling campaigns, suggesting an influence of precedent wetness conditions in the catchments on DON concentrations in the stream. The negative effect of both specific discharge and

precipitation indicates that dryer conditions stimulate DON export. Zhang et al. (2016) found that DON concentrations in soil and stream water are strongly related across different climates. This implies that DON concentrations in the soil are also higher under dry conditions, which could be a consequence of reduced mineralization of organic matter.

Stream water temperature is known to have a positive effect on organic matter decomposition, ammonification and nitrification, i.e. the source process of NO_3-N (Warwick, 1986), which could explain the positive result and correlation between NO_3-N concentration and stream water temperature. Diurnal variations in parameters such as solar radiation and stream temperature can also cause diurnal variation in stream solute concentrations, through influence on in-stream processing of these solutes. This occurs especially in shallow, less-shaded streams (Nimick et al., 2011). Diurnal variation will therefore be more pronounced during baseflow. Since all TTP sites were sampled in the afternoon, this could have resulted in a significantly higher mean stream water temperature in these catchments compared to other sites and thus also higher NO_3-N concentrations through organic matter decomposition. However, it is more common to observe lower NO_3-N concentrations in the afternoon, due to enhanced uptake for in-stream photosynthetic activity (Rusjan and Mikoš, 2010). The coincidence of afternoon sampling of TTP catchments with significantly higher stream water temperatures and higher NO_3-N concentrations, could also explain the positive relationship with stream temperature. Nevertheless, NO_3-N concentrations and stream water temperature also show a significant positive relationship for the TTP catchments alone ($r = 0.678$, $p < 0.05$). Shading of the streams by riparian forests is unlikely to have affected stream temperatures in this study, because mean stream water temperature in the SHA catchments, with the most degraded riparian forests, was not significantly different from the mean temperatures found in the NF and TTP catchments ($p > 0.05$). Furthermore, stream water temperatures in well-shaded NF catchments and less-shaded SHA catchments were similar for sites sampled at the same time of the day.

2.4.3 Interactions between the C and N cycles

Despite the distinctly different drivers for DOC and dissolved N fractions observed in this study, the C and N cycle are not completely independent. Several studies in temperate regions observed a significant positive relationship between DOC and DON (e.g.

Chapman et al., 2001; Hood et al., 2003; Kaushal and Lewis, 2003; Willett et al., 2004), but our data showed no correlation between the two variables ($r = 0.06$, $p > 0.05$). This could be a result of the low use of N fertilizer and the tendency of soil N mining in our study area (Zhou et al., 2014) or different relationships between the two fractions in catchments with different dominant land use. Nevertheless, both dissolved organic C and N concentrations were more influenced by natural than anthropogenic drivers.

Other interactions between the C and N cycles are related to the N inputs and its effect on primary productivity. Nosrati et al. (2012) mention increased organic matter production, utilization of organic fertilizers and increased in-stream productivity due to increased nutrient input as potential causes for such increases in stream water DOC concentrations. It is unlikely that increased nutrient inputs to the stream affected in-stream DOC production and thus DOC concentrations in our study area, because the TTP catchments with the highest nutrient inputs showed lowest DOC concentrations in stream water. On the other hand, there is also evidence that increased soil N-inputs decrease DOC release rates in the soil due to increased microbial metabolism (Gundersen et al., 1998), although results of lab and field studies are not consistent (Kalbitz et al., 2000). This potentially results in reduced stream water DOC concentrations catchments with high fertilizer inputs, which could be a reason for the lower DOC concentrations observed in the TTP catchments. If this mechanism applies here, it implies that DOC concentrations are indirectly affected by land use as well.

2.4.4 Implications for downstream regions

The Sondu River basin studied in this paper eventually discharges into Lake Victoria, which is largely N limited. Since 22%–32.7% of all N inputs to the lake are from riverine origin, large-scale changes in land use could lead to a significant increase in N inputs (Scheren et al., 2000; Zhou et al., 2014). However, despite the significantly higher TDN and NO_3-N concentrations found in non-forest catchments, the effect of land use in the headwaters on the concentration of these solutes downstream is most likely reduced through mixing of water from other catchments. A simple estimation of solute concentrations at the outlet of the Sondu basin, using means of specific solute loads and specific discharge weighted by relative catchment area covered by the three land use types (23% for forest, 68% for smallholder agriculture and 9% for commercial tea and tree plantations, based on the 2013 land use map) reveals that estimated TDN and NO_3-N

concentrations during baseflow (0.90 and 0.74 mg N l^{-1}, respectively) are similar to those of the SHA catchments. Although this is a coarse estimate, it suggests that areas with higher N-export are buffered by the low N-export from forested areas, as long as a substantial forest area remains. Biggs et al. (2004) observed, for example, that TDN concentrations increased in catchments with > 66–75% deforestation. Reduced baseflow and precipitation as consequence of large-scale deforestation (Lawrence and Vandecar, 2015) could also reduce this buffering effect. Further deforestation of the South-West Mau would therefore increase TDN and NO_3-N concentrations during baseflow.

The results of this study cover baseflow conditions only, which occur two to three months per year. During high flow, solute concentrations can increase through mobilization of solutes stored in the topsoil (Creed and Band, 1998) and overland flow, or decrease through dilution. In case of increased mobilization, the difference in TDN and NO_3-N concentrations between the land use types can be amplified during stormflow, because of higher N-availability through fertilizer inputs. Conversely, dilution by increased discharge in combination with mixing with water from forested catchment could further reduce the land use effect on the scale of the Sondu basin. However, the lack of reliable knowledge on the behaviour of nitrate and discharge within the Sondu basin, does not allow extrapolation of our results to periods of stormflow.

2.4.5 Conclusions

This study found a significant effect of land use on TDN and NO_3-N, which agrees with results of many other studies, emphasizing the importance of good land management to reduce N inputs and risks to surface water eutrophication.

Although we found lower DOC concentrations in the tea catchments and a small but significant effect of tree cover on DON, it appears that DOC and DON fractions were more controlled by natural factors than by land use. Both fractions showed an influence of hydrological regime through precipitation and specific discharge, whereas catchment area, topographical wetness index and drainage density were also important drivers for DOC concentrations. Although both models explain the majority of variation in DOC and DON concentrations in stream water, the inclusion of soil properties, such as soil organic matter content and C and N stocks, could increase model performance for both fractions, since many studies identified these as relevant predictors. However, this information was not available for our study area at the time. In addition, sampling throughout different

seasons could further increase our understanding of the role of land use versus physical catchment characteristics and weather variables in determining water quality, because a potential effect of variations in dominant flow paths might be observed.

Some previous studies in East Africa looked at anthropogenic effects on water quality. This study is the first that looks into the role of land use and other catchment characteristics on concentrations of dissolved carbon and nitrogen. These results can help to unravel the complex relationships between these drivers and to identify areas of research that will increase our understanding of the processes behind nutrient cycling in these tropical environments.

Acknowledgements

This work was funded by the CGIAR programme on Forest, Trees and Agroforestry led by the Centre for International Forestry Research (CIFOR). We thank the Deutsche Forschungsgemeinschaft DFG (BR2238/23–1), and the Deutsche Gesellschaft für Internationale Zusammenarbeit GIZ (Grant 81195001) for generously providing additional funding. Additional funding for SJ and KBB was provided by the Helmholtz Association in its ATMO programme and its impulse and networking fund.

3 Using high-resolution data to assess land use impact on nitrate dynamics in East African tropical montane catchments

This chapter is accepted for publication in *Water Resources Research* as:

Jacobs, S. R., Weeser, B., Guzha, A. C., Rufino, M. C., Butterbach-Bahl, K., Windhorst, D. and Breuer, L., 2018. Using high-resolution data to assess land use impact on nitrate dynamics in East African tropical montane catchments. Water Resources Research, doi:10.1002/2017WR021592.

3.1 Introduction

Nitrogen (N) is a key element in terrestrial and aquatic ecosystems and plays an essential role in many biogeochemical processes, including primary productivity. Although organic N frequently constitutes a significant amount of total N export in temperate and tropical rivers (Alvarez-Cobelas et al., 2008; Gücker et al., 2016b; Lewis et al., 1999), nitrate (NO_3-N) is more commonly studied due to its relative ease to measure compared to other forms of N, as well as its strong relation to human activity (Caraco and Cole, 1999). The latter makes it a suitable parameter to assess anthropogenic impacts on catchment water quality and biogeochemistry. The effect of land use on nutrient concentrations in tropical streams, and in particular NO_3-N, has been assessed in the past using spatial sampling campaigns (e.g. Biggs et al., 2004; Deegan et al., 2011; Gücker et al., 2016b; Jacobs et al., 2017; Li et al., 2016), or low frequency monitoring of streams with contrasting land use (Lin et al., 2015; Neill et al., 2001; Ribeiro et al., 2014; Williams and Melack, 1997). Although such studies have provided valuable information on the potential effects of land use on nutrient concentrations, high-frequency long-term time series, facilitated by recent advances in *in situ* sensor technology, are required to obtain detailed information to quantify complex and highly responsive nutrient dynamics in

streams (Blaen et al., 2016; Bowes et al., 2009; Burt, 2003; Kirchner et al., 2004; Rode et al., 2016).

In the case of NO_3-N, such high-frequency data have been used in temperate regions to improve load estimates (Ferrant et al., 2013; Fogle et al., 2003; Pellerin et al., 2014; Rozemeijer et al., 2010), to identify NO_3-N sources (Bowes et al., 2015), to assess responses to rainfall events and hysteresis (Dupas et al., 2016; Lloyd et al., 2016a; Sherson et al., 2015), diurnal nutrient cycling patterns (Aubert et al., 2013; Aubert and Breuer, 2016; Halliday et al., 2013, 2012; Pellerin et al., 2009), responses to disturbances (Sherson et al., 2015), and nutrient dynamics in general (Bende-Michl et al., 2013; Halliday et al., 2013, 2012; Neal et al., 2012). Furthermore, *in situ* instruments can also be used to identify 'hot moments' in nutrient concentrations and export. 'Hot moments' are short periods with enhanced biogeochemical activity (Bernhardt et al., 2017; McClain et al., 2003). Such short-lived events can be easily missed in monitoring programs based on grab sampling, but can still contribute significantly to total stream nutrient export. In contrast to temperate regions, there are very few examples in the tropics whereby *in situ* sensors for high-frequency measurements have been deployed (e.g. Waterloo et al., 2006; Zuijdgeest et al., 2016), and no such studies have been done in East Africa. The tropics generally receive less attention in water quality research compared to the temperate zone, yet tropical countries face higher rates of deforestation and land use change. Additionally, due to differences in climate, seasonality and soil types, which influence hydrological and biogeochemical processes, it is unlikely that knowledge obtained from temperate studies can directly be transferred to the tropics. Therefore, additional research is required to increase our understanding of the effect of land use change on water quality and discharge in tropical, and especially tropical montane regions, since these are generally key sources of fresh water (Bruijnzeel, 2001; Célleri and Feyen, 2009). Furthermore, understanding processes and dynamics of water and solutes, especially by comparing multiple catchments, is essential to increase our understanding of general catchment ecohydrology, which will improve our ability to model and predict nutrient dynamics and transport (Abbott et al., 2016).

The Sondu River is one of the twelve major rivers originating in the Mau Forest Complex, Kenya's largest remaining tropical montane forest and a water source for about 5 million people (UNEP et al., 2008). The forest is under significant human pressure through

encroachment of smallholder farms, illegal tree logging, charcoal burning and grazing, which resulted in a 25% forest loss between 1973 and 2013 (Kinyanjui, 2011; Swart, 2016). Additionally, part of the area has been converted to commercial tea plantations during the 20th century. These changes have led to differences in soil hydraulic properties (Owuor et al., 2018), likely affecting NO_3-N inputs to the stream through changes in flow paths, like increased surface runoff, also referred to as overland flow (Mitchell, 2001). Intensive use of fertilizers specifically by commercial tea plantations, could have led to increased NO_3-N concentrations in the soil, leaching and subsequent sub-surface flow to the stream, depending on the connectivity of the NO_3-N store to the stream (Musolff et al., 2015). Differences in soil C and N stocks as well as gaseous N losses observed for the different land use types in the area by Arias-Navarro et al. (2017b) and Chiti et al. (2018) suggest that land use has strongly affected biogeochemical processes. Moreover, these studies indicate that land use change modified the dynamics of soil organic N and C decomposition, nitrification and denitrification, and soil temperature, soil pH and soil aeration.

The objective of this study was to understand the processes driving stream water NO_3-N dynamics in this tropical montane ecosystem and how these dynamics are affected by land use. We used a 2-year high-resolution dataset from three sub-catchments (27–36 km^2) dominated by either natural forest, smallholder agriculture or commercial tea and tree plantations to investigate: (a) seasonal patterns in stream water NO_3-N concentration and loading, (b) solubility, reactivity and source dynamics of NO_3-N through assessment of concentration-discharge relationships (Moatar et al., 2017; Musolff et al., 2015), (c) flow paths and NO_3-N sources through the analysis of responses to storm events (Dupas et al., 2016; Evans and Davies, 1998), and (d) occurrence of 'hot moments' in NO_3-N concentrations and export. We compared the patterns for the sub-catchments to those observed downstream at the outlet of the main catchment (1,021 km^2), to estimate how NO_3-N responses to land use are reflected at a larger scale. We hypothesized that groundwater is the main source of NO_3-N in stream water and, consequently, that leaching of fertilizer inputs leads to increased NO_3-N concentrations and loads in the tea plantations and smallholder agriculture sub-catchments. Furthermore, we hypothesized that surface runoff occurs more frequently in non-forested catchments, resulting in dilution of NO_3-N concentrations during rainfall events.

3.2 Methods

3.2.1 Study area

This study focuses on the catchment of the Chemosit River in the South-West Mau, a tributary of the Sondu River, which drains into Lake Victoria (Figure 3.1). The elevation in the Chemosit catchment ranges from 2,932 m on top of the Mau Escarpment to 1,715 m at the outlet. The landscape is characterized by three main land use types: natural forest (NF), smallholder agriculture (SHA) and commercial tea and tree plantations (TTP). The upper part of the catchment, above 2,400 m elevation, is dominated by smallholder agriculture. Farmers grow maize, beans, potatoes and cabbage on plots of less than 2 ha. Fertilizer application rates are usually below 20 kg N ha^{-1} yr^{-1}. Crop fields are alternated with pastures for cattle grazing and woodlots of Eucalyptus, Cypress and Pine. In most places the riparian zones are severely degraded.

Natural forest vegetation is mainly found between 1,900 and 2,400 m elevation and is classified as Afromontane mixed forest (Kinyanjui, 2011), changing to montane bamboo forest above 2,300 m. At lower elevation, the landscape is dominated by smallholder farms in the south and by commercial tea plantations in the west. The latter consist of a mosaic of tea fields and Eucalyptus and Cypress plantations to supply the tea factories with fuel wood and timber. Riparian forest strips of up to 30 m width within the commercial tea plantations are well maintained. Fertilizer is applied to tea fields by airplane in pellet form at 150 to 250 kg N ha^{-1} yr^{-1} depending on crop demand.

Geology is fairly similar throughout the catchment, with phonolitic nephelinites dominating the upper part of the catchment with a variety of Tertiary tuffs (Jennings, 1971), whereas the lower part is characterized by phonolites (Binge, 1962). Soils are classified as humic Nitisols (ISRIC, 2007). The long-term (1905–2014) annual rainfall is 1988±328 mm at 2,100 m elevation (Jacobs et al., 2017). Most of the rain falls between April and July (long rainy season) and between October and December (short rainy season). January to March are the driest months. Catchment characteristics and annual precipitation during the study period are shown in Table 3.1. A more detailed description of the study area can be found in Jacobs et al. (2017).

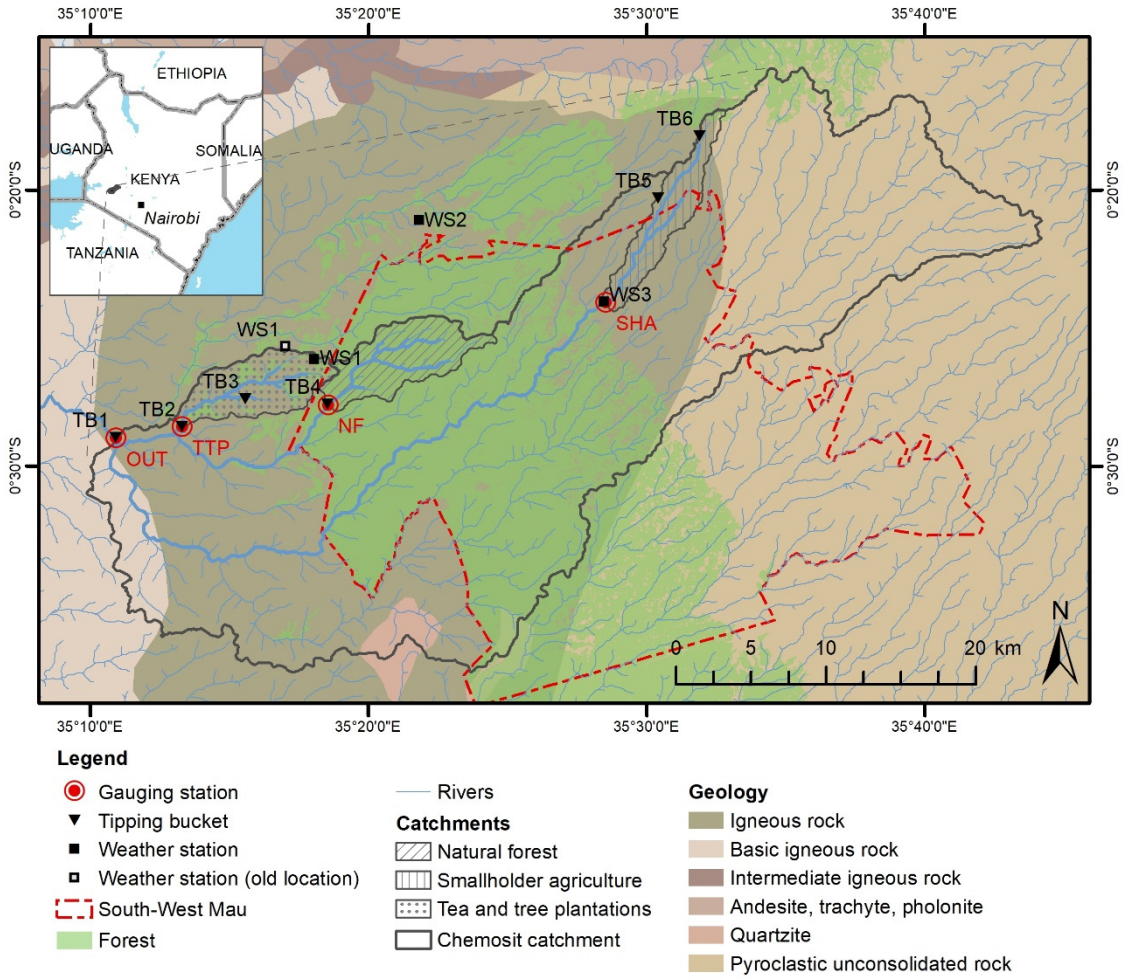

Figure 3.1 Map of the study area, geology and location of the automatic measurement systems (OUT = main outlet, TTP = commercial tea and tree plantations, NF = natural forest, SHA = smallholder agriculture), tipping buckets (TB1–6) and weather stations (WS1–3) in the South-West Mau, Kenya. Monitored rivers indicated with bold lines join at the main outlet (OUT). Geology data is from the Soil and Terrain database for Kenya (KENSOTER) version 2.0 (ISRIC, 2007).

Table 3.1 Characteristics and precipitation[a] data of the three sub-catchments and the main catchment in the South-West Mau, Kenya.

Catchment	Area	Elevation	Mean±SD slope	Precipitation 2015	Precipitation 2016
	km²	*m*	*%*	*mm yr^{-1}*	*mm yr^{-1}*
Natural forest (NF)	35.9	1,954–2,385	15.5±8.0	2,034	1,895
Smallholder agriculture (SHA)	27.2	2,380–2,691	11.5±6.5	1,630	1,373
Tea/tree plantations (TTP)	33.3	1,786–2,141	12.2±7.3	1,934	1,667
Main catchment (OUT)	1,021.3	1,715–2,932	12.8±7.7	1,832	1,648

[a] Annual precipitation for 2015 and 2016 is based on data from six tipping buckets and three weather stations across the main catchment as indicated in Figure 3.1.

3.2.2 Instrumentation

Automatic measurement systems

We used a nested approach, whereby three sub-catchments of 27–36 km² were selected within the Chemosit catchment, based on (a) dominant land use, (b) comparability of geological substrate, (c) security of equipment, and (d) accessibility (Table 3.1; Figure 3.1). The identified sites, i.e. the natural forest (NF), smallholder agriculture (SHA) and tea and tree plantation (TTP) sub-catchments, were instrumented with an automatic measurement system at the start of the short rainy season in October 2014. The outlet of Chemosit catchment, from now on referred to as the main catchment (OUT), was instrumented at the end of the dry season in April 2015.

Each automatic system recorded water level with a radar-based sensor (VEGAPULS WL61, VEGA Grieshaber KG, Schiltach, Germany) with a resolution of < 1 mm and a measurement accuracy < 2 mm. Water level data was complemented with regular discharge measurements using the salt dilution method with slug injection (Moore, 2004), an Acoustic Doppler Velocimeter (ADV; FlowTracker, SonTek, San Diego CA, USA) or an Acoustic Doppler Current Profiler (ADCP; RiverSurveyor S5, SonTek, San Diego CA, USA) depending on river size and discharge to develop a rating curve (see Section 3.2.4). Nitrate (NO_3-N) concentrations were measured *in situ* using UV/Vis spectroscopy (spectro::lyser, s::can Messtechnik GmbH, Vienna, Austria). NO_3-N data were calibrated using reference grab samples (see Section 'Reference grab samples and calibration'). To reduce the influence of sediment and debris, the submerged sensors were cleaned automatically with a pulse of compressed air before each measurement. Although the cleaning system greatly reduced sedimentation on the sensor windows, additional weekly manual cleaning was necessary to remove biofouling. The instruments ran on solar power and measured all parameters at a 10-minute interval.

Reference grab samples and calibration

Weekly or bi-weekly reference stream water samples were taken from all sites for calibration. Flow conditions during sampling covered 71 to 82% of the observed discharge range, missing high flows during storm events. Samples were drawn from the stream using a 60 ml syringe pre-rinsed with stream water. The water was then filtered through a 0.45 µm polypropylene filter (Whatman Puradisc 25 syringe filter, GE Healthcare, Little Chalfont, UK or KX syringe filter, Kinesis Ltd., St. Neods, UK) and

collected in clean 100 ml HDPE bottles. The bottles were transported in a cooler box with ice and frozen at −20°C until final analysis for NO_3-N using ion chromatography (ICS-2000, Dionex, Sunnyvale CA, USA) and total dissolved nitrogen (TDN; TOC cube, Elementar Analysensysteme GmbH, Hanau, Germany) in the laboratory of Justus Liebig University Giessen, Germany. A linear regression model between field and laboratory measurements was used for calibration of the field data for each site.

Rainfall data

Rainfall was measured with tipping buckets at nine locations (TB1–6: Theodor Friedrichs, Schenefeld, Germany, and WS1–3: ECRN-100 high resolution rain gauge, Decagon Devices, Pullman WA, USA; Figure 3.1), recording cumulative rainfall every 10 minutes. WS1 had to be relocated in September 2015 due to construction activities on site. For each catchment, rainfall was calculated by weighting the data from relevant tipping buckets using Thiessen polygons. Weights were adjusted when data were missing due to funnel blockage or instrument malfunctioning, omitting the tipping buckets for which no data were available (NF = 50.0%, SHA = 17.7%, TTP = 19.5% and OUT = 34.9% of time).

3.2.3 Data processing

Flagging unreliable data

A protocol was set up for the processing of all data collected by the automatic stations to ensure reproducibility (Figure 3.7). Unique flags differentiated reasons for classifying a measurement as unreliable (Table 3.4). The flags were categorized as (a) automated, when allocated automatically using a R script (Moatar et al., 2017), or (b) manual, when assigned based on log book information and field observations. A third group of flags (calculation) was added to identify measurements that were adjusted, calibrated or calculated during post-processing. In total, 4.1–7.4% and 0.1–0.4% of the data were flagged as unreliable for NO_3-N and water level, respectively (Figure 3.7).

Biofouling correction

On occasions where the automatic cleaning system failed, biofouling on the windows affected measurements by the spectro::lyser. Laboratory analyses confirmed that the measurement following manual cleaning represented the expected stream water NO_3-N concentration. These data were used to calculate a build-up rate of biofouling (0.02–0.19 mg l^{-1} day^{-1}) and to correct the measurements during periods of cleaning system failure.

Correction was necessary on one occasion for OUT (7 days) and six occasions (3–10 days) for TTP.

Outlier detection

A robust tool for outlier detection is the median absolute deviation (MAD):

$$MAD_i = b\, M_{i2}(|x_i - M_{i1}(x_i)|) \tag{3.1}$$

where x_i is the dataset for which the MAD is calculated, M_{i1} the median of dataset x_i and M_{i2} the median of the absolute deviation of the dataset from its median. Consistency constant b is included to create a robust estimator for the estimation of the standard deviation and is set to 1.4826 for a normal distribution (Leys et al., 2013).

To detect local outliers, we applied a moving window of k measurements around observation x_i at time t_i. The $MAD_{j,i}$ was calculated for observations x_j = ($x_{i-k/2}$…x_{i-1}, x_{i+1}…$x_{i+k/2}$). Measurement x_i was flagged as outlier if:

$$\left|\frac{x_i - M_{j,i}}{MAD_{j,i}}\right| > a \tag{3.2}$$

where a is the threshold for outlier selection, and $M_{j,i}$ and $MAD_{j,i}$ are the median and MAD of x_j. Because the aim was to flag values with large deviation from the remaining dataset, a conservative value of a = 6 was selected. The value of k = 16 was selected based on multiple runs with different values for a and k for NO_3-N and water level data. Outlier detection was carried out after omitting data flagged as unreliable in previous processing steps, as these data could confound the identification of potential outliers.

3.2.4 Data analysis

Discharge calculation

We developed a rating curve (second order polynomial; Figure 3.8) for each catchment using discharge measurements taken at each site over a wide range of water levels, which was then applied to the water level data to estimate discharge. The same polynomial function was used for extrapolation above the highest measured discharge, while extrapolation below the lowest measured discharge was done using a quadratic function through the lowest measured discharge and zero discharge. The rating curves were checked after their establishment by frequent discharge measurements at each site. Discharge was converted to specific discharge ($Q_{s,i}$), also referred to as specific runoff, in mm day^{-1}.

Load calculation

NO_3-N concentrations and discharge were used to calculate loads for the three sub-catchments for 2015 and 2016. For the main catchment loads were only calculated for 2016, because measurements at this site started end of April 2015. Linear interpolation was applied in gaps of ≤ 24 hours in the 10-minute time series data of NO_3-N (0.78–1.22% of data; Table 3.5). Interpolation for gaps > 24 hours (2.82–9.45% of data) was done using a smoothed dataset to minimize the influence of within-day NO_3-N variation due to rainfall events and diurnal cycling at the start and end of the data gap. For smoothing, a rolling median with a 48 h window width was selected to minimize the influence of outliers. Additionally, manual grab samples were used to interpolate data gaps. The final dataset consisted of all points for which both discharge and (estimated) NO_3-N concentration was available. Load (L_i) in g s^{-1} at time t_i was calculated using:

$$L_i = C_i Q_i \tag{3.3}$$

where C_i is the NO_3-N concentration in mg N l^{-1} and Q_i is discharge in m^3 s^{-1} at time t_i. Specific load ($L_{s,y}$) in kg ha^{-1} yr^{-1} in year y was calculated with:

$$L_{s,y} = K_2 \sum_{i=1}^{n} \left(\frac{L_i}{A} \Delta t_i\right) \tag{3.4}$$

where A is catchment area in ha, Δt_i the time interval for the observation in seconds and n the total number of observations. Constant $K_2 = 10^{-3}$ was applied to convert units from g ha^{-1} yr^{-1} to kg ha^{-1} yr^{-1}.

Uncertainty estimation

A 95% confidence interval (CI) for the linear relationship between field and laboratory measurements was used to estimate uncertainty in NO_3-N concentration. This approach considers the uncertainty in the laboratory measurements to be negligible, and treats the spectro::lyser measurements as the primary source of uncertainty. For uncertainty in discharge, we estimated the uncertainty in individual discharge and water level measurements for the rating curve based on the standard deviation (SD) of repeated measurements. Assuming that the size of the SD increases proportionally to the discharge, the SD for salt dilution measurements was 6.9%, while ADV and ADCP measurements had a SD of 4.2 and 6.2% respectively. Water level measurements had a SD of 1.0 mm. Following the procedure of McMillan et al. (2010), we assumed that the true discharge or water level value was within 3*SD from the measured value. For each combination of

water level and discharge on the rating curve, 10,000 random samples within the 3*SD uncertainty limit of water level and discharge were taken and rating curves were generated for each set of samples. The 95% CI was calculated using the empirical cumulative distribution function for discharge estimated with all 10,000 simulated rating curves.

For NO_3-N load, uncertainties in discharge and NO_3-N concentration were included:

$$\frac{\varepsilon_L}{L} = \sqrt{\left(\frac{\varepsilon_C}{C}\right)^2 + \left(\frac{\varepsilon_Q}{Q}\right)^2} \quad (3.5)$$

where ε_L is the uncertainty in the load, ε_C in concentration, and ε_Q the uncertainty in discharge.

Hysteresis analysis

Ten storm events were selected to study the response of NO_3-N concentrations to changes in discharge due to rainfall. The events represented five different periods in the year: dry season (DS), start of the long rainy season (SLR), long rainy season (LR), period of moderate rainfall between the long and short rainy season (MR) and the short rainy season (SR). Event dates were chosen based on occurrence of rainfall events in all catchments in that period and a minimum 30% increase in discharge during the event in each sub-catchment. No data were available for the dry season event in 2015 for TTP and OUT. Hysteresis patterns were assessed using plots of normalized discharge and NO_3-N concentrations:

$$P_{norm,i} = \frac{P_i - P_{min}}{P_{max} - P_{min}} \quad (3.6)$$

where $P_{norm,i}$ and P_i are the normalized and original value of the parameter at time t_i, and P_{min} and P_{max} are the minimum and maximum observed values during the event. In addition to visual assessments of hysteresis patterns and direction of hysteresis loops, we calculated the hysteresis index (*HI*) as proposed by Lloyd et al. (2016b) for every 5th percentile of the normalized discharge of the storm event:

$$HI_i = C_{norm,r,i} - C_{norm,f,i} \quad (3.7)$$

where HI_i is the hysteresis index for percentile *i,* and $C_{norm,r,i}$ and $C_{norm,f,i}$ the normalized NO_3-N concentration on the rising and falling limb for the i^{th} percentile of normalized discharge, respectively. The mean *HI* of all percentiles was used to assess hysteresis of each storm event. Negative and positive mean *HI* generally indicate anti-clockwise and

clockwise hysteresis loops, respectively. However, events with a mean *HI* close to zero usually have a more complex hysteresis pattern and are better interpreted visually. In addition to mean *HI*, a set of storm metrics was calculated to characterize each event: the antecedent precipitation index for 30 days before the event (API_{30}), total precipitation, rainfall intensity during the event, the antecedent concentration and discharge, and relative change in concentration and discharge.

3.3 Results

3.3.1 Specific discharge

The specific discharge time series in the three sub-catchments and main catchment clearly reflected the seasonality in rainfall. The highest discharge peaks were observed during the long rainy season from April to July in both years (Figure 3.2). High specific discharge was also observed during the short rainy season in November and December 2015, but not in 2016. Although mean specific discharge was significantly lower in the smallholder agriculture (SHA; 1.4±1.2 mm day^{-1}) than in the natural forest (NF; 1.9±1.7 mm day^{-1}) and commercial tea and tree plantation (TTP; 1.9±1.8 mm day^{-1}) sub-catchments ($p < 0.001$), TTP had the lowest median specific discharge (1.1 mm day^{-1}) compared NF (1.3 mm day^{-1}) and SHA (1.2 mm day^{-1}), and highest annual runoff coefficient (Table 3.2). The main catchment (OUT) had the highest median specific discharge (1.3 mm day^{-1}) and the temporal discharge pattern reflected the specific discharge patterns of the three sub-catchments. Differences in rainfall patterns between the three sub-catchments resulted in a different timing of peaks in specific discharge.

3.3.2 NO_3-N concentrations

Relationship between field and laboratory measurements

There was a strong relationship between NO_3-N concentrations measured in the field and in the laboratory at all sites (Figure 3.3). TTP had the best linear model fit with $R^2 = 0.899$, whereas measurements at OUT had the poorest fit ($R^2 = 0.565$). Better fits were obtained for sites for which grab samples were taken over a larger range and slightly higher NO_3-N concentrations. The differences among sites could also be related to site-specific surface water properties, such as water temperature, turbidity and colour, that affect sensor performance. The sensor at the outlet of NF tended to overestimate NO_3-N concentrations at concentrations > 0.5 mg N l^{-1}, while the sensors at SHA and TTP slightly underestimated the concentrations. The maximum measured NO_3-N

concentration at NF (2.27 mg N l^{-1}) was more than twice the maximum of the range of values used for calibration (0.99 mg N l^{-1}), but concentrations higher than 0.80 mg N l^{-1} occurred less than 1% of the time.

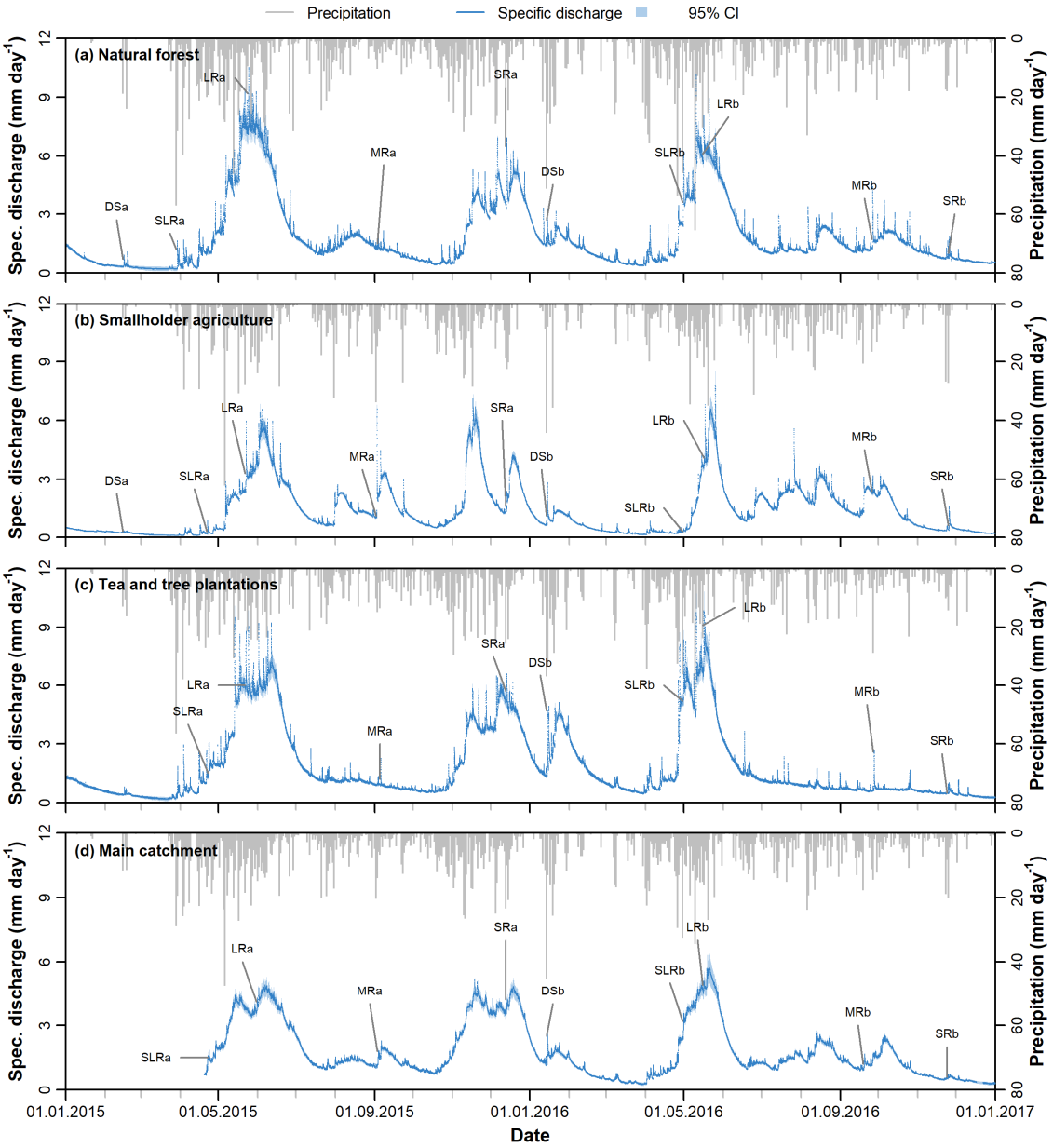

Figure 3.2 Precipitation and specific discharge time series with 95% confidence interval (CI) at the outlet of the (a) natural forest (NF), (b) smallholder agriculture (SHA), and (c) tea and tree plantation (TTP) sub-catchments and (d) the main catchment (OUT) in the South-West Mau, Kenya, between January 2015 and December 2016. Labels indicate selected storm events for hysteresis analysis.

Temporal variations in NO_3-N concentrations

The flow-weighted mean NO_3-N concentration was lowest at NF (0.44±0.043 mg N l^{-1}), followed by SHA (1.10±0.11 mg N l^{-1}) and TTP (2.14±0.19 mg N l^{-1}). The mean NO_3-N concentration at OUT (0.89±0.10 mg N l^{-1}) was slightly lower than at SHA. NO_3-N concentrations at NF were mostly within a range of 0.3–0.5 mg N l^{-1} throughout the year (Figure 3.4). Conversely, concentrations in SHA, TTP and OUT showed a seasonal pattern with higher concentrations during periods of high flow. NO_3-N contributed most to total dissolved nitrogen (TDN) in all catchments, with 83±32% in NF, 75±16% in SHA, 83±17% in TTP and 79±16% in OUT.

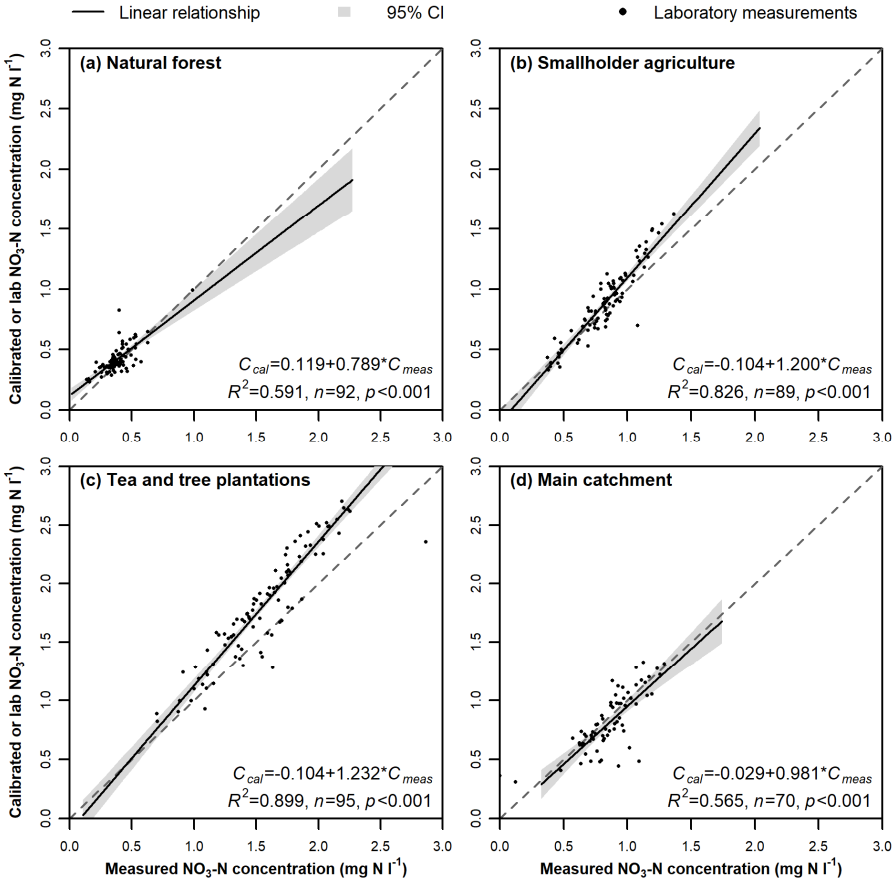

Figure 3.3 Linear relationship and the 95% confidence interval (CI) between measured and calibrated nitrate (NO_3-N) concentrations for the full range of concentrations measured in the field between January 2015 and December 2016 at each site, based on the relationship between values measured by the sensor in the field and as obtained through corresponding grab samples analysed in the laboratory (black dots) for the (a) natural forest (NF), (b) smallholder agriculture (SHA) and (c) tea and tree plantations (TTP) sub-catchments and (d) the main catchment (OUT) in the South-West Mau, Kenya. The dashed line represents the 1:1 relationship between measured and calibrated values.

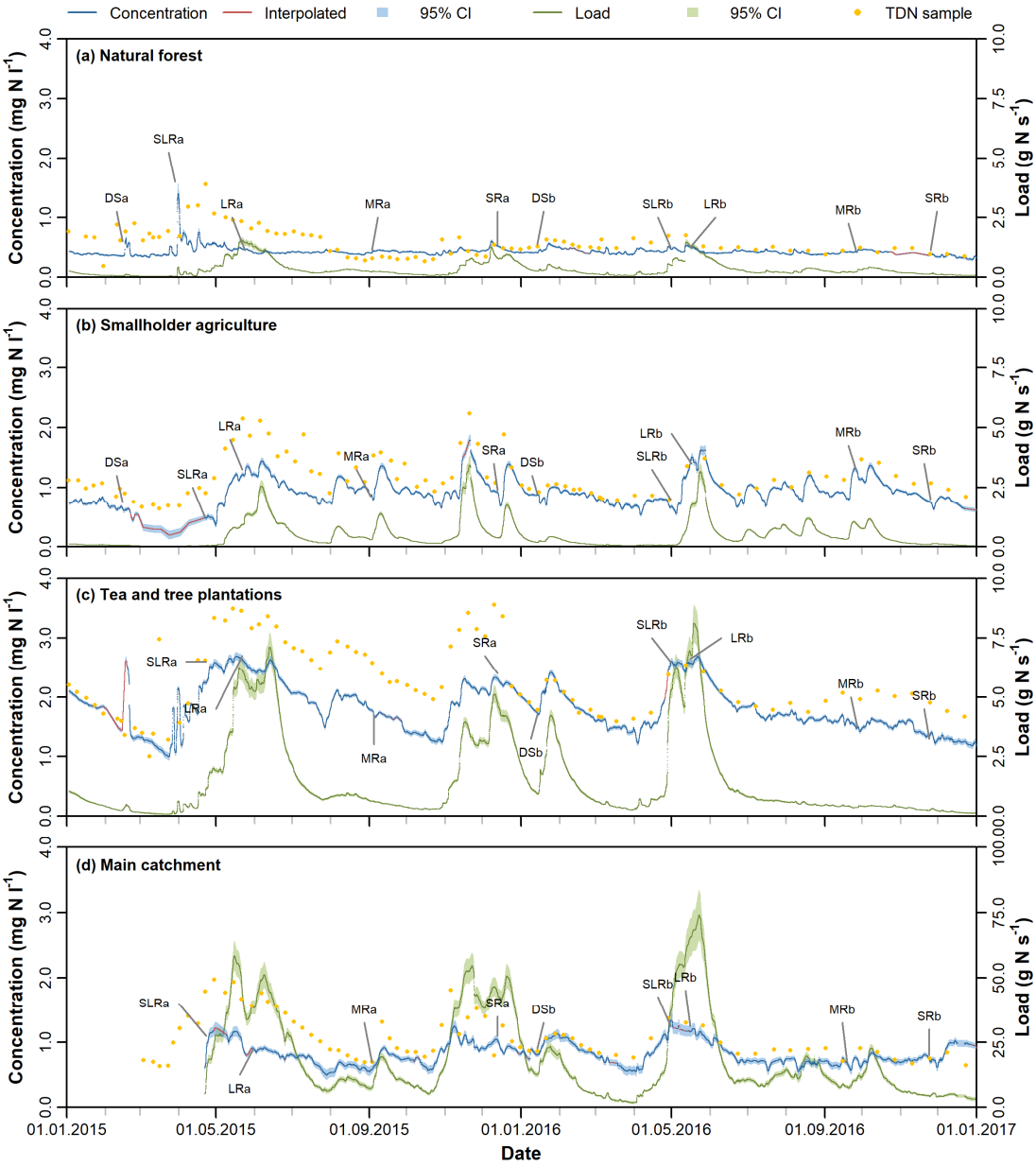

Figure 3.4 Time series of smoothed (48 h rolling median) nitrate (NO_3-N) concentration and loads with 95% confidence interval (CI), and TDN concentration at the outlet of the (a) natural forest (NF), (b) smallholder agriculture (SHA) and (c) tea and tree plantations (TTP) sub-catchments and (d) the main catchment (OUT) in the South-West Mau, Kenya, between January 2015 and December 2016. Labels indicate selected storm events for hysteresis analysis.

Concentration–discharge relationship and hysteresis

The concentration–discharge relationships differed for the sub-catchments: NO_3-N concentrations at NF were not related to discharge (R^2 = 0.070), for SHA and TTP there were positive (log-linear) relationships (R^2 = 0.630 and R^2 = 0.725), whereas for OUT there was a weak positive (log-linear) relationship (R^2 = 0.217; Figure 3.5 and 3.9).

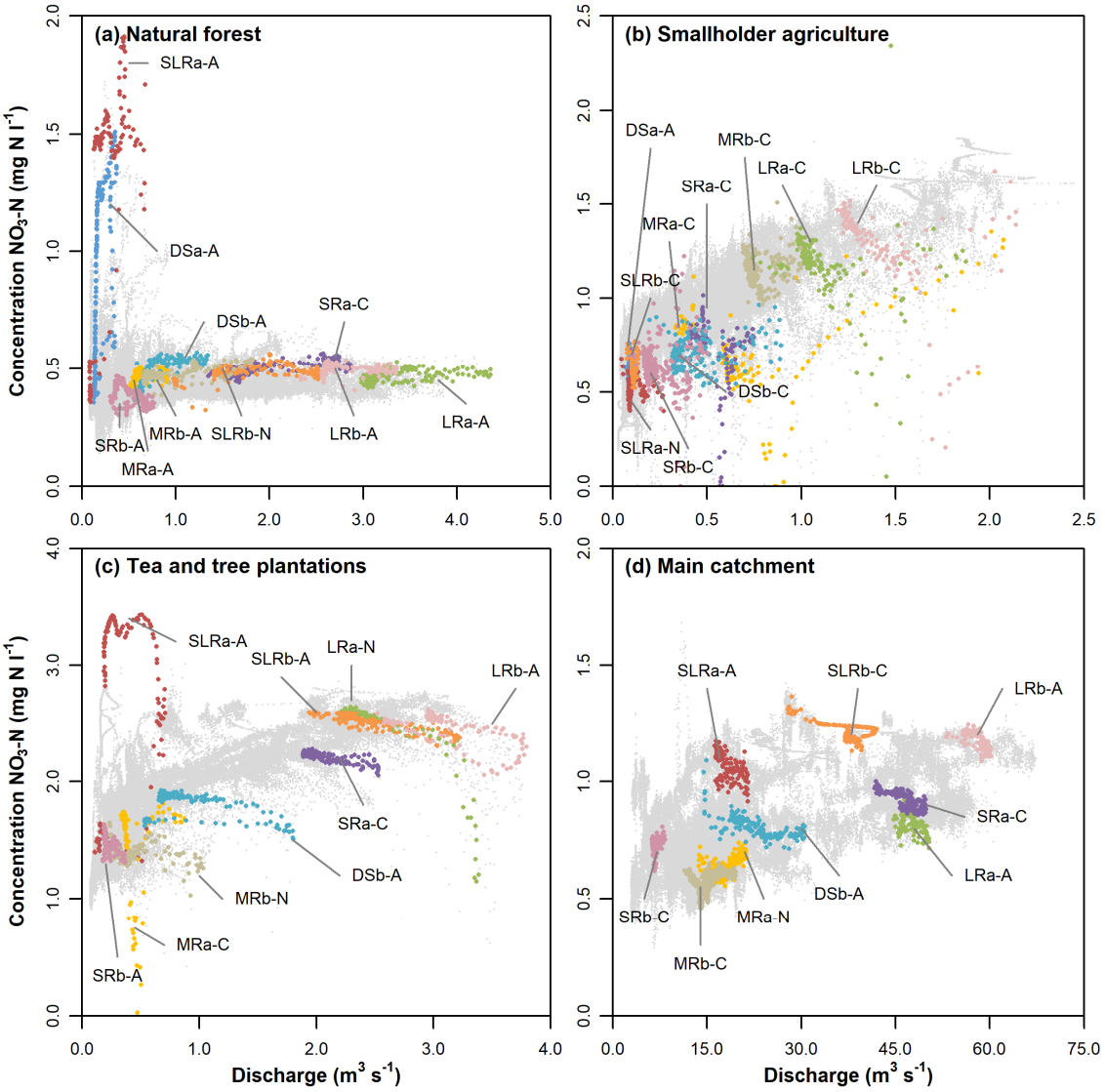

Figure 3.5 Discharge and nitrate (NO_3-N) concentration at the outlet of the (a) natural forest (NF), (b) smallholder agriculture (SHA), and (c) tea and tree plantations (TTP) sub-catchment, and (d) the main catchment (OUT) in the South-West Mau, Kenya, measured between January 2015 and December 2016. The full dataset is represented by grey dots. Selected storm events for hysteresis analysis are indicated by different colours and labels: DS = dry season, SLR = start long rainy season, LR = long rainy season, MR = moderate rainfall between long and short rainy season, and SR = short rainy season), year (a = 2015, b = 2016) and direction of hysteresis loop (A = anti-clockwise, C = clockwise, N = no loop). Labels correspond to the indicated storm events in Figure 3.2 and Figure 3.4.

Normalized concentration–discharge graphs per rainfall event and catchment are provided in Figure 3.10–3.11. Most events at NF followed an anti-clockwise hysteresis loop indicated by negative mean hysteresis indices (*HI*; Table 3.6), with lower

concentrations on the rising limb than on the falling limb of the hydrograph. Events during low flow showed the highest relative increases in NO_3-N concentrations (up to 4-fold). The majority of events in SHA displayed a clockwise hysteresis loop with strong dilution on the falling limb of the hydrograph. Exceptions were event DSa and SLRa, both during or at the end of the low flow period, with an anti-clockwise loop or no clear pattern.

Hysteresis patterns were less consistent for TTP and OUT. Although events in OUT showed anti-clockwise hysteresis loops during the long rainy season and clockwise loops during medium rainfall and the short rainy season, no systematic seasonal changes were observed for TTP. In TTP, larger storm events (high total precipitation and rainfall intensity) usually resulted in lower *HI*, but this was not observed for the other catchments. Similar to NF, event SLRa showed an anti-clockwise hysteresis loop with large increase in NO_3-N concentration in TTP. Most other events in TTP resulted in dilution of the NO_3-N concentration at the peak of the hydrograph. Events with $API_{30} > 250$ mm, mainly coinciding with the long rains, had a *HI* close to or below zero in all catchments. Also events at the start of the long rainy season generally displayed anti-clockwise hysteresis loops ($HI < 0$), whereas storms during the short rains often showed a clockwise loop ($HI > 0$).

3.3.3 NO_3-N loads

Loads in all catchments followed discharge patterns (Figure 3.4). The strong relationship between NO_3-N concentration and discharge in SHA and TTP (Figure 3.5 and 3.9), resulted in pronounced seasonal peaks in NO_3-N loadings. Annual specific loads were more than four times higher in TTP than in NF, while loads for SHA were approximately twice those of NF (Table 3.2). The annual specific load of OUT was similar to that of SHA in 2016. All catchments exported less NO_3-N in 2016 than in 2015.

Table 3.2 Annual specific discharge, runoff coefficient and specific NO_3-N load (and 95% confidence interval) for the studied catchments[a] in the South-West Mau, Kenya.

Catchment	Year	Specific discharge	Runoff coefficient[b]	Specific NO_3-N load
		mm yr^{-1}	-	*kg N ha^{-1} yr^{-1}*
NF	2015	724 (676–772)	0.36 (0.33–0.38)	3.23 (2.98–3.48)
	2016	609 (574–644)	0.32 (0.30–0.34)	2.62 (2.43–2.80)
SHA	2015	535 (500–571)	0.33 (0.31–0.35)	6.04 (5.58–6.49)
	2016	465 (437–493)	0.34 (0.32–0.36)	4.92 (4.57–5.26)
TTP	2015	744 (698–789)	0.38 (0.36–0.41)	16.26 (15.21–17.31)
	2016	582 (547–618)	0.35 (0.33–0.37)	12.04 (11.24–12.83)
OUT	2016	512 (477–547)	0.31 (0.29–0.33)	4.56 (4.12–5.00)

[a] NF = natural forest, SHA = smallholder agriculture, TTP = tea and tree plantations, OUT = main catchment; [b] Annual specific discharge as proportion of annual precipitation.

3.4 Discussion

3.4.1 Seasonal NO_3-N patterns

There was no seasonal pattern in NO_3-N concentrations for the natural forest (NF), while NO_3-N concentrations in the smallholder agriculture (SHA) and commercial tea and tree plantations (TTP) followed a seasonal pattern with higher concentrations in periods of high discharge. Small, short-lived peaks (< 0.2 mg N l^{-1} on top of baseline concentrations) in NO_3-N concentrations during storm events were observed during fertilizer application within TTP, likely as a result of surface runoff. However, the contribution of these peaks to the generally higher NO_3-N concentrations in TTP was very small and the gradual change in NO_3-N concentration during the rainy seasons in TTP and SHA was most likely a consequence of slower transport of NO_3-N to the stream through sub-surface flow paths, as illustrated in Figure 3.6. NO_3-N retention in soils is related to the anion exchange capacity, which depends on mineralogy, soil pH, soil organic carbon (Harmand et al., 2010; Soares et al., 2005) and hydrological properties due to soil age and development (Lohse and Matson, 2005). Although the high kaolinite content of Nitisols, the dominant soil type in the study area, could contribute to NO_3-N retention (Harmand et al., 2010), the relatively high soil organic carbon content of the topsoil (58–97 g kg^{-1}) (Arias-Navarro et al., 2017b) and well-drained soils in the study area could facilitate leaching of NO_3-N from the topsoil to groundwater during the rainy season (Rasiah et al., 2003). Increased NO_3-N input to the streams could also occur when discharge is produced

directly from lateral flow through a NO_3-N rich soil layer (Musolff et al., 2015). During dry periods, this NO_3-N source is likely disconnected from the stream, thus resulting in lower concentrations during periods of low rainfall. The upward shape of the concentration–discharge relationships of SHA and TTP confirms this chemodynamic behaviour (Moatar et al., 2017). A spatially dynamic change in the discharge generating zone has also been observed for other tropical montane ecosystems, such as the Páramo in Ecuador (Correa et al., 2017). Therefore, it is likely that NO_3-N enters the stream via groundwater, a typical pathway discussed for many agricultural catchments (Durand et al., 2011). To further support this hypothesis groundwater measurements are needed, which are currently not available for our study catchments.

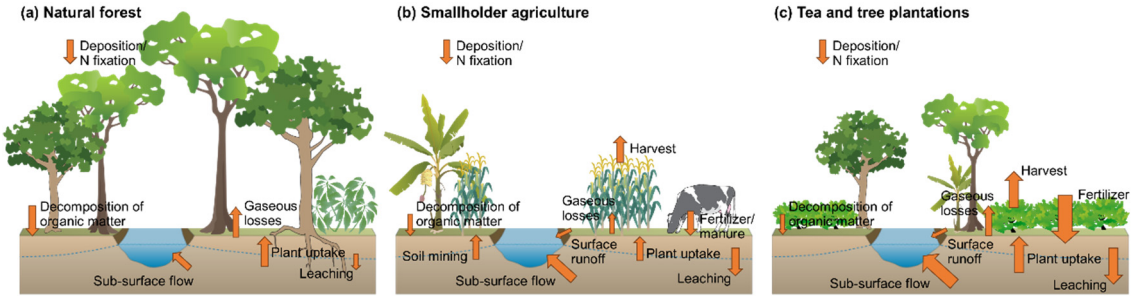

Figure 3.6 Conceptual model of nitrogen (N) fluxes in three land use types in a tropical montane area: (a) natural forest (NF), (b) smallholder agriculture (SHA) and (c) commercial tea and tree plantations (TTP), based on interpretation of the results of this study in the South-West Mau, Kenya. Differences in arrow size indicate relative differences in magnitude of fluxes between the three land use types.

The lack of seasonality in NO_3-N concentrations in NF is reflected in the absence of a relationship between concentration and discharge. This suggests chemostatic behaviour, which could be caused by a uniform distribution of NO_3-N in the soil, continuous hydrological connectivity and temporal stability of flow paths (Moatar et al., 2017; Musolff et al., 2015). Furthermore, unlike SHA and TTP, which receive mainly organic and a significant amount of inorganic fertilizer, respectively, NF does not receive anthropogenic N inputs that accumulate in the soil and are mobilized during the rainy season. Although accumulation of NO_3-N in tropical forests has also been observed, mostly due to nitrification during the dry season (e.g. Kiese et al., 2003), this effect is usually confined to the topsoil and might not result in significant leaching losses. Chaves et al. (2009) reported NO_3-N concentrations two orders of magnitude higher in soil water at 20 cm depth than in groundwater in a tropical forest in the Amazon. They attributed

this reduction along the vertical flow path to uptake by deep-rooted vegetation, denitrification and abiotic N retention in deeper soil layers, which was also observed by Harmand et al. (2010). These processes were also held responsible for a lack of seasonal in-stream NO_3-N variation despite increased NO_3-N concentrations in the upland and riparian zone in a tropical montane forest catchment in Peru (Saunders et al., 2006). However, because of differences between our study area and the aforementioned studies in soil type (e.g. Chaves et al., 2009), topography and soil depth (e.g. Saunders et al., 2006) and annual precipitation and temperature (e.g. Harmand et al., 2010) we cannot reliably conclude that the same processes are responsible for the observed patterns in our study without further empirical evidence.

3.4.2 Response to storm events

Hysteresis occurs when the timing or form of response of the solute concentration and discharge differ, generally resulting in a cyclical relationship between concentration and discharge (Evans and Davies, 1998). These hysteresis loops can be either clockwise, with higher concentrations on the rising limb of the hydrograph, or anti-clockwise, with higher concentrations on the falling limb. The direction and shape of the hysteresis loop reflects the timing of changes in concentration and discharge, as well as mixing processes, and allows interpretation of sources of stormflow and NO_3-N (Evans and Davies, 1998).

The anti-clockwise hysteresis loops with slight increases in NO_3-N concentrations at NF suggest slow mobilization of NO_3-N in top soil during storm events (Van Herpe and Troch, 2000), which has been observed in a Peruvian tropical montane forest (Saunders et al., 2006). According to a classification of hysteresis loops by Evans and Davies (1998) based on a three component mixing model with soil water, groundwater and surface runoff, the shape of most hysteresis loops in NF suggests inflow of NO_3-N rich soil water to the stream during the storm event. Large rainfall events (> 30 mm) during wet periods (API_{30} > 200 mm; SRa and SLRb) showed no clear hysteresis loop and the NO_3-N concentration barely changed during the storm event. This suggests that antecedent moisture conditions and event size affect NO_3-N mobilization in NF, resulting in different hysteresis patterns.

The decrease in NO_3-N concentrations during storm events in TTP and SHA implies dilution of stream water with precipitation which is low in NO_3-N (0.20±0.10 mg N l^{-1}, n = 13). This agrees with findings of Goodridge and Melack (2012), where agricultural

catchments showed dilution during rainfall events, compared to NO_3-N enrichment in undisturbed catchments. Dilution of NO_3-N due to surface runoff was also observed in a sub-tropical agricultural catchment in Japan (Blanco et al., 2010) and a tropical agricultural catchment in the Amazon (Riskin et al., 2017). These results strongly indicate that conversion from natural forest to agricultural land use causes a shift from sub-surface flow to surface runoff during storm events. The generally lower infiltration rates in SHA (40.5±21.5 cm h^{-1} in croplands and 13.8±14.6 cm h^{-1} in pastures) and TTP (43.3±29.2 cm h^{-1} and 60.2±47.9 cm h^{-1} in tea and tree plantations, respectively) than in NF (76.1±50.0 cm h^{-1}), as presented by Owuor et al. (2018), could explain increased surface runoff across agricultural land during storm events. The concave shape and negative direction of the hysteresis loops further suggest that groundwater has higher concentrations than event and soil water (Evans and Davies, 1998), which supports our findings that groundwater enriched through leaching of NO_3-N from fertilizer inputs is the main source of increased NO_3-N concentrations in SHA and TTP (Figure 3.6).

At the outlet of the main catchment (OUT), small rainfall events during wet periods (e.g. events SLRa, LRa and LRb) caused anti-clockwise hysteresis loops while large events after dry periods, indicated by low API_{30}, resulted in clockwise loops indicative of a greater contribution of event water (Evans and Davies, 1998). As observed in the TTP and SHA sub-catchments, most rainfall events led to dilution of the NO_3-N concentration. This indicates that similar flow paths and NO_3-N sources control NO_3-N export in the main catchment, probably as a consequence of the dominance and proximity of these land use types to the outlet of the main catchment (Carey et al., 2014).

3.4.3 Hot moments

A large peak in NO_3-N concentrations was observed at the beginning of the rainy season in 2015 in NF and TTP. This could be caused by rapid mineralization of organic matter and a more active, developing microbial community after rewetting of dry soil (Birch, 1964) or accumulation of NO_3-N in the topsoil during the dry season (Kiese et al., 2003). Rapid onset of mineralization and nitrification with rewetting of soils has been observed at several sites in East Africa (Semb and Robinson, 1969) and elsewhere in the tropics (Borken and Matzner, 2004; Butterbach-Bahl et al., 2004). Alternatively, accumulation of inorganic N from decomposition of organic material could occur during a dry spell as a consequence of decreased uptake by primary producers due to water stress (Borken and

Matzner, 2004; Wong and Nortcliff, 1995). Thus, first rains after a prolonged dry period can cause a flush of the accumulated NO_3-N into the stream. Quick depletion of this source means that such peaks are only observed at the start of the rainy season with rewetting of soils. Atmospheric N deposition during the dry season could also contribute to NO_3-N accumulation, as observed in a dry catchment in California, USA (Homyak et al., 2014), but N deposition is low in the study area at 2.25 kg ha^{-1} yr^{-1} (Zhou et al., 2014). Nevertheless, similar peaks in NO_3-N export were observed in the transition from dry to wet soils through its effect on microbial N-processing (Homyak et al., 2014). Although these peaks are important hot moments for NO_3-N concentrations, increasing the concentration in the NF sub-catchment up to 4 times, their contribution to total annual NO_3-N export was small, due to the low discharge at the end of the dry season. The absence of similar peaks at the start of the rainy season in 2016 suggests that prolonged dry periods are necessary for such flushing events to occur, which is in line with the concept that a combination of a sufficient supply of reactants and suitable environmental conditions are required for this phenomenon to occur (Bernhardt et al., 2017). Nevertheless, the nature of hot moments is that they are difficult to predict.

3.4.4 NO_3-N loads

The increased NO_3-N loading in agricultural compared to forested sub-catchments in this study, has also been observed in a study comparing 20 tropical catchments in Brazil, where agricultural catchments exported on average 10 times more NO_3-N than natural vegetation catchments (Gücker et al., 2016b). Annual loads for NF fall within the range of loads observed in other forests in the tropics (0.02–6.1 kg N ha^{-1} yr^{-1}; Table 3.7). The large range of loads obtained from different studies are likely caused by the high variability between tropical catchments, whereby differences in precipitation amount and patterns, hydrological response, temperature, soils, vegetation and topography will result in different flow paths, timing and magnitude of NO_3-N export.

Loads for the SHA and TTP sub-catchments are much lower than those observed in agricultural catchments that were converted more than 10 years ago in western Kenya, while a catchment 5 years after conversion had a lower annual NO_3-N load (Recha et al., 2013). The latter did not receive any fertilizer input (Recha et al., 2013), which probably resulted in lower NO_3-N export. Recha et al. (2013) attributed the high NO_3-N load of the older catchments to increased mineralization of soil organic matter, higher population

density and higher fertilizer inputs (40 kg N ha^{-1}), which are lower than fertilizer inputs in TTP. However, soils in the study area of Recha et al. (2013) had a higher sand content and pH, which could have increased NO_3-N leaching (Gaines and Gaines, 1994; Sharpley, 1991). In our study, differences in annual NO_3-N exports are most likely related to fertilizer inputs in the agricultural catchments. Although part of the added fertilizer (less than 20 kg N ha^{-1} yr^{-1}, mainly as organic fertilizer in SHA and 150–250 kg N ha^{-1} yr^{-1} predominantly synthetic fertilizer in TTP) is removed through harvesting of crops in SHA and continuous harvesting of young tea leaves in TTP, excess N inputs will be lost through surface runoff, leaching, microbial uptake and as gaseous losses (Figure 3.6; Arias-Navarro et al., 2017b; Mitchell et al., 2009).

Forest cover loss results on average in an increase of annual specific discharge or water yield, the magnitude depending on the amount of forest cover loss (Bosch and Hewlett, 1982; Brown et al., 2005). However, these reviews also show there is a large variability in the change in specific discharge as response to deforestation. In addition to deforestation extent, local climate, soils, topography and geology play an important role. In our case, specific discharge was smaller in SHA than in the other sub-catchments, which could be explained by the 14–28% lower annual precipitation than in NF and TTP. Precipitation in the Mau Forest area generally decreases to the northeast and south of the forest (Williams, 1991) and SHA could be less influenced by thunderstorms originating from Lake Victoria in the west than NF and TTP (Krhoda, 1988). Consequently, in addition to differences in fertilizer inputs and N cycling between the three sub-catchments, annual NO_3-N loads in our study are presumably affected by differences in annual specific discharge, but the difference in specific discharge could be largely a result of variation in annual precipitation rather than primarily an effect of land use.

3.4.5 Downstream effects

The mean NO_3-N concentration and annual specific load in 2016 at the main outlet was higher than in NF, but not as high as in TTP. Since NO_3-N concentrations and loads in SHA and TTP seem to depend strongly on the amount of fertilizer input, we conclude that fertilizer application on agricultural land increases NO_3-N concentrations and loads and that values observed at OUT will depend on the overall fertilizer input within the catchment. Despite the small share of commercial tea plantations (11%) to the area of the main catchment, but due to the high fertilizer inputs compared to other land use types, tea

plantations contributed 27% of the annual NO_3-N load at the outlet of the main catchment (Table 3.3). The forest and smallholder agriculture contributed 20 and 53%, respectively. Load estimation based on annual specific load and surface area covered by each land use led to a small overestimation of the annual load calculated with data measured at OUT (470 t N yr^{-1}) of 4.9%, showing that land use is a reasonable predictor for annual load estimation within this tropical catchment.

Table 3.3 Annual load estimation for the Chemosit and Sondu basins in Kenya for 2016 and two scenarios based on changes in land use and fertilizer use.

	Annual specific load[a]	Catchment area	Annual load	Contribution
	kg N ha^{-1} yr^{-1}	*%*	*t N yr^{-1}*	*%*
Chemosit (1,021 km²)				
Natural forest (NF)	2.6	37	98	20
Smallholder agriculture (SHA)	4.9	52	260	53
Tea and tree plantations (TTP)	12.0	11	135	27
Total estimated annual load			496	
Sondu (3,452 km²) – Current land use				
Natural forest (NF)	2.6	23	206	12
Smallholder agriculture (SHA)	4.9	68	1,150	66
Tea and tree plantations (TTP)	12.0	9	373	22
Total estimated annual load			1,729	
Sondu (3,452 km²) – Scenario 1: All forest converted to smallholder agriculture				
Natural forest (NF)	2.6	0	0	0
Smallholder agriculture (SHA)	4.9	91	1,539	81
Tea and tree plantations (TTP)	12.0	9	373	19
Total estimated annual load			1,912	
Sondu (3,452 km²) – Scenario 2: Same fertilizer use in smallholder agriculture as in tea and tree plantations				
Natural forest (NF)	2.6	23	206	6
Smallholder agriculture (SHA)	12.0	68	2,817	83
Tea and tree plantations (TTP)	12.0	9	373	11
Total estimated annual load			3,396	

[a] Based on annual specific load for land use types calculated from the sub-catchments in this study.

From these results, one can expect that downstream water bodies, such as Lake Victoria in this case, will receive increased NO_3-N loads as a consequence of past and future land use changes. Evidence suggests that the water quality and ecology of Lake Victoria declined in the last decades as consequence of population and economic growth in the region (Juma et al., 2014; Verschuren et al., 2002). Extrapolating the specific loads of the three sub-catchments to the Sondu Basin and assuming that loads do not vary regionally

and in-stream N removal is negligible, Lake Victoria would have received 1,729 t N in the form of NO_3-N from the Sondu River in 2016 (Table 3.3). This is 1.5% of the estimated total annual N input to the lake, while the basin covers 1.8% of the complete Lake Victoria basin (2.7% of terrestrial surface area) (Scheren et al., 2000). Further population growth and agricultural expansion (e.g., conversion of forest to smallholder agriculture in Scenario 1, Table 3.3) or intensification of fertilizer use (e.g. same level of fertilizer use in smallholder agriculture as in commercial tea plantations in Scenario 2, Table 3.3) could lead to a 11% and 96% increase in annual N loads from the basin, respectively. This would affect the lake through increased eutrophication. Our annual load estimate is, however, 28% higher than the estimated load of 1,347 t N yr^{-1} from the Sondu basin by Kayombo and Jorgensen (2005). Because our estimate is only based on NO_3-N, the total N load is likely higher, since also other forms of N, such as particulate N, ammonium (NH_4-N), nitrite (NO_2-N) and dissolved inorganic N (DON) need to be considered. The difference between our load estimate and the value reported by Kayombo and Jorgensen (2005) could also be due to the quality and frequency of collected data and the use of different load estimation methods (Littlewood, 1992; Zamyadi et al., 2007). Also, in-stream NO_3-N transformation and uptake between our sub-catchments and the outlet of the Sondu Basin, could change NO_3-N concentrations. The calculated specific loads of our study might differ throughout the whole Sondu basin because of differences in underlying geology and soil type, drier and warmer climate, and changes in topography downstream. However, the data presented here is the first approximation to discharge and NO_3-N dynamics and annual N loads and a good basis for upscaling and calibrating hydrological models.

3.5 Conclusion

This study presented the first high-resolution dataset in East Africa. The two years of data from natural forest, smallholder agriculture and commercial tea and tree plantations and the main catchment offer valuable insights in NO_3-N dynamics within a tropical montane region in Kenya, as summarized in Figure 3.6. Our study does not only quantify how land use change impacts the area under change, but also the ecosystems downstream, as shown with the estimated NO_3-N input from the Sondu River to Lake Victoria. A change from natural forest to agriculture seems to increase NO_3-N yields and the occurrence of surface runoff during storm events, in which could lead to increased erosion rates and sediment

loads in rivers. Increased nutrient concentrations as a consequence of fertilization can reduce ecological quality of rivers and lakes and affect aquatic life. The high-resolution data collected in this study shows responses to storm events, the processes behind the different responses and hot moments for NO_3-N export. This study highlights the need for wider application of high-resolution monitoring to better understand catchment functioning through analysis of hysteresis loops and hot moments. Although the use of *in situ* instruments has its own challenges, such as security, power supply and maintenance, continuous development of sensor technology and reduction in costs increasingly enables deployment of such sensors, also in remote areas. This is especially relevant in many tropical regions that are vulnerable to land use and climate change. While there is some similarity in general NO_3-N dynamics between our study catchments and temperate catchments, such as increased NO_3-N concentrations and yields due to fertilizer application, dilution of NO_3-N concentrations during rainfall events and the importance of groundwater as source of NO_3-N, underlying biogeochemical processes, like denitrification and decomposition of organic matter, that strongly depend on climatic factors such as precipitation, soil moisture and temperature, are likely to respond differently in tropical regions, where seasonality is often defined by precipitation rather than temperature differences. Therefore, studies using such high-resolution monitoring systems provide valuable data and information to reduce the current knowledge gap in the understanding of the hydrological functioning of and nutrient fluxes in tropical ecosystems.

Acknowledgements

We would like to thank Kenya Forest Service (KFS) for supporting the research team to conduct this research in the Mau Forest. This work was partially funded by the CGIAR program on Forest, Trees and Agroforestry led by the Centre for International Forestry Research (CIFOR). We thank the Deutsche Forschungsgemeinschaft DFG (BR2238/23-1), and the Deutsche Gesellschaft für Internationale Zusammenarbeit GIZ (Grants 81195001 “Low Cost methods for monitoring water quality to inform upscaling of sustainable water management in forested landscapes in Kenya” and Grant 81206682 “The Water Towers of East Africa: policies and practices for enhancing co-benefits from joint forest and water conservation”) for generously providing additional support. We are also grateful for the valuable feedback from the reviewers to improve this manuscript. The raw data are currently available in an online database (http://fb09-pasig.umwelt.uni-giessen.de:8050/wiki/publications) hosted by Justus Liebig University, Giessen, Germany.

3.6 Supporting information

This supporting information contains details on data processing: flow-chart of the data processing protocol and percentage of data left after flagging of unreliable measurements (Figure 3.7), flags used in the data processing protocol (Table 3.4), details on gaps in the nitrate (NO_3-N) dataset used for annual load calculation (Table 3.5) and the rating curves used for discharge estimation (Figure 3.8). It also provides a comparison of annual NO_3-N export from tropical catchments across the world (Table 3.7), the log-linear relationship between NO_3-N concentration and discharge in the four catchments (Figure 3.9), and graphs of individual normalised hysteresis loops per storm event per catchment (Figures 3.10–3.11) with their corresponding storm event metrics (Table 3.6).

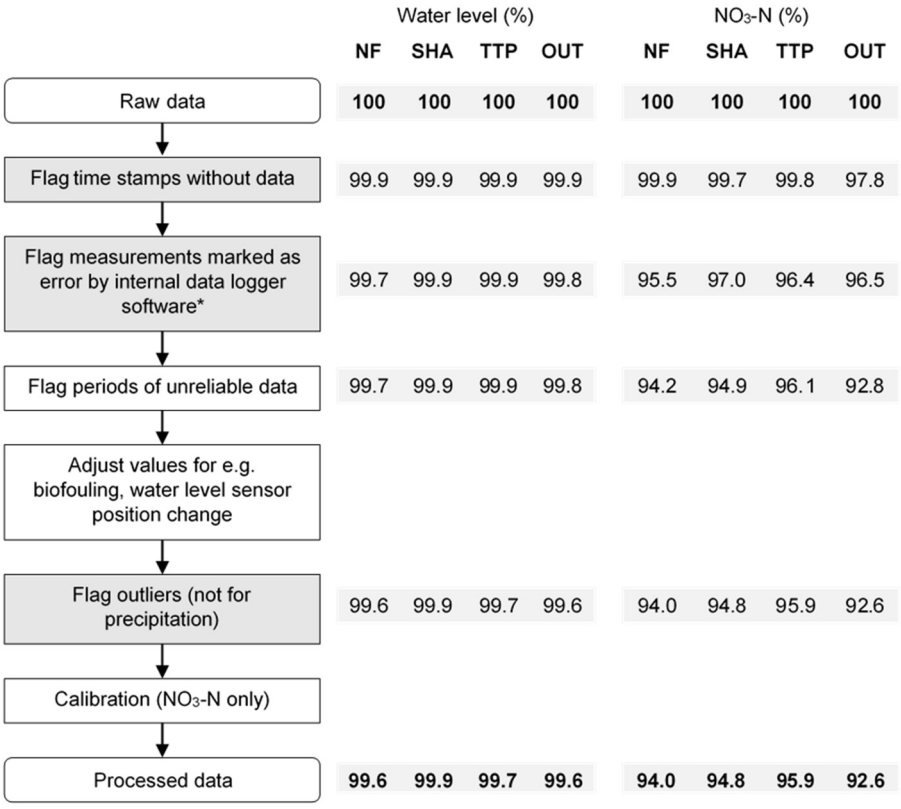

Figure 3.7 Flowchart describing the processing protocol for high-resolution data. Grey boxes indicate automated processes, while white boxes represent manual processes. Steps marked with an asterisk (*) were only carried out for data from the automatic measurement systems and not for weather data. Percentages indicate the amount of data remaining after each step for water level and nitrate (NO_3-N) concentration for the four catchments (NF = natural forest, SHA = smallholder agriculture, TTP = tea and tree plantations and OUT = main catchment) in the South-West Mau, Kenya between January 2015 and December 2016.

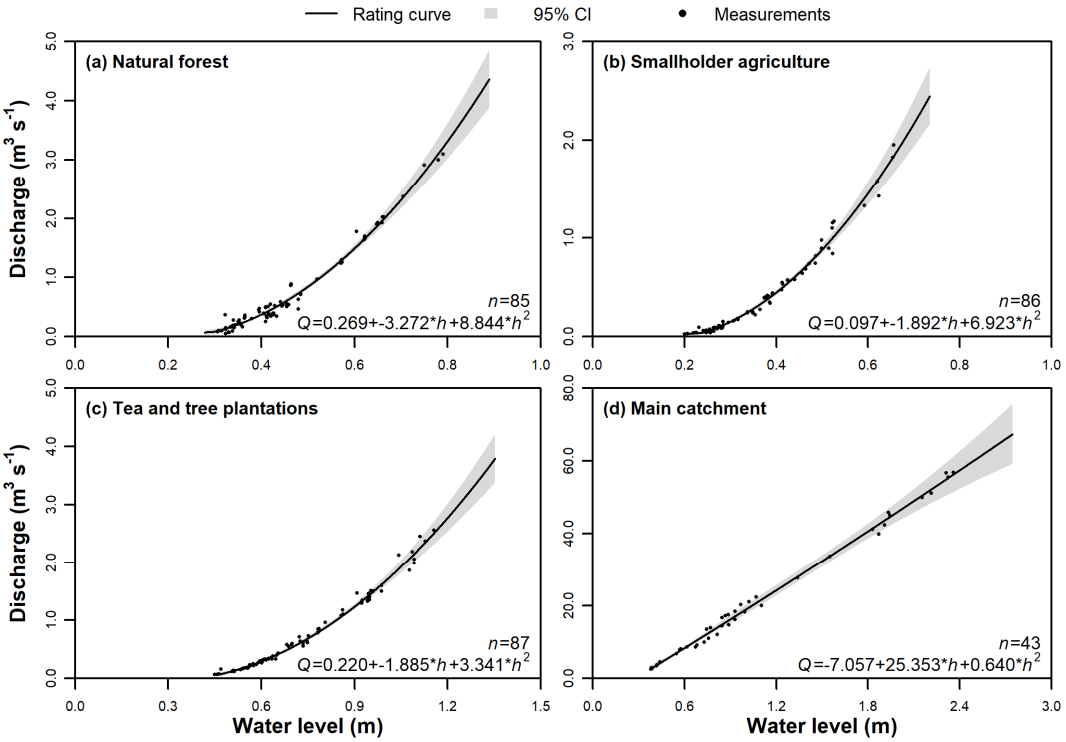

Figure 3.8 Rating curves with 95% confidence interval (CI) for the outlet of the (a) natural forest (NF), (b) smallholder agriculture (SHA) and (c) tea and tree plantations (TTP) sub-catchments and (d) the main catchment (OUT) in the South-West Mau, Kenya.

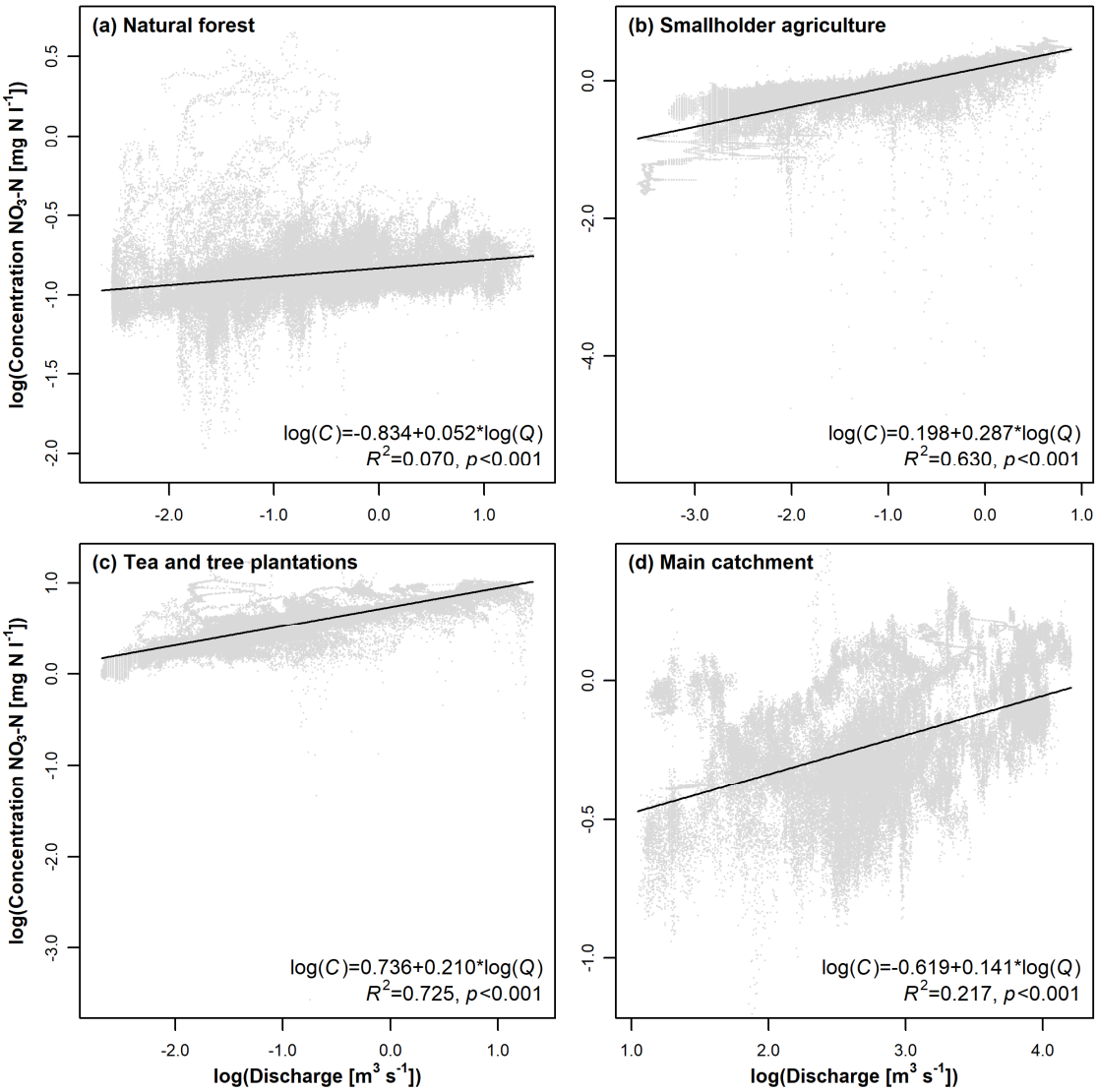

Figure 3.9 Relationship between log-transformed discharge (*Q*) and nitrate (NO_3-N; *C*) concentrations in the (a) natural forest (NF), (b) smallholder agriculture (SHA) and (c) tea and tree plantation (TTP) sub-catchment and (d) the main catchment (OUT) in the South-West Mau, Kenya, between January 2015 and December 2016.

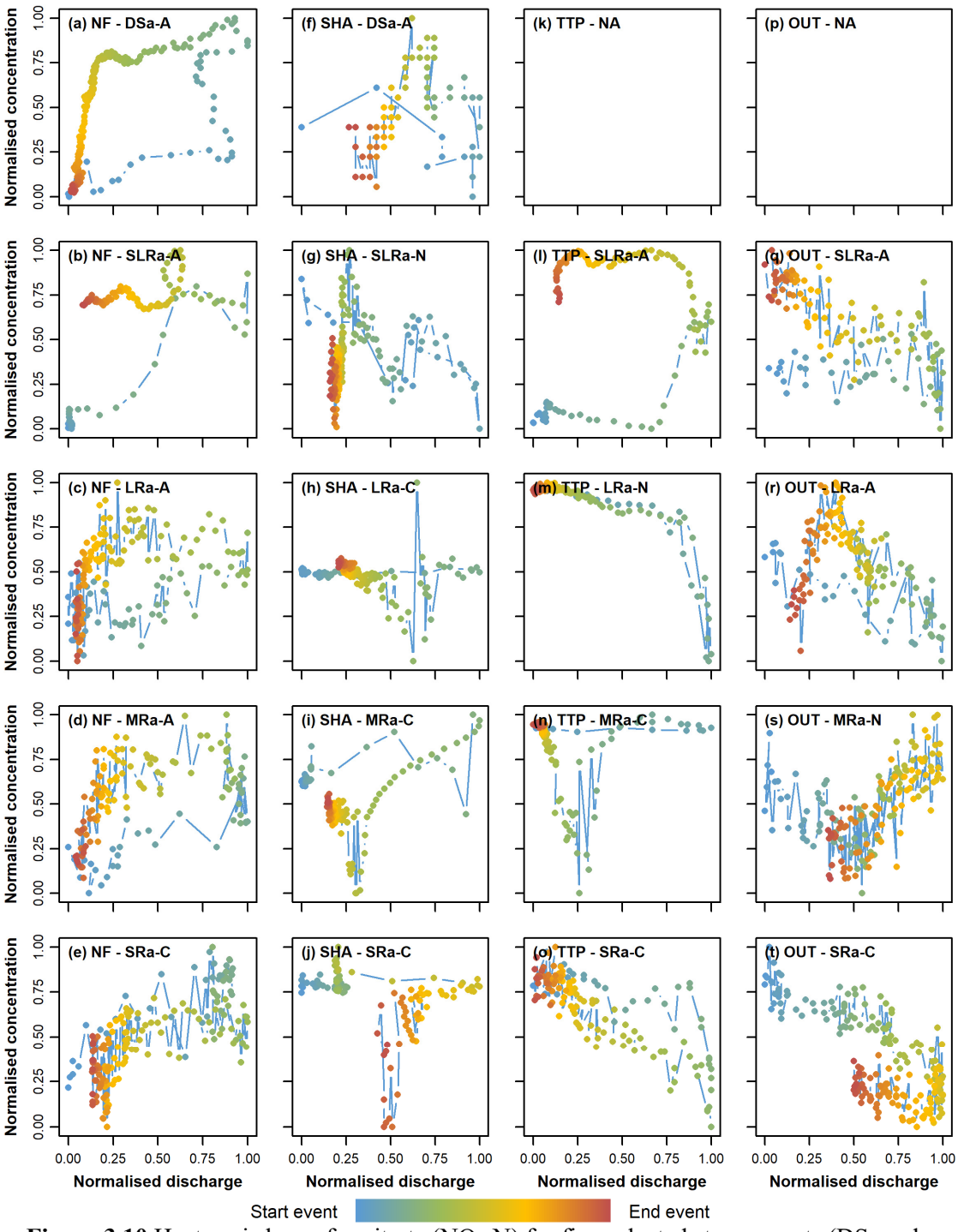

Figure 3.10 Hysteresis loops for nitrate (NO_3-N) for five selected storm events (DSa = dry season, SLRa = beginning long rainy season, LRa = long rainy season, MRa = moderate rainfall between long and short rainy season, and SRa = short rainy season) in 2015 in the three sub-catchments with (a–e) natural forest (NF), (f–j) smallholder agriculture (SHA), (k–o) tea and tree plantations (TTP) and (p–t) the main catchment (OUT) in the South-West Mau, Kenya. Last letter in the graph title indicates the direction of the hysteresis loop (A = anti-clockwise, C = clockwise, N = no loop).

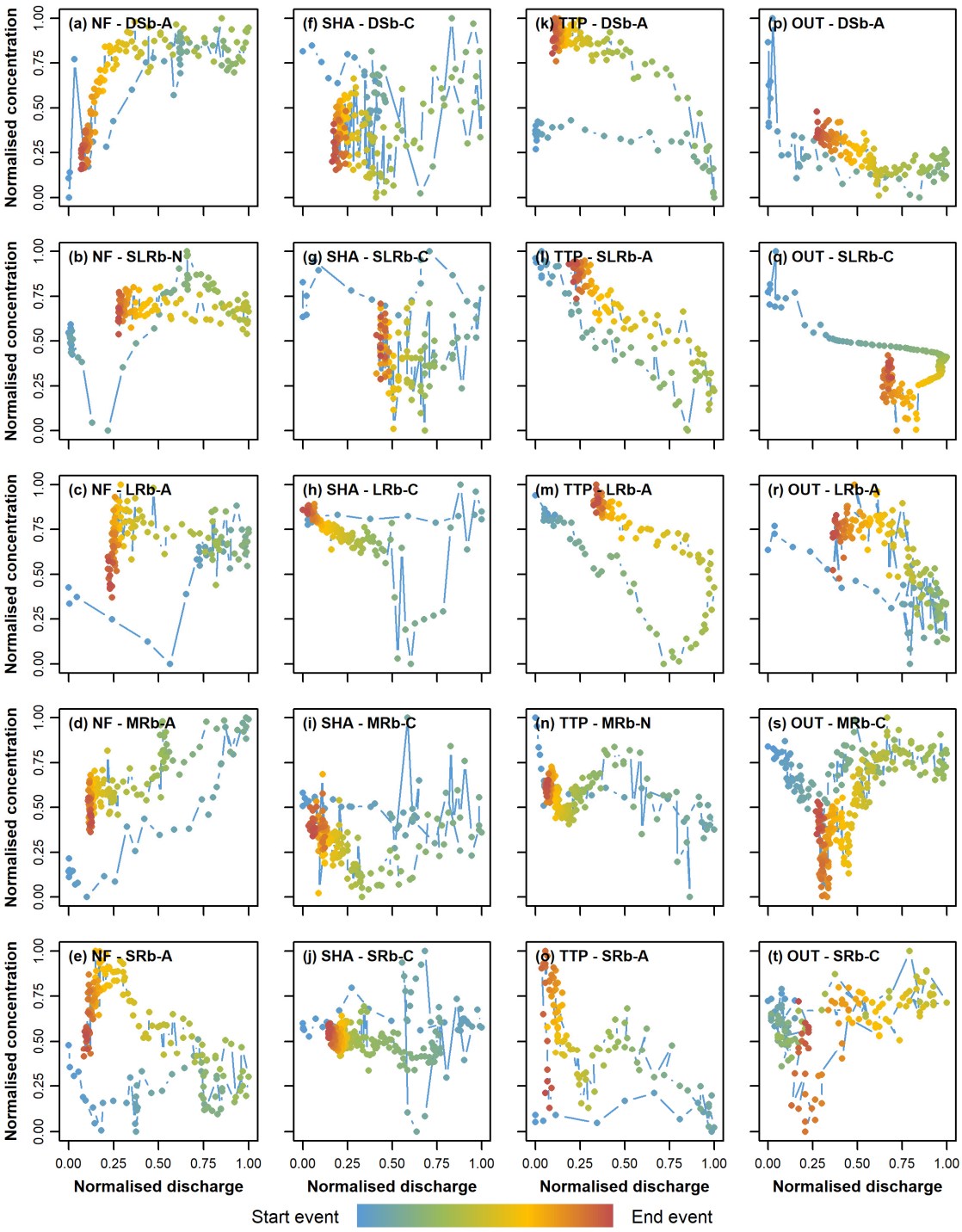

Figure 3.11 Hysteresis loops for nitrate (NO_3-N) for five selected storm events (DSb = dry season, SLRb = beginning long rainy season, LRb = long rainy season, MRb = moderate rainfall between long and short rainy season, and SRb = short rainy season) in 2016 in the three sub-catchments with (a–e) natural forest (NF), (f–j) smallholder agriculture (SHA), (k–o) tea and tree plantations (TTP) and (p–t) the main catchment (OUT) in the South-West Mau, Kenya. Last letter in the graph title indicates the direction of the hysteresis loop (A = anti-clockwise, C = clockwise, N = no loop).

Table 3.4 Flags used in post-processing of data collected by the automatic instruments. Automatic flags were assigned based on a script, while manual flags were assigned based on information from an instrument log book and field observations. Calculation flags identify data that were adjusted, calibrated or calculated during post-processing. Some flags were instrument-specific.

Type	Flag	Description	Instrument
Automatic	e	Measurement marked as error by internal data logger software	spectro::lyser, condu::lyser
	n	Time stamp without data	All
	o	Outlier, based on Median Absolute Deviation (*MAD*) of moving window j with length k at time t_i and threshold a: $\left\lvert \frac{x_i - M_{j,i}}{MAD_{j.i}} \right\rvert > a$	All
Manual	a	Sensor above water	spectro::lyser, condu::lyser
	b	Sensor buried in sediments	spectro::lyser, condu::lyser
	c	Cleaning or maintenance	All
	f	Sensor failure not identified by data logger software	All
	h	Funnel blockage	Tipping bucket
	p	Problem with power supply	All
	r	Measurement affected by poor reference measurement	spectro::lyser
	s	Cables cut	Weather station
	t	Problem with automatic cleaning system	spectro::lyser, condu::lyser
	v	Instrument disturbed by insects	All
	w	Sensor too close to water level	VEGAPULS WL61
	x	Sensor above object	VEGAPULS WL61
Calculation	A	Measurement value adjusted in post-processing	All
	C	Measurement calibrated	spectro::lyser
	R	Discharge calculated using rating curve	VEGAPULS WL61

Table 3.5 Details of data gaps and interpolation of the nitrate (NO_3-N) data of the three sub-catchments (NF = natural forest, SHA = smallholder agriculture, TTP = tea and tree plantations) and the main catchment (OUT) in the South-West Mau, Kenya between January 2015 and December 2016.

	NF	SHA	TTP	OUT
Data gaps ≤ 24 hours				
Count	482	252	351	319
Median length (count)	20 min (354)	20 min (204)	20 min (280)	20 min (273)
Maximum length	760 min	1,220 min	1,020 min	1,110 min
Data gaps > 24 hours				
Count	1	4	2	10
Range	43,860 min	2,210–73,600 min	3,440–27,360 min	2,180–14,620 min
Final data set				
Number of measurements	105,031	105,183	104,915	88,161
Interpolated	5.71%	10.44%	3.95%	6.37%

Table 3.6 Characteristics of the selected storm events (DS = dry season, SLR = start long rainy season, LR = long rainy season, MR = moderate rainfall between long and short rainy season, SR = short rainy season, a = 2015, b = 2016) in the studied catchments (NF = natural forest, SHA = smallholder agriculture, TTP = tea and tree plantations, OUT = main catchment) in the South-West Mau, Kenya. Hysteresis index was calculated after Lloyd et al. (2016b).

Site	Event	API_{30}	Total precipitation	Rainfall intensity	Start concentration	Concentration change	Total load per event	Start discharge	Discharge change	Total event discharge	Hysteresis index
		mm	*mm*	*mm* h^{-1}	*mg N* l^{-1}	*%*	*g N* ha^{-1}	$m^3 s^{-1}$	*%*	*mm*	
NF	DSa	3.9	18.9	3.4	0.36	321	6.7	0.13	188	0.7	−0.41
	SLRa	21.6	57.0	10.1	0.37	420	8.8	0.08	742	0.6	−0.46
	LRa	353.6	9.3	0.9	0.46	24	46.2	2.98	46	9.8	−0.23
	MRa	97.2	10.2	1.3	0.42	30	7.2	0.52	81	1.6	−0.34
	SRa	213.0	33.8	6.1	0.47	27	30.1	1.35	113	5.9	0.19
	DSb	93.8	51.3	9.3	0.39	52	11.1	0.56	140	2.2	−0.13
	SLRb	347.9	44.8	5.5	0.45	54	20.3	0.97	161	4.2	−0.09
	LRb	381.8	30.2	8.6	0.45	29	33.9	2.34	44	6.8	−0.31
	MRb	143.3	10.9	3.6	0.40	42	12.3	0.52	252	2.6	−0.46
	SRb	75.6	12.8	1.7	0.38	43	5.2	0.30	156	1.4	−0.42
SHA	DSa	0.7	5.0	1.0	0.63	34	1.1	0.07	47	0.2	−0.07
	SLRa	161.0	9.2	2.4	0.59	57	2.5	0.06	372	0.5	0.08
	LRa	267.8	27.3	4.0	1.18	194	47.7	0.75	151	4.1	−0.01
	MRa	109.8	31.9	17.4	0.85	159	21.6	0.33	508	2.5	0.28
	SRa	154.7	16.6	3.0	0.79	129	8.7	0.41	82	1.3	0.28
	DSb	55.2	44.1	7.6	0.89	49	12.5	0.20	348	1.7	0.21
	SLRb	157.1	12.3	1.4	0.73	35	1.9	0.08	76	0.3	0.34
	LRb	257.1	10.9	5.0	1.46	101	50.8	1.22	77	4.0	0.07
	MRb	115.1	16.4	3.6	1.26	43	36.9	0.70	44	3.2	0.18
	SRb	50.6	26.9	4.5	0.70	175	11.1	0.11	356	1.7	0.15
TTP	SLRa	40.4	56.3	9.1	1.40	151	21.4	0.11	547	0.8	−0.73
	LRa	265.6	14.4	2.4	2.59	58	171.2	2.21	54	7.0	−0.01
	MRa	108.9	13.4	3.5	1.71	104	16.6	0.34	159	1.1	0.13
	SRa	211.8	24.8	5.3	2.23	10	115.6	1.88	34	5.3	0.14
	DSb	98.5	37.0	8.5	1.62	25	42.1	0.54	235	2.4	−0.43
	SLRb	266.5	36.6	4.5	2.59	12	142.2	1.95	66	5.7	−0.22
	LRb	322.6	23.5	8.3	2.59	22	165.3	2.52	50	6.8	−0.35
	MRb	113.2	28.6	13.2	1.65	38	20.3	0.23	348	1.5	0.06
	SRb	71.5	9.5	5.2	1.34	24	6.7	0.18	100	0.5	−0.39
OUT	SLRa	274.0	6.7	2.5	1.00	26	14.5	16.37	33	1.4	−0.33
	LRa	339.1	6.4	0.8	0.84	25	34.6	44.70	13	4.2	−0.21
	MRa	111.8	13.9	1.8	0.68	27	11.6	13.95	55	1.8	0.07
	SRa	196.7	22.6	2.8	0.98	15	48.2	41.74	20	5.3	0.36
	DSb	81.6	45.4	7.8	0.95	40	16.2	14.59	110	2.0	−0.10
	SLRb	246.0	34.0	3.0	1.31	18	40.1	27.88	43	3.3	0.09
	LRb	309.9	12.7	3.8	1.19	14	60.1	53.12	13	5.1	−0.25
	MRb	127.6	17.6	2.2	0.62	31	14.1	11.47	71	2.5	0.19
	SRb	68.8	8.2	2.5	0.75	25	4.4	6.56	32	0.6	0.30

Table 3.7 Flow-weighted mean or range of mean concentrations and annual loads of NO_3-N in stream water in catchments across the tropics. Elev. = elevation, *n* = number of samples for annual load estimate, AP = annual precipitation during study period, SD = specific discharge, Conc. = NO_3-N concentration, AL = annual NO_3-N load.

Source	Location	Study period	Coordinates	Land use	Elev.	Area	*n*	AP	SD	Conc.	AL
					m	*km²*		*mm*	*mm*	*mg N l^{-1}*	*kg N ha^{-1}*
Boy et al. (2008)	San Francisco catchment, Andes, Ecuador	Apr 1998–Apr 2003	4°00' S, 79°05' W	Montane forest	1900–2200	0.08–0.13	254	2340–2667	958–1101	0.08–0.14	0.88–1.4
Bücker et al. (2011)	San Francisco catchment, Andes, Ecuador	Apr 2007–May 2008	3°58'30" S, 79°4'25" W	Montane forest	1800–3140	1.3–4.5	n.a.	n.a.	n.a.	0.54–0.69	4.3–5.0
				Mixed	1800–3140	0.7–76	n.a.	n.a.	n.a.	0.55–0.62	0.07–3.4
McDowell and Asbury (1994)	Rio Icacos, Luquillo Experimental Forest, Puerto Rico	Jun 1983–May 1986	18°15' N, 65°50' W	Rainforest	375–1050	0.162–3.26	164–188	2880–4640	145–4030	0.054–0.066	0.75–2.78
Newbold et al. (1995)	Río Tempisque, Guanacaste Conservation Area, Costa Rica	Oct 1990–Sep 1993	n.a.	Evergreen forest	580–1340	0.36–3.19	20–48	2400	1400–4300	0.080–0.206	4.0–6.1
Recha et al. (2013, 2012)	Kapchorwa, Nandi County, Kenya	2007–2008	0°10'0" N, 35°0'0" E	Rainforest	1750–1900	0.128	12	2065–2100	296–370	0.40	1.18
				Maize 5 years	1750–1900	0.144	12	2065–2100	462–549	0.58	2.68
				Maize 10 years	1750–1900	0.091	12	2065–2100	574–637	4.71	27.09
				Maize 50 years	1750–1900	0.100	12	2065–2100	645–702	4.52	29.16
Riskin et al. (2017)	Tanguro Ranch, Mato Grosso, Brazil	Aug 2008–Aug 2009	n.a.	Evergreen forest	n.a.	5.13–13.12	14–17	1300	141	0.057–0.091	0.02–0.15
				Soybean	n.a.	1.98–4.11	14–17	1300	614	0.042–0.120	0.14–0.81
Taylor et al. (2015)	Quebrada Mariposa, Golfo Dulce Forest Reserve, Costa Rica	Jun–May	8°43' N, 83°37' W	Tropical forest	n.a.	0.0935	936	3220	1111	0.0128–0.0653	0.26
Williams and Melack (1997)	Braço do Mota and Igarapé de Mota, central Amazon, Brazil	Jul 1989–Jul 1990	3°15' S, 60°34' W	Rainforest	n.a.	0.18	26	n.a.	n.a	0.115	n.a.
				Agriculture	n.a.	0.234	27	2754	2080	0.167	3.64
Lesack (1993)	Braço do Mota, central Amazon, Brazil	1984	3°15' S, 60°34' W	Rainforest	n.a.	0.234	n.a.	2870	1650	n.a.	2.67
Yusop et al. (2006)	Bukit Tarek Experimental Catchment, Selangor, Malaysia	Jul 1991–Jun1994	3°31'30" N, 101°35' E	Tropical forest	48–2013	0.328–0.343	234–237	2348–3169	1081–1606	0.10–0.42	2.12–5.78
Current study	Sondu Basin, South-West Mau, Kenya	Jan 2015–Dec 2016	0°27'47" S, 35°18'32" E	Montane forest	1954–2385	35.9	52478–52543	1895–2034	609–724	0.43–0.45	2.61–3.23
			0°24'03" S, 35°28'32" E	Smallholder agriculture	2380–2691	27.2	52536–53647	1373–1630	465–535	1.06–1.13	4.92–6.04
			0°28'34" S, 35°13'17" E	Tea and tree plantations	1786–2141	33.3	52337–52578	1667–1934	582–744	2.07–2.19	12.05–16.29
			0°28'59" S, 35°10'53" E	Mixed	1715–2932	1,021.3	51393	1832	512	0.89	4.56

4 Land use alters dominant water sources and flow paths in tropical montane catchments in East Africa

This chapter was submitted to *Hydrology and Earth System Sciences* as:

Jacobs, S. R., Timbe, E., Weeser, B., Rufino, M. C., Butterbach-Bahl, K. and Breuer, L. Land use alters dominant water sources and flow paths in tropical montane catchments in East Africa. Under review for Hydrology and Earth System Sciences, https://doi.org/10.5194/hess-2018-61

4.1 Introduction

Tropical montane forests are under high anthropogenic pressure through deforestation. Evidence from tropical montane regions in Central and South America shows that conversion of montane forests to pastures increases the contribution of surface runoff to streamflow, caused by changes in flow paths and stream water sources (Ataroff and Rada, 2000; Germer et al., 2010; Muñoz-Villers and McDonnell, 2013). This could affect the timing and quantity of water supply through reduced infiltration of precipitation and increased occurrence of flood events, and could decrease water quality as a result of soil erosion. In Africa, where much of the population relies on surface water as main water source, understanding the effect of land use change on water supply and quality is crucial to manage resources sustainably. However, the hydrological functioning of tropical catchments is generally less well understood than that of temperate catchments. This is specifically true for tropical montane forest catchments, as those have received less attention in hydrological research compared to the tropical lowlands. Nevertheless, tropical montane forests are known for their high biodiversity (Burgess et al., 2007; Martínez et al., 2009) and provision several other important ecosystem services, including carbon storage (Spracklen and Righelato, 2014) and water supply (Célleri and Feyen, 2009; Martínez et al., 2009).

Stable water isotopes (^{2}H, ^{18}O) provide a useful tool to study the movement of water through a catchment (McGuire and McDonnell, 2007). Stable isotopes, usually expressed as the ratio of heavy to light isotopes (e.g. ^{2}H to ^{1}H) relative to a known standard (e.g. VSMOW, the Vienna Standard Mean Ocean Water), are useful tracers in hydrology, since these enter the environment naturally through precipitation. The isotopic composition of water only changes due to mixing with other water sources and fractionation by evaporation and condensation. Due to decreasing costs of analysis, stable isotope-based methods are used more frequently worldwide to trace water through catchments and to identify the origin and flow paths of water inputs to streams. Most case studies in tropical montane areas are from Latin America (e.g. Correa et al., 2017; Crespo et al., 2012; Mosquera et al., 2016b; Roa-García and Weiler, 2010; Timbe et al., 2014; Windhorst et al., 2014), whereas no data is available from African tropical montane catchments.

Mean transit time (MTT), i.e. the time required for rainfall to reach the stream, is a good indicator to assess flow paths, water storage capacity and mixing at the catchment scale (Asano and Uchida, 2012). Transit time also has implications for water quality, since the contact time between water and the soil will affect the chemical composition of the water that finally enters the stream through biogeochemical processes (McGuire and McDonnell, 2006). MTT can be influenced by catchment soil cover (Capell et al., 2012; Rodgers et al., 2005b; Soulsby et al., 2006), soil depth, hydraulic conductivity and topographic parameters, such as slope (Heidbüchel et al., 2013; Mosquera et al., 2016b; Muñoz-Villers et al., 2016) or a combination of these factors (Hrachowitz et al., 2009). Changes in vegetation cover and especially soil hydraulic properties as consequence of changes in land management can also modify MTT.

Other naturally occurring tracers, such as the elements Ca, Mg, K, Na and Fe, can also be used to study water flow through a catchment, for example through end member mixing analysis (EMMA). In EMMA, stream water is assumed to be a mixture of different 'end members' or water sources, such as precipitation, throughfall, groundwater and soil water (Christophersen et al., 1990). A quantification of the contribution of different end members in a catchment provides relevant insight into dominant flow paths and stream water sources (Barthold et al., 2010; Burns et al., 2001; Correa et al., 2017; Crespo et al., 2012; Soulsby et al., 2003) or water provenance (Fröhlich et al., 2008b, 2008a). Application of EMMA in the south-western Amazon revealed, for example, a higher

contribution of surface runoff in catchments converted from forest to pasture (Chaves et al., 2008; Neill et al., 2011). Increased surface runoff could result in higher soil erosion and changes in flow paths that generally affect transport of solutes and contaminants to streams, potentially resulting in decreased water quality.

The Mau Forest Complex in western Kenya is the largest tropical montane rainforest in the country and considered a major 'water tower', supplying fresh water to approximately 5 million people living downstream (Kenya Water Towers Agency, 2015). However, conversion of forest to agricultural land resulted in a 25% forest loss in the past decades (Kinyanjui, 2011). This has supposedly led to changes in flow regime (Baldyga et al., 2004; Mango et al., 2011; Mwangi et al., 2016) and increased surface runoff (Baker and Miller, 2013). These observations strongly suggest changes in dominant flow paths as a consequence of land use change, but no scientific evidence is available to confirm this. In this study, we combined MTT analysis and EMMA (Crespo et al., 2012; Katsuyama et al., 2009) to assess the effect of land use on spatial and temporal dynamics of water sources and flow paths in catchments with contrasting land use (i.e. natural forest, smallholder agriculture and commercial tea and tree plantations) in the Mau Forest Complex. This knowledge is essential in the tropics, where population growth puts significant pressure on forests and water resources, but where little is known about the consequences of deforestation. Previous studies in the South-West Mau block of the Mau Forest Complex observed reduced infiltration rates in agricultural compared to forested land use types (Owuor et al., 2018). Furthermore, analysis of nitrate concentration–discharge relationships of rainfall events suggested more surface runoff in catchments dominated by smallholder agriculture or commercial tea and tree plantations than in a montane forest catchment (Jacobs et al., 2018). Based on these results, we hypothesised that (a) the natural forest catchment has a longer MTT than the tea and tree plantation catchment and the smallholder catchment, and (b) precipitation contributes more to streamflow in the smallholder catchment, followed by the tea and tree plantation catchment and forest catchment. Furthermore, we expected that (c) the contribution of different end members varies throughout the year due to seasonality in rainfall.

4.2 Methods

4.2.1 Study area

This study was conducted in the South-West Mau block of the Mau Forest Complex, western Kenya (Figure 4.1, Table 4.1). Three sub-catchments (27–36 km²) were characterised by different land use types: natural forest (NF), smallholder agriculture (SHA) and commercial tea and tree plantations (TTP). These were nested in a 1,021 km² large catchment, referred to as the main catchment (OUT), which is characterized by a mixture of these three land use types. The natural forest is classified as Afromontane mixed forest, with species including *Podocarpus milanjianus*, *Juniperus procera* and *Olea hochstetteri* (Kinyanjui, 2011; Krhoda, 1988). The vegetation changes into bamboo forest (*Arundinaria alpina*) above 2,300 m elevation. The north-western side of the forest, bordering smallholder agriculture, is degraded through encroachment of farms, livestock grazing, charcoal burning and logging (Bewernick, 2016). The smallholder agriculture area is characterised by small farms of less than 2 ha, where beans, maize, cabbage and potatoes are grown interspersed with grazing fields for livestock and small woodlots of Eucalyptus, Pine and Cypress. The riparian zones are severely degraded by vegetation clearance for grazing or cultivation and access to the river by humans and livestock. Commercial tea plantations, covering approximately 20,000 ha, are found at lower elevation (1,700–2,200 m) closer to Kericho town (0°22'08" S, 35°17'10" E) and consist of a mosaic of tea fields and Eucalyptus plantations, the latter mainly being used for tea processing. Riparian forests of up to 30 m width are well-maintained and contain native tree species, such as *Macaranga kilimandscharica*, *Polyscias kikuyuensis*, *Olea hochstetteri* and *Casearia battiscombei* (Ekirapa and Shitakha, 1996). A more detailed description of land use in the study area can be found in Jacobs et al. (2017).

The geology in OUT originates from the early Miocene, with the lower part, encompassing NF and TTP, dominated by phonolites and the upper part, covering SHA, by phonolitic nephelinites with a variety of Tertiary tuffs (Binge, 1962; Jennings, 1971). The soils are deep and well-drained, classified as humic Nitisols (ISRIC, 2007; Krhoda, 1988). The area has a bi-modal rainfall pattern with highest rainfall between April and July (long rains) and October and December (short rains). January to March are the driest months. Long-term annual precipitation at 2,100 m elevation is 1,988±328 mm yr^{-1} (Jacobs et al., 2017).

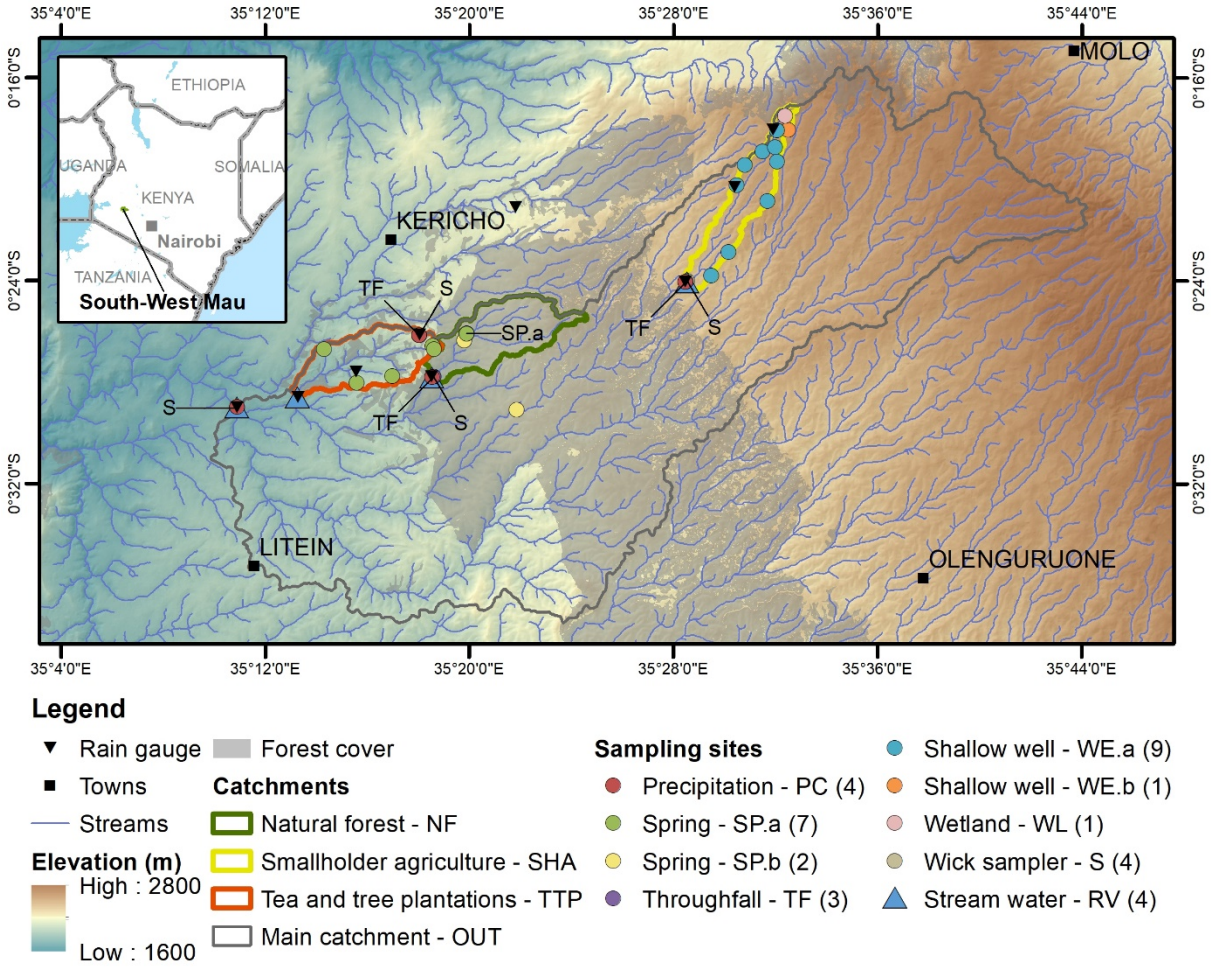

Figure 4.1 Map of the study area in the South-West Mau, Kenya, showing the three sub-catchments with different land use types within the main catchment, location of rain gauges, and sampling sites for stream water and selected end members. Sampling sites with overlapping symbols are indicated with labels instead of symbols. Numbers in brackets in the legend indicate the number of sampling sites per end member.

Table 4.1 Physical and hydroclimatic characteristics of the study catchments in the South-West Mau, Kenya. Precipitation, specific discharge and runoff ratio are presented for the study period of 15 October 2015 to 14 October 2016.

Catchment	Area	Elevation	Slope[a]	Precipitation	Specific discharge	RR[b]
	km²	*m*	*%*	*mm yr^{-1}*	*mm yr^{-1}*	-
Natural forest (NF)	35.9	1,954–2,385	15.5±8.0	2,299	744	0.323
Smallholder agriculture (SHA)	27.2	2,380–2,691	11.5±6.5	1,738	607	0.349
Tea and tree plantations (TTP)	33.3	1,786–2,141	12.2±7.3	2,045	791	0.387
Main catchment (OUT)	1021.3	1,715–2,932	12.8±7.7	2,019	701	0.347

[a] Mean±SD; [b] Runoff ratio, i.e. ratio of specific discharge to precipitation

4.2.2 Hydroclimatic instrumentation

Hydroclimatic data has been measured in the study area since October 2014 at a 10 minute interval (Jacobs et al., 2018). Water level data was recorded at the outlet of each catchment with a radar based sensor (VEGAPULS WL61, VEGA Grieshaber KG, Schiltach, Germany). Discharge was estimated from this data using a site-specific second order polynomial rating curve (Jacobs et al., 2018). Nine tipping bucket rain gauges (Theodor Friedrichs, Schenefeld, Germany and ECRN-100 high resolution rain gauge, Decagon Devices, Pullman WA, USA) were installed in the study area across an elevation gradient of 1,717 to 2,602 m (Figure 4.1). Each tipping bucket recorded cumulative precipitation (resolution of 0.2 mm per tip) per 10 minutes. Precipitation in each catchment was calculated using Thiessen polygons.

4.2.3 Sampling and laboratory analysis

Each catchment had one site with a precipitation and throughfall sampler, constructed of a 1 litre glass bottle covered with aluminium foil and a funnel of 12.5 cm diameter with a table tennis ball to reduce sample fractionation due to evaporation (Windhorst et al., 2013). The throughfall sampler was placed inside the forest, underneath maize or sugar cane (depending on growing season) and underneath tea bushes in NF, SHA and TTP, respectively. The main catchment only had a precipitation sampler. Additionally, a passive capillary wick sampler was installed in each catchment to collect soil water (Brown et al., 1989). Three PE plates of 30 by 30 cm were inserted horizontally at 15, 30 and 50 cm depth in the soil with as little disturbance of the soil above and around the plate as possible. A glass fibre wick was unravelled and draped on top of each plate to maximize surface area. The remaining wick length was led through a hosepipe to a 1 litre glass bottle, which was placed at 1 to 1.5 m depth in the soil. The installation of all samplers was carried out in September 2015 and stable isotope samples were collected from 15 October 2015 to 17 March 2017. Stream water samples were taken at the outlet of all catchments on a weekly basis. The samples were filtered with 0.45 µm polypropylene filters (Whatman Puradisc 25 syringe filter, GE Healthcare, Little Chalfont, UK or KX syringe filter, Kinesis Ltd., St. Neods, UK) and stored in 2 ml glass vials with screw cap. Weekly integrated stable isotope samples were collected from the wick, precipitation and throughfall samplers. Water samples were analysed for isotopic composition in the laboratory of Justus Liebig University Giessen, Germany, with cavity ring-down spectroscopy (Picarro, Santa Clara CA, USA). Precipitation water samples

from all four sites were used to calculate the local meteoric water line (LMWL) with a linear regression model and the 95% confidence interval was estimated for the slope and intercept. Only samples with a sampling volume of more than 100 ml were included to avoid the effect of evaporative enrichment of small sample volumes stored in the collector over the period between collections (Prechsl et al., 2014).

For end member mixing analysis (EMMA), samples were filtered with 0.45 µm polypropylene filters and collected in 25 to 30 ml HDPE bottles with screw cap. Samples were immediately acidified with nitric acid to pH < 2 and stored frozen until analysis for trace elements Li, Na, Mg, Al, Si, K, Ca, Cr, Fe, Cu, Zn, Rb, Sr, Y, Ba, Ce, La and Nd with inductively coupled plasma mass spectrometry (ICP-MS) in the laboratory of Justus Liebig University Giessen, Germany (n = 122) or the University of Hohenheim, Germany (n = 231). At the University of Hohenheim, samples were analysed for Al, Ca, K, Mg, Na and Si with inductively coupled plasma optical emission spectrometry (ICP-OES) instead of ICP-MS. Samples for EMMA were collected between 15 October 2015 and 21 October 2016. Weekly samples were taken for stream water, while precipitation and throughfall were sampled approximately every 4–6 weeks (n = 9–11). Due to difficult access to sampling sites, other potential water sources were sampled less frequently: wetland SHA-WL (n = 4) and spring NF-SP.b (n = 3). Springs NF-SP.a and TTP-SP.a were a combination of samples taken at different locations rather than different points in time with n = 2 and n = 5, respectively. Ten shallow wells (SHA-WE.a and SHA-WE.b) in SHA were sampled twice. Initially all samples for this end member were combined, but SHA-WE.b showed a chemical composition that strongly differed from the remaining samples and was therefore treated as a separate end member. No separate end member sampling was carried out for OUT, except for one spring sample and regular precipitation samples. Since all end members from the sub-catchments were sampled within OUT, these end members were used to identify potential streamflow sources for OUT. It was not possible to use samples collected from the wick samplers for EMMA, because the glass fibre wick could have contaminated the samples and the sample volume was generally too low (< 25 ml).

4.2.4 End member mixing analysis

The EMMA was carried out following the procedures described in Christophersen and Hooper (1992) and Hooper (2003). The final set of solutes to be included in the EMMA

was selected based on conservative behaviour of the solutes, which was assessed with bivariate scatter plots of all possible solute combinations, including stable water isotopes. A solute was considered conservative when it showed at least one significant ($p < 0.01$) linear relationship with another solute with $R^2 > 0.5$ (Hooper, 2003; James and Roulet, 2006). In our case these were Li, Na, Mg, K, Rb, Sr and Ba, i.e. elements which are commonly used in EMMA (Barthold et al., 2011).

The relative root mean square error (RRMSE) was calculated based on the measured and projected stream water concentrations for the selected solutes for up to four dimensions (i.e. principal components in EMMA). This was used to assess how many dimensions should be included in the analysis. Although higher-dimensional end member mixing models had lower RRMSE scores, the residual analysis (Hooper, 2003) and 'Rule of One' (last included dimension needs to explain at least $1/n^{th}$ of the variation, where n is the number of solutes included in the analysis) both indicated that a 2-dimensional end member mixing model with three end members was sufficient for all catchments. Median end member concentrations were projected in the 2-dimensional mixing space of the stream water samples of the respective catchments and the three end members enclosing most of the stream water samples in this mixing space were selected for EMMA. Then, contributions of each end member to streamflow were calculated. Although it is common practice to project stream water samples that fall outside the triangle enclosed by the three selected end members back into the mixing space to constrain end member contributions to a range of 0 to 100%, we decided to omit this step as it is indicative of uncertainty in the analysis caused by uncertainty in field and laboratory analyses, non-conservative solute behaviour, unidentified end members, and temporal variability of end members (Barthold et al., 2010).

4.2.5 Mean transit time analysis

Model selection

Mean transit time (MTT) estimations of stream and soil water were obtained through lumped parameter models. In this approach, the transport of a tracer through a catchment is expressed mathematically by a convolution integral (Maloszewski and Zuber, 1982) in which the composition of the outflow (e.g. stream or soil water) C_{out} at a time t (time of exit) consists of a tracer C_{in} that falls uniformly on the catchment in a previous time step t' (time of entry), C_{in} becomes lagged according to its transit time distribution $g(t - t')$.

Having in mind that the time span $t - t'$ is in fact the tracer's transit time τ, the convolution integral could be expressed as Eq. (1), in which $g(\tau)$ is the weighting function (i.e. the tracer's transit time distribution TTD) that describes the normalized distribution of the tracer added instantaneously over an entire area (McGuire and McDonnell, 2006).

$$C_{\text{out}}(t) = \int_0^{\infty} C_{\text{in}}(t-\tau)g(\tau)d\tau \tag{4.1}$$

When using the convolution approach, any type of weighting function is referred as a lumped parameter model. In case preliminary insights of a system are to be obtained with scarce data, it is common practice to apply a set of models to analyse whether they yield similar results. Among the diverse model types, two-parameter models such as the gamma model (GM) or the exponential piston flow model (EPM) are commonly used for MTT estimations (Hrachowitz et al., 2010; McGuire and McDonnell, 2006) and were identified by Timbe et al. (2014) as most suited to infer MTT estimations of spring, stream and soil water in an Andean tropical montane forest catchment. We therefore chose to apply these models in our study (Table 4.2). For EPM, the parameter η is the ratio of the total volume to the volume of water with exponential distribution of transit times. If $\eta = 1$, the function corresponds to a fully exponential one-parameter model (EM), but there is no physical meaning for cases where $\eta < 1$. GM is a more general and flexible exponential-type of model. If $\alpha = 1$, the GM becomes an exponential model, but when $\alpha < 1$, a significant part of the flow is quickly transported to the river. Conversely, the signal of the concentration peak is delayed for $\alpha > 1$.

Table 4.2 Lumped parameter models used for the calculation of the mean transit times in the South-West Mau, Kenya.

Model	Transit time distribution $g(\tau)$	Parameter range for Monte Carlo simulations[a]
Gamma model (GM)	$\frac{\tau^{\alpha-1}}{\beta^{\alpha}\Gamma(\alpha)}\exp\left(-\frac{\tau}{\beta}\right)$	α [0.0001–10] τ [1–400] $\beta = \alpha/\tau$
Exponential piston flow model (EPM)	$\frac{\eta}{\tau}\exp\left(-\frac{\eta t}{\tau}+\eta-1\right)$ for $t \geq \tau(1-\eta^{-1})$ 0 for $t < \tau(1-\eta^{-1})$	τ [1–400] η [0.1–4]

[a] τ = tracer's mean transit time; α and β = shape parameters; η ratio of the total volume to the volume of water with exponential distribution of transit times. Units for parameters and their respective ranges are a-dimensional except for τ, which has units of time.

The selection of acceptable model parameters was based on the statistical comparison of 50,000 random simulations (Monte Carlo approach), which assumes a uniform random distribution of the variables of each model. For each site and model, the performance was evaluated based on the best matches to a predefined objective function: the Nash-Sutcliffe efficiency (NSE). Quantification of errors and deviations from the observed data were calculated using the root mean square error (RMSE) and the bias, respectively. MatLab R2017a was used for data handling and solving the convolution equation, while R was used for weighting the range of behavioural solutions (generalised likelihood uncertainty estimation, GLUE). When using GLUE, the range of behavioural solutions is discrete. In our case, the lower limit was set to 5% below the best fitting efficiency. In order to refine the limits of behavioural solutions, the 90% of the prediction limits were calculated for every variable through weighted quantiles between 0.05 and 0.95.

Selection of isotope data for the MTT analyses

Only $\delta^{18}O$ was used for MTT analysis, because the two measured conservative isotopes ($\delta^{18}O$ and $\delta^{2}H$) showed a strong linear relationship, meaning that similar estimations could be obtained by using just one isotope (Mosquera et al., 2016a). The isotopic signals of precipitation (weekly scheme, $n = 75$) were considered as input function of the lumped parameter models. The isotopic composition of throughfall samples, which were also collected (data not presented here), was not significantly different from that of precipitation, hence the same MTT could be obtained using data from throughfall samples. All the available weekly isotope data for stream water ($n = 75$) were included in the analysis, because the seasonal isotopic signatures of stream water (i.e., TTP-RV, SHA-RV, NF-RV and OUT-RV) were considerably damped compared to the seasonal isotopic signatures of rainfall (Figure 4.4). This means that, although some of the stream water samples could have been taken during interflow or high flow conditions, the isotopic signatures of those samples still showed a major component of 'old' or baseflow water.

The number of soil water samples ($n = 4$–47) was smaller than for stream water ($n = 75$). This was because wick samplers – the devices used to collect soil water – only collect the portion of the water moving through the soil, i.e. they start to collect water for soil conditions near to saturation. Only three sites had enough data to perform model

calibration and were therefore considered: NF-S15 (n = 47), OUT-S15 (n = 47) and OUT-S50 (n = 46).

4.3 Results

4.3.1 Solute concentrations

Most end members and stream water showed differences in median solute concentrations (Figure 4.2). Especially samples from shallow well WE.b in the smallholder agriculture catchment (SHA) had higher concentrations for most solutes than other end members. Concentrations were lowest in precipitation (PC) in all catchments, while throughfall (TF) in some catchments showed higher concentrations and more variation. These patterns were reflected in the total solute concentrations of the different end members, although the difference between shallow well WE.b and the other end members was not as pronounced.

4.3.2 Isotopic composition

Isotopic values for precipitation plotted slightly above the global meteoric water line (GMWL), resulting in a local meteoric water line (LMWL) with a slope of 8.05±0.21 δ^{18}O and an intercept of 15.31±0.61 δ^{2}H ($p < 0.001$, $R^2 = 0.962$; Figure 4.3). The slopes of the LMWL and GMWL were not significantly different ($p = 0.619$), but the intercepts were ($p < 0.001$). Samples far below the LMWL represented samples with a low sample volume (< 100 ml) affected by evaporative enrichment. There was no significant effect of elevation on δ^{18}O values of the precipitation samples, but precipitation samples collected at higher altitude (SHA-PC) were generally more depleted than those collected at lower altitudes (NF-PC, TTP-PC and OUT-PC). The linear regression slope for stream water samples was 5.00±0.54 δ^{18}O, which was significantly lower than the slope of the LMWL ($p < 0.001$). There was very little variation in isotopic values in streamflow throughout the study period, while values for precipitation showed pronounced minima in November 2015, May 2016 and November 2016 in all catchments (Figure 4.4).

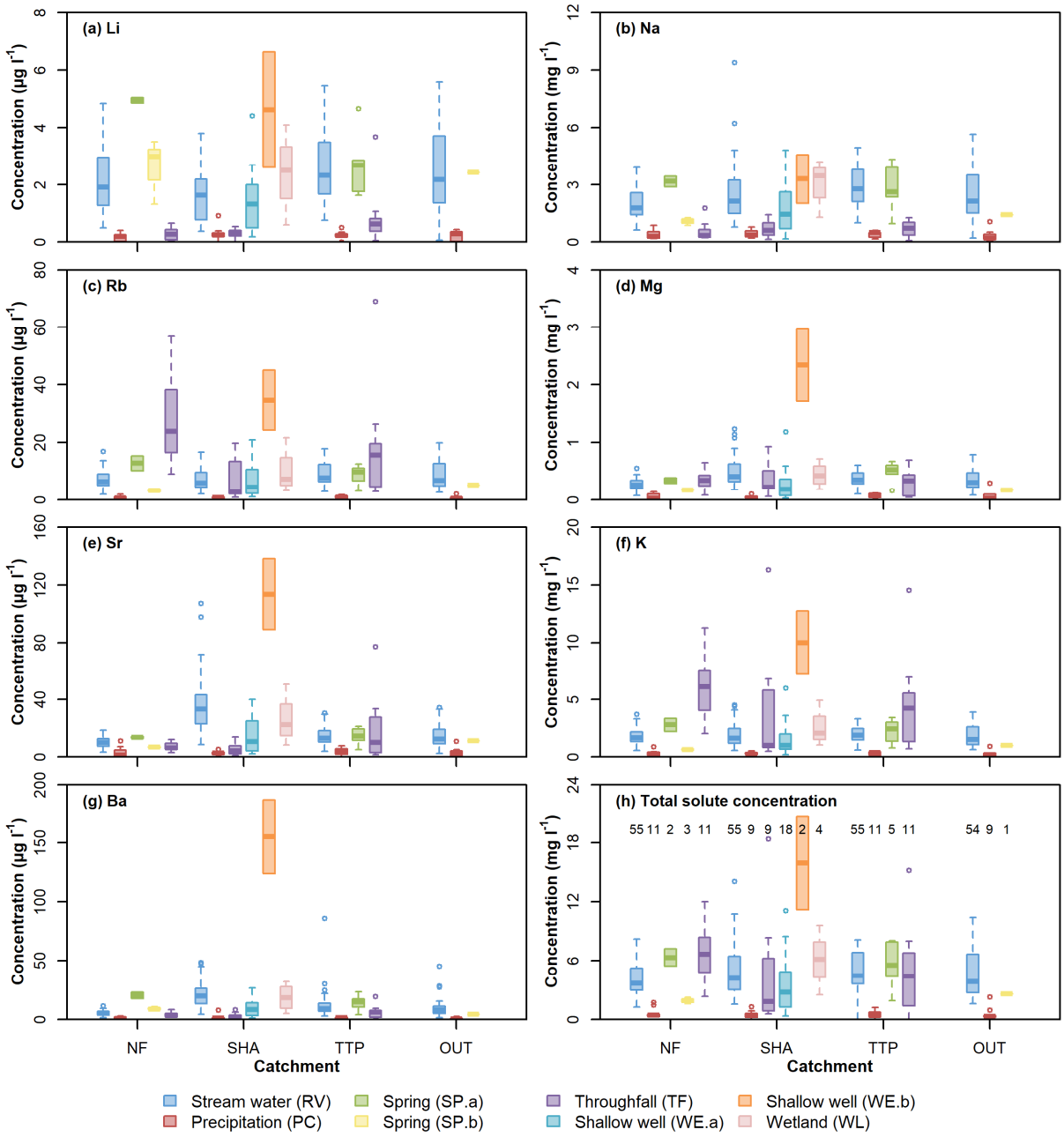

Figure 4.2 Box plots with concentrations of (a) Li, (b) Na, (c) Rb, (d) Mg, (e) Sr, (f) K and (g) Ba, and (h) total concentration of the selected solutes in stream water and sampled end members in the three sub-catchments with different land use (NF = natural forest, SHA = smallholder agriculture, TTP = tea and tree plantations) and the main catchment (OUT). The thick line represents the median, the box shows the interquartile range and the whiskers the minimum and maximum values within 1.5 times the interquartile range. Outliers are indicated with open circles. Numbers in plot (h) indicate the number of samples per end member.

4.3.3 End member contributions

Based on the projection of all end members in the stream water mixing space for each catchment, it was possible to identify three end members that would enclose most of the stream water samples for NF and SHA (Figure 4.5). However, this involved selection of two very specific sources with a low number of samples ($n = 2$), i.e. a combination of two springs NF-SP.a located close to each other, sampled on the same day for NF, and two samples taken from shallow well SHA-WE.b in the smallholder area. The sampled end members were not sufficient to capture the variability in stream water samples in TTP and OUT, with more than a third of the stream water samples falling outside the area enclosed by the three selected end members. Precipitation in all catchments plotted similarly in the mixing space of OUT. Also springs OUT-SP.b and NF-SP.b and the combination of nine shallow wells SHA-WE.a, as well as springs TTP-SP.a and NF-SP.a and wetland SHA-WL were similar, whereas there was considerable variation in chemical composition of throughfall (TF) samples, both within and between sub-catchments. Shallow well SHA-WE.b plotted far outside the mixing space of NF, TTP and OUT.

Predicted stream water solute concentrations, based on median solute concentrations of the selected end members, matched well with observed stream water solute concentrations ($R^2 > 0.85$ for most solutes). The EMMA resulted in a dominant contribution of precipitation (PC) in NF (45%) and SHA (59%), while spring water (TTP-SP.a) dominated in TTP (56%) (Figure 4.6). The three selected end members for OUT generally had similar contributions (30–40%). In NF and OUT the contribution of precipitation dropped towards the end of the dry season from more than 50% to less than 10% (March–April) and increased again to around 25% during the long rains. In this period, the contribution of throughfall was higher in NF (62%) and OUT (65%). Conversely, in SHA a strong drop in contribution of precipitation (from 86 to 30%) was observed at the start of the long rains in May 2016. Precipitation did not contribute to streamflow in TTP during the dry season, whereas the contribution of spring water TTP-SP.a was highly overestimated (up to 853%). Contributions of end members during the second half of the study period in SHA differed from the first half, with an increase in contributions of wetland SHA-WL from 1 to 58%. Generally, the contribution of the wetland was higher during periods of high flow in SHA (51%) – similar to contributions of springs SP.a in NF and TTP. Conversely, shallow well SHA-WE.b in SHA showed highest contributions during the dry season (up to 54%).

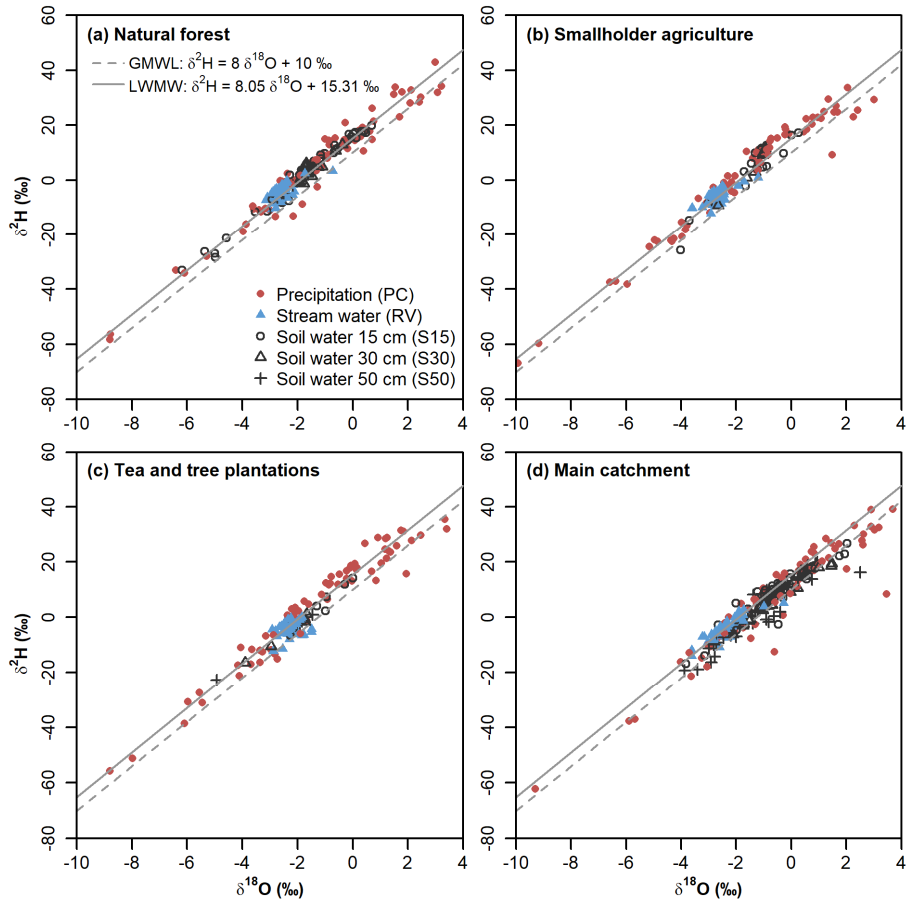

Figure 4.3 Relationship between $\delta^{18}O$ and $\delta^{2}H$ values in precipitation (PC), stream water (RV) and soil water at 15, 30 and 50 cm depth (S15, S30 and S50, respectively) for the (a) natural forest (NF), (b) smallholder agriculture (SHA), and (c) tea and tree plantations (TTP) sub-catchments, and (d) the main catchment (OUT) between 15 October 2015 and 17 March 2017 in the South-West Mau, Kenya. The global meteoric water line (GMWL) and local meteoric water line (LMWL) are indicated as dashed and solid lines, respectively.

4.3.4 MTT estimates for stream and soil water

Based on the Nash-Sutcliffe efficiency (NSE), it was clear that the gamma model (GM) provided a better mean transit time (MTT) estimate for stream water than the exponential piston flow model (EPM; Table 4.3). The best performance was observed for OUT-RV (NSE = 0.33), while TTP-RV had a very low performance (NSE = 0.05) and was therefore discarded. The generally low fitting efficiencies were caused by the low amplitude of seasonal isotopic signatures of $\delta^{18}O$ in stream water samples from all four catchments (see standard deviation of observed values in Table 4.3; Figure 4.3–4.4). There was a moderate positive relationship between the standard deviation of the observed values and corresponding NSE of modelled results (R^2 = 0.84). NF-RV and SHA-RV had a similar

estimated MTT of approximately 4 years (Table 4.3). However, similar to TTP-RV, the poor fit to the objective functions (NSE = 0.15 and NSE = 0.22, respectively) could be related to the highly damped isotopic signature and should be interpreted with care. The shortest estimated MTT of 2.5 years was for OUT-RV.

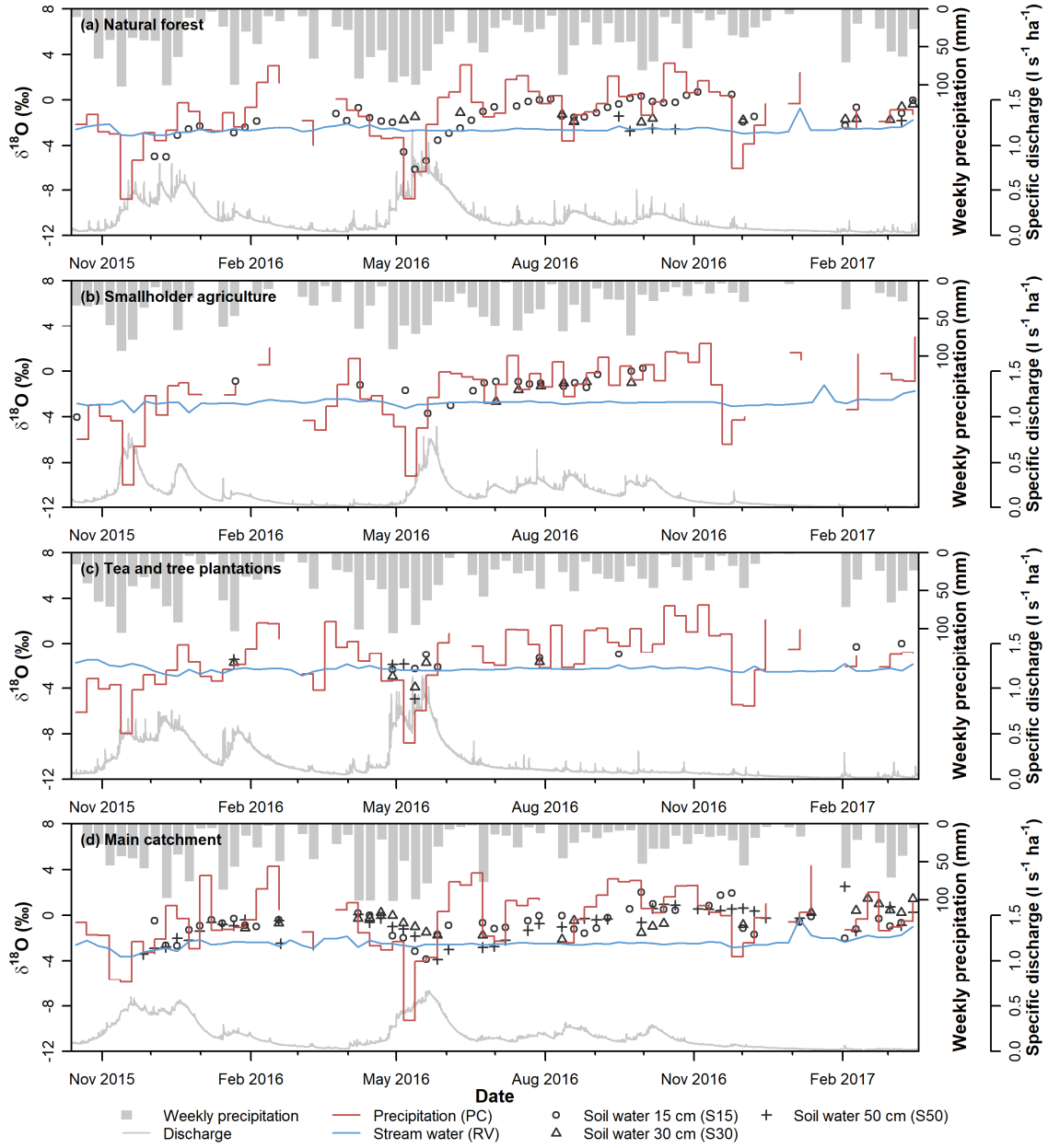

Figure 4.4 Time series of $\delta^{18}O$ values in precipitation (PC), stream water (RV) and soil water at 15, 30 and 50 cm depth (S15, S30 and S50, respectively), specific discharge and weekly precipitation in the (a) natural forest (NF), (b) smallholder agriculture (SHA), and (c) tea and tree plantations (TTP) sub-catchments, and (d) the main catchment (OUT) between 15 October 2015 and 17 March 2017 in the South-West Mau, Kenya.

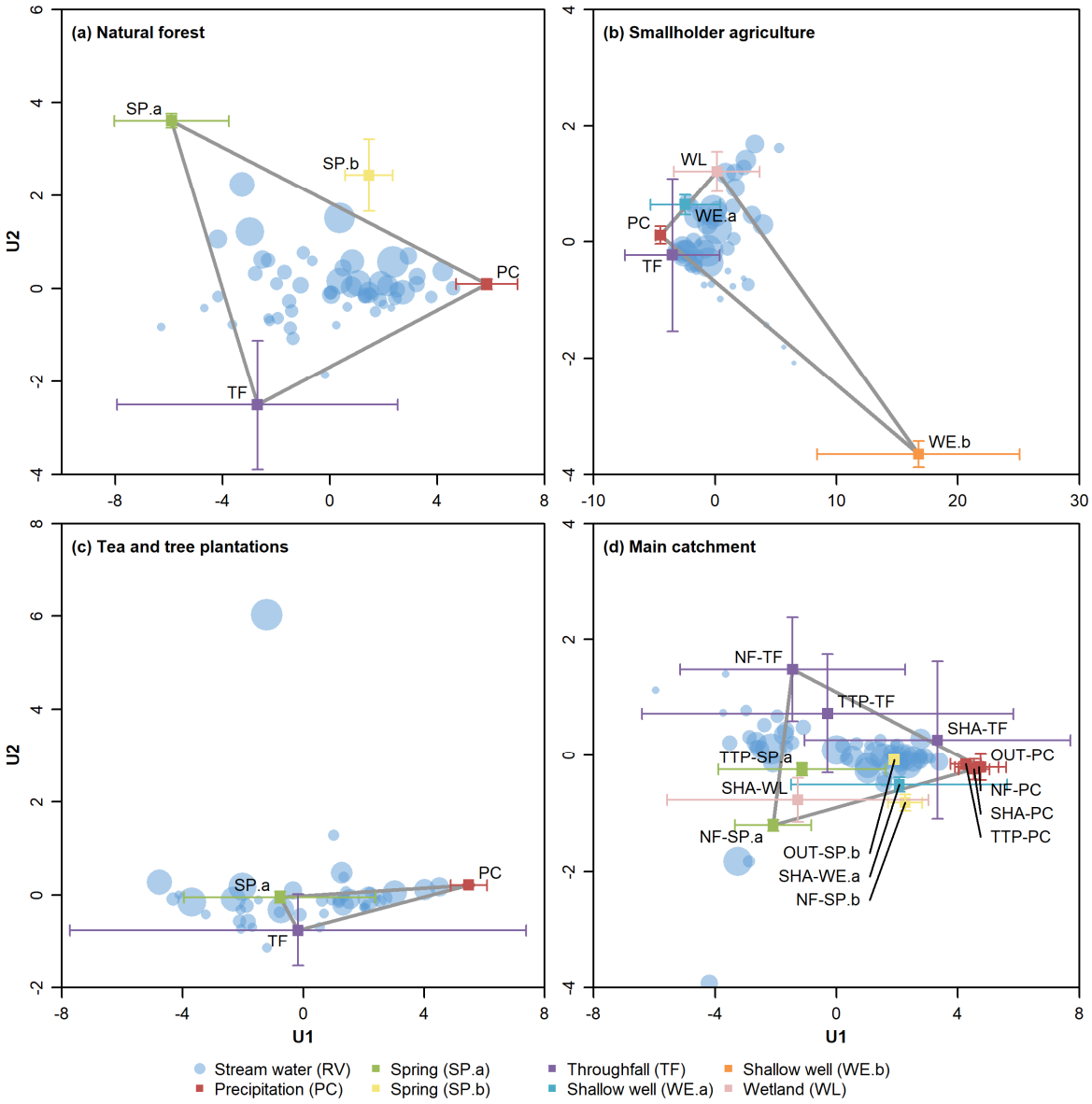

Figure 4.5 Projection of end members in the 2-dimensional (U1 and U2) mixing space of stream water samples of the (a) natural forest (NF), (b) smallholder agriculture (SHA), and (c) tea and tree plantation (TTP) sub-catchments and (d) the main catchment (OUT) in the South-West Mau, Kenya between 15 October 2015 and 21 October 2016. The size of the symbol for stream water represents the relative discharge at the time of sampling (larger symbol means higher discharge).

For soil water, both models (GM and EPM) yielded similar results in terms of fitting efficiencies (NSE), MTT estimations and uncertainty ranges (Table 4.4). NF-S15 showed the shortest estimated transit time (3.2–3.3 weeks). The estimated transit time for OUT-S15 (4.5–7.5 weeks) was longer than for NF-S15, but shorter than for OUT-S50 (10.4–10.8 weeks).

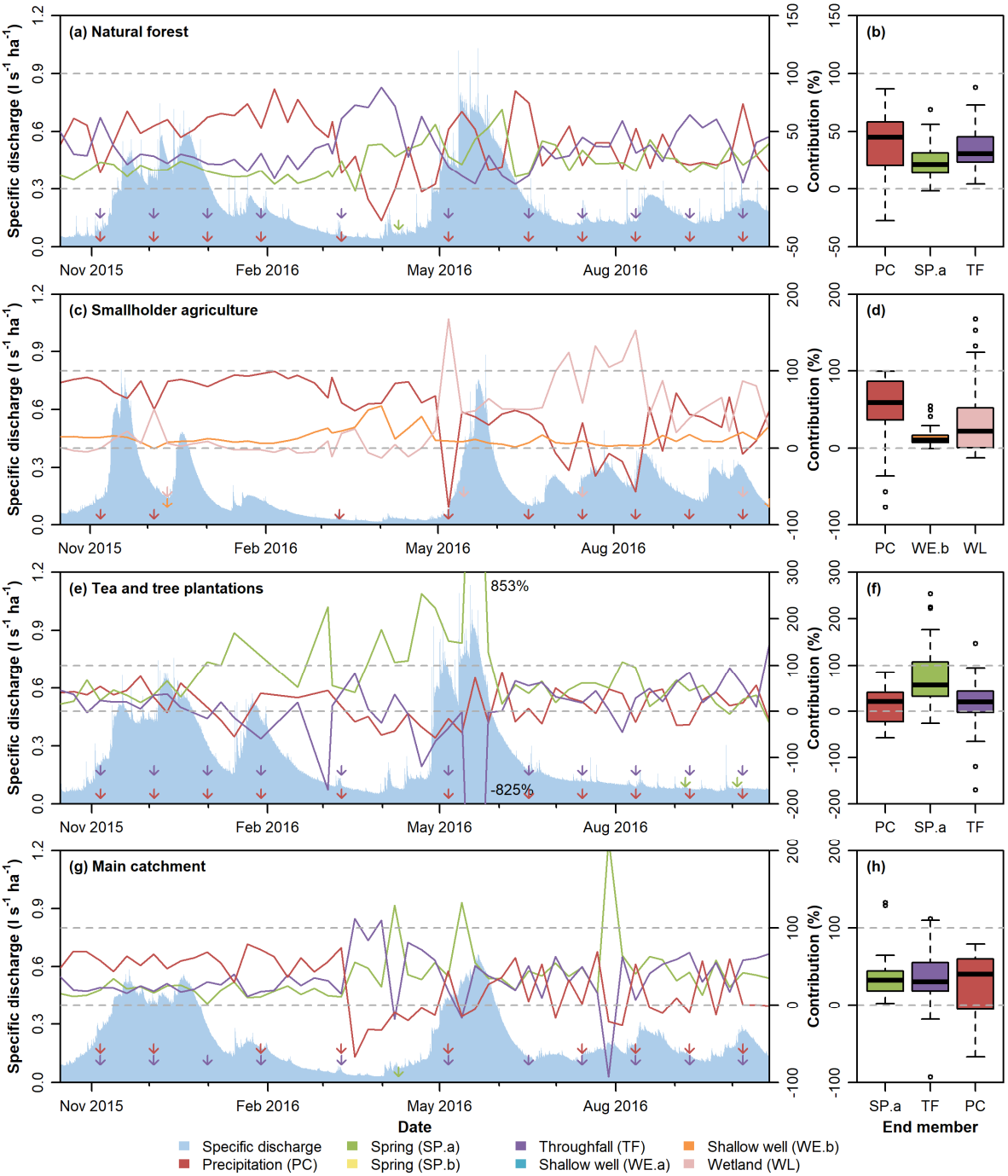

Figure 4.6 Specific discharge (shaded) and contribution of selected end members to streamflow for the (a–b) natural forest (NF), (c–d) smallholder agriculture (SHA) and (e–f) tea and tea plantation (TTP) sub-catchments and (g–h) the main catchment (OUT) in the South-West Mau, Kenya between 15 October 2015 and 21 October 2016. The grey dashed lines indicate the realistic range of end member contributions and arrows show sampling dates for end members. The thick line in the box plots represents the median, the box shows the interquartile range and the whiskers the minimum and maximum values within 1.5 times the interquartile range. Outliers are indicated with open circles.

Table 4.3 Main statistical parameters of observed and modelled $\delta^{18}O$ for stream water in the three sub-catchments and the main catchments for the gamma model (GM) and exponential piston flow model (EPM). Uncertainty bounds of the modelled parameters (MTT and α or η), in parentheses, were calculated through generalized likelihood uncertainty estimation (GLUE).

Site[a]	Area	Elevation	Observed $\delta^{18}O$		Modelled $\delta^{18}O$						
			Mean	SD[b]	Mean	SD[b]	NSE[c]	RMSE[d]	Bias	MTT[e]	α/η[f]
	km²	*m*	*‰*	*‰*	*‰*	*‰*	-	*‰*	*‰*	*years*	-
Gamma model (GM)											
NF-RV	35.9	1,969	−2.58	0.32	−2.56	0.13	0.15	0.30	0.021	4.0 (3.3–4.6)	0.65 (0.63–0.71)
SHA-RV	27.2	2,386	−2.72	0.31	−2.69	0.16	0.22	0.27	0.029	3.8 (3.1–4.5)	0.61 (0.57–0.66)
TTP-RV	33.3	1,788	−2.29	0.26	−2.29	0.06	0.05	0.25	0.000	3.3 (2.8–4.3)	1.09 (0.99–1.17)
OUT-RV	1021.3	1,717	−2.42	0.47	−2.36	0.26	0.33	0.38	0.061	2.5 (1.8–3.4)	0.48 (0.43–0.54)
Exponential piston flow model (EPM)											
NF-RV	35.9	1,969	−2.58	0.32	−2.58	0.10	0.09	0.31	0.000	2.4 (2.1–2.9)	1.000 (0.994–1.003)
SHA-RV	27.2	2,386	−2.72	0.31	−2.72	0.11	0.12	0.29	0.000	2.2 (1.9–2.6)	1.001 (0.994–1.004)
TTP-RV	33.3	1,788	−2.29	0.26	−2.29	0.07	0.07	0.25	0.000	3.5 (3.1–4.1)	1.011 (1.009–1.018)
OUT-RV	1,021.3	1,717	−2.42	0.47	−2.42	0.20	0.14	0.43	0.001	1.2 (1.0–1.4)	1.001 (0.998–1.007)

[a] NF = natural forest, SHA = smallholder agriculture, TTP = tea and tree plantations, OUT = main catchment, RV = stream water; [b] standard deviation; [c] Nash-Sutcliffe efficiency of objective function; [d] root mean square error; [e] estimated mean transit time (in years); [f] model parameters for GM (α) and EPM (η).

Table 4.4 Main statistical parameters of observed and modelled $\delta^{18}O$ for soil water at 15 cm depth in the natural forest sub-catchment and at 15 and 50 cm depth in the main catchment for the gamma model (GM) and exponential piston flow model (EPM). Uncertainty bounds of the modelled parameters (MTT and α or η), in parentheses, were calculated through generalized likelihood uncertainty estimation (GLUE).

Site[a]	n[b]	Elevation	Observed $\delta^{18}O$		Modelled $\delta^{18}O$						
			Mean	SD[c]	Mean	SD[c]	NSE[d]	RMSE[e]	Bias	MTT[f]	α/η[g]
	-	*m*	‰	‰	‰	‰	-	‰	‰	*weeks*	-
Gamma model (GM)											
NF-S15	47	1,971	−1.62	1.64	−1.74	1.48	0.79	0.75	−0.12	3.2 (2.8–4.1)	1.5 (0.9–2.2)
OUT-S15	47	1,721	−0.68	1.20	−0.71	0.99	0.50	0.84	−0.03	7.9 (6.1–11.3)	0.9 (0.6–1.2)
OUT-S50	46	1,721	−0.84	1.35	−0.92	0.93	0.47	0.97	−0.08	10.4 (8.8–12.6)	1.4 (1.1–2.0)
Exponential piston flow model (EPM)											
NF-S15	47	1,971	−1.62	1.64	−1.67	1.38	0.78	0.77	−0.05	3.3 (2.6–4.4)	1.0 (0.9–1.1)
OUT-S15	47	1,721	−0.68	1.20	−0.58	0.94	0.52	0.82	0.11	4.5 (3.2–6.7)	0.8 (0.7–1.1)
OUT-S50	46	1,721	−0.84	1.35	−0.90	0.85	0.46	0.99	−0.06	10.8 (8.0–13.9)	1.0 (0.9–1.3)

[a] NF = natural forest, OUT = main catchment, S15 = soil water 15 cm depth, S50 = soil water 50 cm depth; [f] number of samples; [c] standard deviation; [d] Nash-Sutcliffe efficiency of objective function; [e] root mean square error; [f] predicted mean transit time (in weeks); [g] model parameters for GM (α) and EPM (η).

4.4 Discussion

4.4.1 Hydrochemistry

While precipitation (PC) had low solute concentrations at all sites, throughfall (TF) concentrations were much more variable in space and time, although solute concentrations were generally not significantly different between sites. This has been observed elsewhere as well (e.g. Ali et al., 2010; Germer et al., 2007) and can be attributed to seasonal variations in plant growth and dry and wet atmospheric deposition of elements such as Na, K and Mg originating from sea salts or biomass burning. Shallow well SHA-WE.b had trace element concentrations that were much higher than those of the other nine sampled shallow wells SHA-WE.a. Wetland SHA-WL, located near shallow well SHA-WE.b, did not show these high concentrations, which could indicate that the shallow well received water from a different groundwater source than the wetland and other shallow wells. Similarity in solute concentrations in springs NF-SP.b and OUT-SP.b and shallow wells SHA-WE.a indicate that these end members represent the same water source, despite their different geographical location. The same was observed for wetland SHA-WL and springs NF-SP.a and TTP-SP.a.

The higher intercept of the local meteoric water line (LMWL) than of the global meteoric water line (GMWL) indicates deuterium-excess (*d*-excess) as consequence of more arid vapour sources (McGuire and McDonnell, 2007) or re-evaporated rainfall (Goldsmith et al., 2012). Similar *d*-excess values have been observed in many tropical montane environments (e.g. Goldsmith et al., 2012; Mosquera et al., 2016a; Muñoz-Villers et al., 2016; Otte et al., 2017; Windhorst et al., 2013). The value for the slope of the linear relation between stream water isotopic values (5.00±0.54) was similar to that found by Craig (1961) for East African rivers and lakes and suggests evaporative enrichment of stream water. The observed altitude effect (−0.099‰ δ^{18}O per 100 m) is smaller than the −0.22‰ δ^{18}O per 100 m found in an Andean tropical montane forest (Windhorst et al., 2013), −0.31‰ δ^{18}O per 100 m in an Ecuadorian Páramo ecosystem (Mosquera et al., 2016a), but similar to values of −0.10 and −0.11‰ δ^{18}O per 100 m observed on Mt. Kilimanjaro in Tanzania (Mckenzie et al., 2010; Otte et al., 2017). The occurrence of the lowest precipitation δ^{18}O values during the rainy seasons also agrees with seasonal observations by Otte et al. (2017) on Mt. Kilimanjaro and is most likely related to the different isotopic composition of precipitation from storms caused by the movement of the intertropical convergence zone (ITCZ) over the study area during the rainy seasons (Otte et al., 2017). Furthermore, most storm trajectories originate from south-easterly direction during the long and short rainy season, while coming from an easterly direction during the dry season, suggesting different origin and thus isotopic composition of precipitation (Soderberg et al., 2013).

4.4.2 Dominant water sources

The end member mixing analysis (EMMA) showed that precipitation (PC) was always one of the three selected end members in all catchments, as depicted in our conceptual model of the rainfall–runoff generation processes in the three sub-catchments with different land use (Figure 4.7). Although the use of a single throughfall sampler might not be sufficient to capture the spatial variation in throughfall chemistry (Zimmermann et al., 2007), throughfall (TF) was selected as an additional end member for all catchments, except in the smallholder agriculture sub-catchment (SHA). The high contribution of precipitation (21–59%) in all catchments and throughfall (31–40%) in the natural forest (NF) sub-catchment and the main catchment (OUT) suggest high contributions of channel precipitation, surface runoff or rapid sub-surface flow. However, given the size of streams, it is unlikely that channel precipitation alters the stream's composition to such

an extent. Although surface runoff can occur in tropical forests (e.g. Chaves et al., 2008; de Moraes et al., 2006; Johnson et al., 2006b) and was observed on paths in NF, a major contribution of surface runoff is unlikely due to high infiltration rates and hydraulic conductivity of forest soils (Owuor et al., 2018). We therefore conclude that the observed signatures were caused by shallow sub-surface flow during rainfall events, which agrees with findings in NF by Jacobs et al. (2018) and is commonly observed in tropical montane forested catchments (e.g. Boy et al., 2008; Muñoz-Villers and McDonnell, 2012; Saunders et al., 2006). The extent to which the chemical composition of water changes through contact with the soil depends on the contact time (McGuire and McDonnell, 2006; Mulholland et al., 1990). Therefore, if event water, i.e. precipitation or throughfall, is only in contact with the soil for a short time (e.g. several hours), the chemical composition of the water that enters the stream might be comparable to the composition of precipitation or throughfall. Furthermore, if the riparian zone is near saturation, which occurs in the relatively flat valley bottoms in NF, only a small fraction of the precipitation can infiltrate and storage capacity is limited, resulting in shallow flow from the riparian zone during rainfall events (Mosquera et al., 2015; von Freyberg et al., 2014). Similar to our study, Chaves et al. (2008) found that the precipitation/throughfall end member contributed most to streamflow in a forested Amazonian catchment.

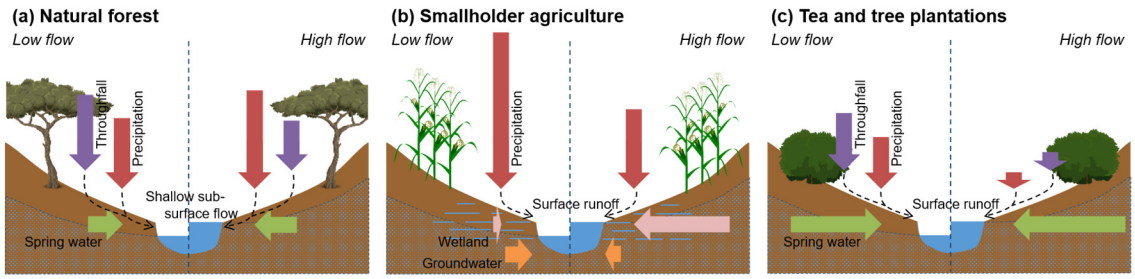

Figure 4.7 Conceptual model of dominant water sources and flow paths in different land use types during low (≤ mean discharge) and high flows (> mean discharge) in a tropical montane area: (a) natural forest (NF), (b) smallholder agriculture (SHA) and (c) commercial tea and tree plantations (TTP), based on results of end member mixing and mean transit time analysis in the South-West Mau, Kenya. Arrow length represents the median contribution (%) of each end member. Black dashed arrows show the most likely pathway for precipitation and throughfall to reach the stream.

The relatively low contribution of precipitation to streamflow in the tea and tree plantation sub-catchment (TTP) compared to the other sub-catchments suggests a minor input of

surface runoff to streamflow during both wet and dry conditions (Figure 4.7). This seemingly contradicts previous findings in the same sub-catchment, where rainfall events led to significant dilution of nitrate concentrations in stream water due to surface runoff (Jacobs et al., 2018). However, surface runoff could have a different chemical signature than precipitation (Chaves et al., 2008). Most of the surface runoff in TTP seems to be generated on footpaths and roads. Emissions from traffic and wear of tyres could also change the surface runoff composition (Gan et al., 2008). However, the chemical composition of stream water samples did not correspond to trace elements related to traffic (Mn, Pb, Cu, Zn and Cr; Gunawardena et al., 2015), but rather indicated mineral origin (high concentrations of Si, Li, K, Na and Rb; data not presented here). Specific sampling of surface runoff and subsequent inclusion as separate end member could improve the end member mixing model performance. Similar to Muñoz-Villers and McDonnell (2012) and Chaves et al. (2008), the contribution of precipitation and throughfall decreased in all sub-catchments during high flows (Figure 4.7, right hillslopes in each graph). This suggests increased inputs from groundwater through wetlands (SHA-WL) or springs (TTP-SP.a and NF-SP.a) during the rainy season. These findings support our hypothesis that there are temporal changes in the contribution of the different end members in this African tropical montane ecosystem, similar to South American tropical montane catchment (Chaves et al., 2008; Correa et al., 2017). Groundwater end member SHA-WE.b in SHA showed contrasting behaviour, with highest contributions during low flow periods, suggesting that this is a different groundwater source and an important component of baseflow in SHA.

The triangle bounded by the three selected end members in the stream water mixing space of NF (precipitation, throughfall and springs SP.a; Figure 4.5) encompassed most of the stream water samples, with only 9% of the samples falling outside the triangle. However, in SHA, TTP and OUT 42, 49 and 33% of the samples fell outside the triangle of the three selected end members, respectively. Although this could be attributed to the variability in end member composition, uncertainty in laboratory analysis or non-conservative solute behaviour (Barthold et al., 2010), it is very likely that one or more end members are missing, which could be better suited to explain the observed chemical composition of stream water at the catchment outlet. Alternatively, inclusion of additional end members to increase dimensionality of the end member model may be required to satisfactorily represent the behaviour and stream water sources in these catchments, as observed for an

Andean Páramo ecosystem (Correa et al., 2017). The selection of tracers and number of end members is highly subjective and can therefore significantly affect the outcomes of the EMMA (Barthold et al., 2011). Furthermore, although the chemical signature of end members should be invariable in space and time according to the EMMA assumptions, a more consistent sampling approach whereby all end members are sampled on a regular basis could also improve the performance of the models, because the full range of chemical variation in time would be captured (Neill et al., 2011). In our case this was not possible, because most sampling sites were difficult to access.

Another shortcoming of our sampling approach is that springs, shallow wells and wetlands might not accurately represent groundwater, although this could be an important end member, as observed in many studies (e.g. Barthold et al., 2011; Chaves et al., 2008; Crespo et al., 2012; Katsuyama et al., 2009). Access to groundwater in the study area is complicated by the absence of wells or boreholes in NF and TTP, and the existing wells in SHA are often not properly sealed, which means that groundwater can mix with water from shallower soil layers and precipitation, obscuring the groundwater signal. Jacobs et al. (2018) suggested that discharge contributing zones change with the seasons, which could be tested by inclusion of soil water as end member. This was not possible with the current experimental set-up, because the glass fibre wick in the wick samplers could contaminate the trace element samples. Especially soil water from different topographical locations within the catchment (e.g. riparian zone and hillslope) or different soil types could yield further insight in the dynamics of discharge contributing zones and important flow paths during different seasons.

4.4.3 Mean transit times

The low variation in isotopic signatures (−3.6 to −0.3‰ for $\delta^{18}O$) observed for stream water compared to precipitation (−9.9 to 4.4‰) at all sites suggests long travel times. Equally damped signals (−8.0 to −6.2‰ versus −15.2 to −0.4‰ for $\delta^{18}O$ in stream water and precipitation, respectively) were observed in a Mexican tropical montane forest catchment (Muñoz-Villers and McDonnell, 2012). The long transit time could be explained by the deep and well-drained soils in our study area (Cooper, 1979; Edwards and Blackie, 1981), which promote slow flow paths through deeper soil layers and longer transit times (Asano and Uchida, 2012). The most damped isotopic signature was observed at TTP (SD = 0.26‰ for $\delta^{18}O$; Table 4.3), which suggests that stream water in

this sub-catchments is older than at all other sites. Most likely, the MTT is longer than 4 years and is therefore beyond the reliability of the present used method with $\delta^{18}O$ or $\delta^{2}H$ tracers, which also explains the very low Nash-Sutcliffe efficiency (NSE). Better predictions could be obtained by using more appropriate tracers for estimating transit times of several years to decades, such at tritium (^{3}H) (Cartwright et al., 2017). A longer sampling period of at least 4 years would also improve the reliability of the mean transit time estimates (McGuire and McDonnell, 2006). Although the gamma model (GM) used in this study was found to be most suitable for the estimation of stream water MTT in other tropical montane catchments (Muñoz-Villers and McDonnell, 2012; Timbe et al., 2014), it is also possible that the applied method for MTT estimation is less suitable for tropical catchments with highly damped isotope signals and low seasonal variation, as indicated by the low NSE for all stream water sites.

Because of the similar estimated MTTs for NF and SHA and the most likely longer MTT for TTP, we rejected our hypothesis that agricultural catchments have a shorter MTT than forested catchments due to increased importance of faster flow paths such as surface runoff. Evidence from other studies suggests that the role of vegetation cover in water storage and MTT could be suppressed by geomorphology (Timbe et al., 2017) or soil hydraulic properties (Geris et al., 2015; Mueller et al., 2013; Muñoz-Villers et al., 2016). The latter, however, can also be influenced by land use. The MTT of ~4 years in the three sub-catchments suggests that most of the stream water originates from 'old' water or groundwater, which corresponds with the importance of groundwater-related end members springs TTP-SP.a and NF-SP.a and wetland SHA-WL in the sub-catchments. The runoff ratios in all catchments (0.323–0.387) confirm that a small part of the precipitation leaves the catchment as discharge. Similar runoff ratios (0.30) and MTT (~3 years) were obtained in a Mexican montane forest catchment with deep volcanic soils, but higher annual precipitation (Muñoz-Villers and McDonnell, 2012). However, Andean tropical montane catchments had higher runoff ratios (0.76–0.81) and correspondingly shorter MTTs (< 1 year) (Crespo et al., 2012), which could be caused by steeper slopes and shallower soils compared to our study area. The importance of groundwater does, however, contradict the generally high contribution of precipitation and throughfall to streamflow in most catchments. The use of bulked precipitation and weekly stream water samples as input could cause a bias towards older groundwater, because the direct effect of storm events on stream water isotope composition are removed from the analysis

(McGuire and McDonnell, 2006). Although samples obtained during high flow in the rainy season were not removed from our analysis, the use of bulked samples could have underestimated the importance of faster flow paths during rainfall events and therefore partly explain the discrepancy between the long transit times and high contribution of precipitation and throughfall to streamflow in most catchments.

The shorter estimated MTT for OUT compared to the sub-catchments is counterintuitive, since it is the largest catchment. One could also expect that, since OUT is a mixture of the three land use types dominating the sub-catchments, the MTT should be similar to or an average of the estimated MTTs of the sub-catchments. MTT is, however, not always correlated to catchment area (McGuire et al., 2005; Rodgers et al., 2005b), but seems more related to other hydrological and topographical metrics such as drainage density and slope (Capell et al., 2012). Also geology and presence of hydrologically responsive soils seem to be important determinants for MTT (Capell et al., 2012; Tetzlaff et al., 2007). The occurrence of other soil types (mollic Andosols) and underlying geology (pyroclastic unconsolidated rock) in the upper part of OUT (ISRIC, 2007) compared to the humic Nitisols and igneous rock dominating the three sub-catchments could lead to differences in soil hydraulic properties and sub-surface water storage and eventually MTT, but not enough data are available for the study area to test this.

The longer MTT for soil water for OUT-S15, located in a pasture, than for NF-S15 contradicts findings by Timbe et al. (2014), who compared pasture and forest soil water MTT and found longer MTTs for forested sites. In our case, the difference could be caused by differences in hydraulic conductivity. Pasture soils in our study area had a generally lower hydraulic conductivity (2–53 cm h^{-1}) than natural forest soils (10–207 cm h^{-1}) due to soil compaction by animal trampling (Owuor et al., 2018). Differences in soil hydraulic properties between land use types are, however, mainly restricted to the topsoil, while deeper soil layers are usually less affected by land management (Zimmermann et al., 2006). The estimated MTTs fell within the range observed for soil water from 30 to 60 cm depth (20–62 days) in a tropical montane catchment in Mexico (Muñoz-Villers and McDonnell, 2012). For soil water MTT estimation, the second parameter (α) for GM was around 1.5 for the best-modelled efficiencies for NF-S15 and OUT-S50. However, according to the range of behavioural solutions, all soil sites could be well represented by gamma functions with α values of 1 (Table 4.4), which means a

simple exponential distribution function (EM). Similarly, the exponential piston flow model (EPM) can yield similar results with $\eta = 1$ for all analysed cases, meaning that EPM could also be simplified as EM, i.e. without any portion of piston flow participating in the transport. Therefore, results from both models point out that the same predictions could be obtained with a simpler, single parameter exponential model, as was used for estimation of MTT of soil water at 30 cm by Muñoz-Villers and McDonnell (2012). In order to avoid over-parametrization, models with less parameters are preferred when they provide comparable results.

4.5 Conclusion

In this study we aimed to identify the dominant water sources and flow paths in three sub-catchments with contrasting land use (i.e. natural forest, smallholder agriculture and commercial tea and tree plantations) using mean transit time (MTT) analysis and end member mixing analysis (EMMA) to assess the effect of land use on catchment hydrology. The analyses revealed a similar MTT of approximately 4 years in all catchments, which is longer than observed in other tropical montane headwater catchments. In the three sub-catchments, springs and wetlands fed by groundwater were selected as important end member, with increased contribution to streamflow during high flows. A second, different groundwater source was identified in the smallholder agriculture catchment, which was an important end member during baseflow. These results emphasize the importance of sufficient groundwater recharge and sustainable management of groundwater resources to maintain streamflow throughout the year.

Despite the observed similarities, the three sub-catchments showed clear differences in the contribution of precipitation and throughfall to stream water, with highest contributions in the natural forest and smallholder agriculture and lowest contribution in the tea and tree plantations. However, we expect that the contribution of precipitation and throughfall in the natural forest sub-catchment occurs as shallow sub-surface flow, while surface runoff could still play a significant role in the smallholder agriculture sub-catchment. Further evidence to support this statement is necessary, because surface runoff generally has negative impact on soil fertility, erosion and sedimentation. Due the similar soils and geology in the three sub-catchments, the differences in end member selection and behaviour can mainly be attributed to land use. However, over- and under-prediction

of end member contributions, especially during the dry season and at the peak of the rainy season, indicate that important end members were missing in the mixing models. Identification of additional end members and regular sampling of all end members to capture the variation in chemical composition of the end members throughout the year, might therefore improve the end member mixing models and thus our knowledge on dominant water sources and flow paths in the three land use types under different hydrological regimes. Because changes in flow paths will affect the transport and fate of nutrients and pollutants, which could have an adverse effect on montane ecosystems and downstream areas, the results of this study can be used to assess the potential impact of future land use changes on surface water supply and quality.

Acknowledgements

We would like to thank the Kenya Forest Service (KFS) for supporting us to conduct this study in the South-West Mau. This work was partially funded by the CGIAR program on Forest, Trees and Agroforestry led by the Centre for International Forestry Research (CIFOR). We thank the Deutsche Forschungsgemeinschaft DFG (BR2238/23-1) and the Deutsche Gesellschaft für Internationale Zusammenarbeit GIZ (Grants 81195001 “Low cost methods for monitoring water quality to inform upscaling of sustainable water management in forested landscapes in Kenya”) for generously providing additional support.

References

Abbott, B.W., Baranov, V., Mendoza-Lera, C., Nikolakopoulou, M., Harjung, A., Kolbe, T., Balasubramanian, M.N., Vaessen, T.N., Ciocca, F., Campeau, A., Wallin, M.B., Romeijn, P., Antonelli, M., Gonçalves, J., Datry, T., Laverman, A.M., de Dreuzy, J.-R., Hannah, D.M., Krause, S., Oldham, C., Pinay, G., 2016. Using multi-tracer inference to move beyond single-catchment ecohydrology. Earth-Sci. Rev. 160, 19–42. https://doi.org/10.1016/j.earscirev.2016.06.014

Ali, G.A., Roy, A.G., Turmel, M.-C., Courchesne, F., 2010. Source-to-stream connectivity assessment through end-member mixing analysis. J. Hydrol. 392, 119–135. https://doi.org/10.1016/j.jhydrol.2010.07.049

Alvarez-Cobelas, M., Angeler, D.G., Sánchez-Carrillo, S., 2008. Export of nitrogen from catchments: A worldwide analysis. Environ. Pollut. 156, 261–269. https://doi.org/10.1016/j.envpol.2008.02.016

Arias-Navarro, C., Díaz-Pinés, E., Klatt, S., Brandt, P., Rufino, M.C., Butterbach-Bahl, K., Verchot, L.V., 2017a. Spatial variability of soil N_2O and CO_2 fluxes in different topographic positions in a tropical montane forest in Kenya. J. Geophys. Res. Biogeosci. 122, 2016JG003667. https://doi.org/10.1002/2016JG003667

Arias-Navarro, C., Díaz-Pinés, E., Zuazo, P., Rufino, M.C., Verchot, L., Butterbach-Bahl, K., 2017b. Quantifying the contribution of land use to N_2O, NO and CO_2 fluxes in a montane forest ecosystem of Kenya. Biogeochemistry. https://doi.org/DOI 10.1007/s10533-017-0348-3

Asano, Y., Uchida, T., 2012. Flow path depth is the main controller of mean base flow transit times in a mountainous catchment. Water Resour. Res. 48, W03512. https://doi.org/10.1029/2011WR010906

Ataroff, M., Rada, F., 2000. Deforestation impact on water dynamics in a Venezuelan Andean cloud forest. Ambio 29, 440–444. https://doi.org/10.1579/0044-7447-29.7.440

Aubert, A.H., Breuer, L., 2016. New seasonal shift in in-stream diurnal nitrate cycles identified by mining high-frequency data. PLOS ONE 11, e0153138. https://doi.org/10.1371/journal.pone.0153138

Aubert, A.H., Gascuel-Odoux, C., Merot, P., 2013. Annual hysteresis of water quality: A method to analyse the effect of intra-and inter-annual climatic conditions. J. Hydrol. 478, 29–39. https://doi.org/10.1016/j.jhydrol.2012.11.027

Baker, T.J., Miller, S.N., 2013. Using the Soil and Water Assessment Tool (SWAT) to assess land use impact on water resources in an East African watershed. J. Hydrol. 486, 100–111. https://doi.org/10.1016/j.jhydrol.2013.01.041

Baldyga, T.J., Miller, S.N., Driese, K.L., Gichaba, C.M., 2008. Assessing land cover change in Kenya's Mau Forest region using remotely sensed data. Afr. J. Ecol. 46, 46–54. https://doi.org/10.1111/j.1365-2028.2007.00806.x

Baldyga, T.J., Miller, S.N., Shivoga, W., Gichaba, M., 2004. Assessing the impact of land cover change in Kenya using remote sensing and hydrologic modelling, in: ASPRS Annual Conference Proceedings. Presented at the ASPRS - 70 years of service to the profession, Denver, Colourado.

Barthold, F.K., Tyralla, C., Schneider, K., Vaché, K.B., Frede, H.-G., Breuer, L., 2011. How many tracers do we need for end member mixing analysis (EMMA)? A sensitivity analysis. Water Resour. Res. 47, W08519. https://doi.org/10.1029/2011WR010604

Barthold, F.K., Wu, J., Vaché, K.B., Schneider, K., Frede, H.-G., Breuer, L., 2010. Identification of geographic runoff sources in a data sparse region: Hydrological processes and the limitations of tracer-based approaches. Hydrol. Process. 24, 2313–2327. https://doi.org/10.1002/hyp.7678

Bartsch, S., Peiffer, S., Shope, C.L., Arnhold, S., Jeong, J.-J., Park, J.-H., Eum, J., Kim, B., Fleckenstein, J.H., 2013. Monsoonal-type climate or land-use management: Understanding their role in the mobilization of nitrate and DOC in a mountainous catchment. J. Hydrol. 507, 149–162. https://doi.org/10.1016/j.jhydrol.2013.10.012

Bende-Michl, U., Verburg, K., Cresswell, H.P., 2013. High-frequency nutrient monitoring to infer seasonal patterns in catchment source availability, mobilisation and delivery. Environ. Monit. Assess. 185, 9191–9219. https://doi.org/10.1007/s10661-013-3246-8

Bernhardt, E.S., Blaszczak, J.R., Ficken, C.D., Fork, M.L., Kaiser, K.E., Seybold, E.C., 2017. Control points in ecosystems: Moving beyond the hot spot hot moment concept. Ecosystems 20, 665–682. https://doi.org/10.1007/s10021-016-0103-y

Beven, K.J., Kirkby, M.J., 1979. A physically based, variable contributing area model of basin hydrology. Hydrol. Sci. B. 24, 43–69. https://doi.org/10.1080/02626667909491834

Bewernick, T., 2016. Mapping forest degradation in the Mau Forest Complex using NDFI time series (MSc thesis). Wageningen University, Wageningen, the Netherlands.

Biggs, T.W., Dunne, T., Martinelli, L.A., 2004. Natural controls and human impacts on stream nutrient concentrations in a deforested region of the Brazilian Amazon basin. Biogeochemistry 68, 227–257. https://doi.org/10.1023/B:BIOG.0000025744.78309.2e

Billett, M.F., Cresser, M.S., 1996. Evaluation of the use of soil ion exchange properties for predicting streamwater chemistry in upland catchments. J. Hydrol. 186, 375–394. https://doi.org/10.1016/S0022-1694(96)03041-7

Billett, M.F., Deacon, C.M., Palmer, S.M., Dawson, J.J.C., Hope, D., 2006. Connecting organic carbon in stream water and soils in a peatland catchment. J. Geophys. Res. 111, G02010. https://doi.org/10.1029/2005JG000065

Binge, F.W., 1962. Geology of the Kericho area (No. 50). Ministry of Commerce, Industry and Communications, Geological Survey of Kenya.

Birch, H.F., 1964. Mineralisation of plant nitrogen following alternate wet and dry conditions. Plant Soil 20, 43–49.

Bjørndalen, J.E., 1992. Tanzania's vanishing rain forests — Assessment of nature conservation values, biodiversity and importance for water catchment. Agr. Ecosyst. Environ. 40, 313–334. https://doi.org/10.1016/0167-8809(92)90100-P

Blackie, J.R., 1972. Hydrological effects of a change in land use from rain forest to tea plantation in Kenya, in: Studies and Reports in Hydrology No. 12. International Association of Hydrological Sciences, UNESCO, pp. 312–329.

Blaen, P.J., Khamis, K., Lloyd, C.E.M., Bradley, C., Hannah, D., Krause, S., 2016. Real-time monitoring of nutrients and dissolved organic matter in rivers: Capturing event dynamics, technological opportunities and future directions. Sci. Total Environ. 569–570, 647–660. https://doi.org/10.1016/j.scitotenv.2016.06.116

Blanco, A.C., Nadaoka, K., Yamamoto, T., Kinjo, K., 2010. Dynamic evolution of nutrient discharge under stormflow and baseflow conditions in a coastal agricultural watershed in Ishigaki Island, Okinawa, Japan. Hydrol. Process. 24, 2601–2616. https://doi.org/10.1002/hyp.7685

Bonell, M., 1998. Selected challenges in runoff generation research in forests from the hillslope to headwater drainage basin scale. J. Am. Water Resour. As. 34, 765–785. http://dx.doi:10.1111/j.1752-1688.1998.tb01514.x

Borken, W., Matzner, E., 2004. Reappraisal of drying and wetting effects on C and N mineralization and fluxes in soils. Glob. Change Biol. 15, 808–824. https://doi.org/10.1111/j.1365-2486.2008.01681.x

Bosch, J.M., Hewlett, J.D., 1982. A review of catchment experiments to determine the effect of vegetation changes on water yield and evapotranspiration. J. Hydrol. 55, 3–23.

Bouillon, S., Abril, G., Borges, A.V., Dehairs, F., Govers, G., Hughes, H.J., Merckx, R., Meysman, F.J.R., Nyunja, J., Osburn, C., Middelburg, J.J., 2009. Distribution, origin and cycling of carbon in the Tana River (Kenya): A dry season basin-scale survey from headwaters to the delta. Biogeosciences 6, 2475–2493. https://doi.org/10.5194/bg-6-2475-2009

Bowes, M.J., Jarvie, H.P., Halliday, S.J., Skeffington, R.A., Wade, A.J., Loewenthal, M., Gozzard, E., Newman, J.R., Palmer-Felgate, E.J., 2015. Characterising phosphorus and nitrate inputs to a rural river using high-frequency concentration-flow relationships. Sci. Total Environ. 511, 608–620. https://doi.org/10.1016/j.scitotenv.2014.12.086

Bowes, M.J., Smith, J.T., Neal, C., 2009. The value of high-resolution nutrient monitoring: A case study of the River Frome, Dorset, UK. J. Hydrol. 378, 82–96. https://doi.org/10.1016/j.jhydrol.2009.09.015

Boy, J., Valarezo, C., Wilcke, W., 2008. Water flow paths in soil control element exports in an Andean tropical montane forest. Eur. J. Soil Sci. 59, 1209–1227. https://doi.org/10.1111/j.1365-2389.2008.01063.x

Breuer, L., Hiery, N., Kraft, P., Bach, M., Aubert, A.H., Frede, H.-G., 2015. HydroCrowd: A citizen science snapshot to assess the spatial control of nitrogen solutes in surface waters. Sci. Rep.-UK 5, 16503. https://doi.org/10.1038/srep16503

Brown, A.E., Zhang, L., McMahon, T.A., Western, A.W., Vertessy, R.A., 2005. A review of paired catchment studies for determining changes in water yield resulting from alterations in vegetation. J. Hydrol. 310, 28–61. https://doi.org/10.1016/j.jhydrol.2004.12.010

Brown, K.W., Thomas, J.C., Holder, M.W., 1989. Development of a capillary wick unsaturated zone pore water sampler (No. EPA/600/S4-88/001). United States Environmental Protection Agency, Las Vegas, USA.

Bruijnzeel, L.A., 2005. Tropical montane cloud forest: A unique hydrological case, in: Bonell, M., Bruijnzeel, L.A. (Eds.), Forests, Water and People in the Humid Tropics. Cambridge University Press, Cambridge, UK.

Bruijnzeel, L.A., 2004. Hydrological functions of tropical forests: Not seeing the soil for the trees? Agr. Ecosyst. Environ. 104, 185–228. https://doi.org/10.1016/j.agee.2004.01.015

Bruijnzeel, L.A., 2001. Hydrology of tropical montane cloud forests: A reassessment. Land Use and Water Resources Research 1, 1.1-1.18.

Bruijnzeel, L.A., 1990. Hydrology of moist tropical forests and effects of conversion: A state of knowledge review. Faculty of Earth Sciences, Free University, Amsterdam, the Netherlands.

Bücker, A., Crespo, P., Frede, H.-G., Breuer, L., 2011. Solute behaviour and export rates in neotropical montane catchments under different land-uses. J. Trop. Ecol. 27, 305–317. https://doi.org/10.1017/S0266467410000787

Burgess, N., Butynski, T., Cordeiro, N., Doggart, N., Fjeldsa, J., Howell, K., Kilahama, F., Loader, S., Lovett, J., Mbilinyi, B., 2007. The biological importance of the Eastern Arc Mountains of Tanzania and Kenya. Biol. Conserv. 134, 209–231. https://doi.org/10.1016/j.biocon.2006.08.015

Burns, D.A., McDonnell, J.J., Hooper, R.P., Peters, N.E., Freer, J.E., Kendall, C., Beven, K., 2001. Quantifying contributions to storm runoff through end-member mixing analysis and hydrologic measurements at the Panola Mountain Research Watershed (Georgia, USA). Hydrol. Process. 15, 1903–1924. https://doi.org/10.1002/hyp.246

Burns, D.A., Plummer, L.N., McDonnell, J.J., Busenberg, E., Casile, G.C., Kendall, C., Hooper, R.P., Freer, J.E., Peters, N.E., Beven, K., Schlosser, P., 2003. The geochemical evolution of riparian ground water in a forested Piedmont catchment. Ground Water 41, 913–925. https://doi.org/10.1111/j.1745-6584.2003.tb02434.x

Burt, T.P., 2003. Monitoring change in hydrological systems. Sci. Total Environ. 310, 9–16. https://doi.org/10.1016/S0048-9697(02)00618-6

Bustillo, V., Victoria, R.L., Moura, J.M.S. de, Victoria, D. de C., Toledo, A.M.A., Collicchio, E., 2011. Factors driving the biogeochemical budget of the Amazon River and its statistical modelling. C. R. Geosci. 343, 261–277. https://doi.org/10.1016/j.crte.2011.01.003

Butterbach-Bahl, K., Kock, M., Willibald, G., Hewlett, B., Buhagiar, S., Papen, H., Kiese, R., 2004. Temporal variations of fluxes of NO, NO_2, N_2O, CO_2, and CH_4 in a tropical rain forest ecosystem. Global Biogeochem. Cy. 18, GB3012. https://doi.org/doi:10.1029/2004GB002243

Butynski, T.M., De Jong, Y.A., 2016. South Western Mau Forest Reserve. Game-proof barrier feasibility study. Sustainability Centre Eastern Africa, Nanyuki, Kenya.

Caine, N., Thurman, E.M., 1990. Temporal and spatial variations in the solute content of an alpine stream, Colorado Front Range. Geomorphology 4, 55–72. https://doi.org/10.1016/0169-555X(90)90026-M

Calder, I.R., 2002. Forest and hydrological services - Reconciling public and science perceptions. Land Use and Water Resources Research 2, 2.1-2.12.

Camberlin, P., Moron, V., Okoola, R., Philippon, N., Gitau, W., 2009. Components of rainy seasons' variability in Equatorial East Africa: Onset, cessation, rainfall frequency and intensity. Theor. Appl. Climatol. 98, 237–249. https://doi.org/10.1007/s00704-009-0113-1

Capell, R., Tetzlaff, D., Hartley, A.J., Soulsby, C., 2012. Linking metrics of hydrological function and transit times to landscape controls in a heterogeneous mesoscale catchment. Hydrol. Process. 26, 405–420. https://doi.org/10.1002/hyp.8139

Caraco, N.F., Cole, J.J., 1999. Human impact on nitrate export: An analysis using major world rivers. Ambio 28, 167–170.

Carey, R.O., Wollheim, W.M., Mulukutla, G.K., Mineau, M.M., 2014. Characterizing storm-event nitrate fluxes in a fifth order suburbanizing watershed using in situ sensors. Environ. Sci. Technol. 48, 7756–7765. https://doi.org/10.1021/es500252j

Cartwright, I., Cendón, D., Currell, M., Meredith, K., 2017. A review of radioactive isotopes and other residence time tracers in understanding groundwater recharge: Possibilities, challenges, and limitations. J. Hydrol. 555, 797–811. https://doi.org/10.1016/j.jhydrol.2017.10.053

Cauvy-Fraunié, S., Condom, T., Rabatel, A., Villacis, M., Jacobsen, D., Dangles, O., 2013. Technical Note: Glacial influence in tropical mountain hydrosystems evidenced by the diurnal cycle in water levels. Hydrol. Earth Syst. Sci. 17, 4803–4816. https://doi.org/10.5194/hess-17-4803-2013

Célleri, R., Feyen, J., 2009. The hydrology of tropical Andean ecosystems: Importance, knowledge status, and perspectives. Mt. Res. Dev. 29, 350–355. https://doi.org/10.1659/mrd.00007

Chacha, J.S., 2015. Building local capacity and creating awareness in conserving the Mau Forest and water resources, in: Picard, L.A., Buss, T.F., Seybolt, T.B., Lelei, M.C. (Eds.), Sustainable Development and Human Security in Africa. Governance as the Missing Link. CRC Press, Taylor and Francis Group, Boca Raton FL, USA, pp. 121–131.

Chapman, P.J., Edwards, A.C., Cresser, M.S., 2001. The nitrogen composition of streams in upland Scotland: Some regional and seasonal differences. Sci. Total Environ. 265, 65–83. https://doi.org/10.1016/S0048-9697(00)00650-1

Chaves, J., Neill, C., Germer, S., Neto, S.G., Krusche, A., Elsenbeer, H., 2008. Land management impacts on runoff sources in small Amazon watersheds. Hydrol. Process. 22, 1766–1775. https://doi.org/10.1002/hyp.6803

Chaves, J., Neill, C., Germer, S., Neto, S.G., Krusche, A.V., Bonilla, A.C., Elsenbeer, H., 2009. Nitrogen transformations in flowpaths leading from soils to streams in Amazon Forest and pasture. Ecosystems 12, 961–972. https://doi.org/10.1007/s10021-009-9270-4

Chiti, T., Díaz-Pinés, E., Butterbach-Bahl, K., Marzaioli, F., Valentini, R., 2018. Soil organic carbon changes following degradation and conversion to cypress and tea

plantations in a tropical mountain forest in Kenya. Plant Soil 422, 527–539. https://doi.org/10.1007/s11104-017-3489-1

Christophersen, N., Hooper, R.P., 1992. Multivariate analysis of stream water chemical data: The use of principal components analysis for the end-member mixing problem. Water Resour. Res. 28, 99–107. https://doi.org/10.1029/91WR02518

Christophersen, N., Neal, C., Hooper, R.P., Vogt, R.D., Andersen, S., 1990. Modelling streamwater chemistry as a mixture of soilwater end-members — A step towards second-generation acidification models. J. Hydrol. 116, 307–320. https://doi.org/10.1016/0022-1694(90)90130-P

Chuman, T., Hruška, J., Oulehle, F., Gürtlerová, P., Majer, V., 2013. Does stream water chemistry reflect watershed characteristics? Environ. Monit. Assess. 185, 5683–5701. https://doi.org/10.1007/s10661-012-2976-3

Conrad, O., Bechtel, B., Bock, M., Dietrich, H., Fischer, E., Gerlitz, L., Wehberg, J., Wichmann, V., Boehner, J., 2015. System for Automated Geoscientific Analyses (SAGA) v. 2.4.1. Geosci. Model Dev. 8, 1991–2007.

Cook, K.H., Vizy, E.K., 2013. Projected changes in East African rainy seasons. J. Climate 26, 5931–5948. https://doi.org/10.1175/JCLI-D-12-00455.1

Cooper, J.D., 1979. Water use of a tea estate from soil moisture measurements. E. Afr. Agr. Forestry J. 43, 102–121.

Correa, A., Windhorst, D., Tetzlaff, D., Crespo, P., Célleri, R., Feyen, J., Breuer, L., 2017. Temporal dynamics in dominant runoff sources and flow paths in the Andean Páramo. Water Resour. Res. 53. https://doi.org/10.1002/2016WR020187

Covaleda, S., Gallardo, J.F., García-Oliva, F., Kirchmann, H., Prat, C., Bravo, M., Etchevers, J.D., 2011. Land-use effects on the distribution of soil organic carbon within particle-size fractions of volcanic soils in the Transmexican Volcanic Belt (Mexico). Soil Use Manage. 27, 186–194. https://doi.org/10.1111/j.1475-2743.2011.00341.x

Craig, H., 1961. Isotopic variations in meteoric waters. Science 133, 1702–1703. https://doi.org/10.1126/science.133.3465.1702

Creed, I.F., Band, L.E., 1998. Export of nitrogen from catchments within a temperate forest: Evidence for a unifying mechanism regulated by variable source area dynamics. Water Resour. Res. 34, 3105–3120. https://doi.org/10.1029/98WR01924

Crespo, P., Bücker, A., Feyen, J., Vaché, K.B., Frede, H.-G., Breuer, L., 2012. Preliminary evaluation of the runoff processes in a remote montane cloud forest basin using Mixing Model Analysis and Mean Transit Time. Hydrol. Process. 26, 3896–3910. https://doi.org/10.1002/hyp.8382

Da Costa, E.N.D., De Souza, J.C., Pereira, M.A., De Souza, M.F.L., De Souza, W.F.L., Da Silva, D.M.L., 2017. Influence of hydrological pathways on dissolved organic carbon fluxes in tropical streams. Ecol. Evol. 7, 228–239. https://doi.org/10.1002/ece3.2543

Da Silva, D.M.L., Ometto, J.P.H.B., Lobo, G. de A., Lima, W. de P., Scaranello, M.A., Mazzi, E., Rocha, H.R. da, 2007. Can land use changes alter carbon, nitrogen and major ion transport in subtropical Brazilian streams? Sci. Agr. 64, 317–324. https://doi.org/10.1590/S0103-90162007000400002

de Moraes, J.M., Schuler, A.E., Dunne, T., Figueiredo, R. de O., Victoria, R.L., 2006. Water storage and runoff processes in plinthic soils under forest and pasture in

eastern Amazonia. Hydrol. Process. 20, 2509–2526. https://doi.org/10.1002/hyp.6213

Deegan, L.A., Neill, C., Haupert, C.L., Ballester, M.V.R., Krusche, A.V., Victoria, R.L., Thomas, S.M., Moor, E. de, 2011. Amazon deforestation alters small stream structure, nitrogen biogeochemistry and connectivity to larger rivers. Biogeochemistry 105, 53–74. https://doi.org/10.1007/s10533-010-9540-4

Defersha, M.B., Melesse, A.M., 2012. Field-scale investigation of the effect of land use on sediment yield and runoff using runoff plot data and models in the Mara River basin, Kenya. CATENA 89, 54–64. https://doi.org/10.1016/j.catena.2011.07.010

Defersha, M.B., Melesse, A.M., McClain, M.E., 2012. Watershed scale application of WEPP and EROSION 3D models for assessment of potential sediment source areas and runoff flux in the Mara River Basin, Kenya. CATENA 95, 63–72. https://doi.org/10.1016/j.catena.2012.03.004

Dudgeon, D., Arthington, A.H., Gessner, M.O., Kawabata, Z.-I., Knowler, D.J., Lévêque, C., Naiman, R.J., Prieur-Richard, A.-H., Soto, D., Stiassny, M.L.J., Sullivan, C.A., 2006. Freshwater biodiversity: Importance, threats, status and conservation challenges. Biol. Rev. 81, 163–182. https://doi.org/10.1017/S1464793105006950

Dupas, R., Jomaa, S., Musolff, A., Borchardt, D., Rode, M., 2016. Disentangling the influence of hydroclimatic patterns and agricultural management on river nitrate dynamics from sub-hourly to decadal time scales. Sci. Total Environ. 571, 791–800. https://doi.org/10.1016/j.scitotenv.2016.07.053

Durand, P., Breuer, L., Johnes, P.J., Billen, G., Butturini, A., Pinay, G., van Grinsven, H., Garnier, J., Rivett, M., Reay, D.S., Curtis, C., Siemens, J., Maberly, S., Kaste, O., Humborg, C., Loeb, R., de Klein, J., Hejzlar, J., Skoulikidis, N., Kortelainen, P., Lipistö, A., Wright, R., 2011. Nitrogen processes in aquatic ecosystems, in: Sutton, M.A., Howard, C.M., Erisman, J.W., Billen, G., Bleeker, A., Grennfelt, P., van Grinsven, H., Grizzetti, B. (Eds.), The European Nitrogen Assessment. Cambridge University Press, Cambridge, UK.

Dutton, C., Anisfeld, S.C., Ernstberger, H., 2013. A novel sediment fingerprinting method using filtration: Application to the Mara River, East Africa. J Soils Sediments 13, 1708–1723. https://doi.org/10.1007/s11368-013-0725-z

Edwards, K.A., Blackie, J.R., 1981. Results of the East African Catchment Experiments 1958-1974, in: Tropical Agricultural Hydrology. John Wiley & Sons Ltd, pp. 163–200.

Edwards, K.A., Blackie, J.R., 1979. The Kericho research project. E. Afr. Agr. Forestry J. 43, 44–50.

Ekirapa, E.A., Shitakha, F.M., 1996. Semi detailed soil survey of the African Highland Produce Company farm (No. S29 1996). Kenya Agricultural Research Institute, Nairobi, Kenya.

Ellison, D., N. Futter, M., Bishop, K., 2012. On the forest cover–water yield debate: from demand- to supply-side thinking. Glob. Change. Biol. 18, 806–820. https://doi.org/10.1111/j.1365-2486.2011.02589.x

Evans, C., Davies, T.D., 1998. Causes of concentration/discharge hysteresis and its potential as a tool for analysis of episode hydrochemistry. Water Resour. Res. 34, 129–137. https://doi.org/10.1029/97WR01881

FAO, 2016. State of the world's forest 2016. Forests and agriculture: Land-use challenges and opportunities. FAO, Rome, Italy.

FAO, 2013. Forests and water: International momentum and action. FAO, Rome, Italy.

Ferrant, S., Laplanche, C., Durbe, G., Probst, A., Dugast, P., Durand, P., Sanchez-Perez, J.M., Probst, J.L., 2013. Continuous measurement of nitrate concentration in a highly event-responsive agricultural catchment in south-west of France: Is the gain of information useful? Hydrol. Process. 27, 1751–1763. https://doi.org/10.1002/hyp.9324

Figueiredo, R.O., Markewitz, D., Davidson, E.A., Schuler, A.E., dos S. Watrin, O., de Souza Silva, P., 2010. Land-use effects on the chemical attributes of low-order streams in the eastern Amazon. J. Geophys. Res. 115, G04004. https://doi.org/10.1029/2009JG001200

Fogle, A.W., Taraba, J.L., Dinger, J.S., 2003. Mass load estimation errors utilizing grab sampling strategies in a Karst watershed. J. Am. Water Resour. As. 39, 1361–1372. https://doi.org/10.1111/j.1752-1688.2003.tb04423.x

Fröhlich, H.L., Breuer, L., Frede, H.-G., Huisman, J.A., Vaché, K.B., 2008a. Water source characterization through spatiotemporal patterns of major, minor and trace element stream concentrations in a complex, mesoscale German catchment. Hydrol. Process. 22, 2028–2043. https://doi.org/10.1002/hyp.6804

Fröhlich, H.L., Breuer, L., Vaché, K.B., Frede, H.-G., 2008b. Inferring the effect of catchment complexity on mesoscale hydrologic response. Water Resour. Res. 44, W09414. https://doi.org/10.1029/2007WR006207

Gaines, T.P., Gaines, S.T., 1994. Soil texture effect on nitrate leaching in soil percolates. Commun. Soil Sci. Plan. 25, 2561–2570. https://doi.org/10.1080/00103629409369207

Gan, H., Zhuo, M., Li, D., Zhou, Y., 2008. Quality characterization and impact assessment of highway runoff in urban and rural area of Guangzhou, China. Environ. Monit. Assess. 140, 147–159. https://doi.org/10.1007/s10661-007-9856-2

Geris, J., Tetzlaff, D., McDonnell, J., Soulsby, C., 2015. The relative role of soil type and tree cover on water storage and transmission in northern headwater catchments. Hydrol. Process. 29, 1844–1860. https://doi.org/10.1002/hyp.10289

Germer, S., Neill, C., Krusche, A.V., Elsenbeer, H., 2010. Influence of land-use change on near-surface hydrological processes: Undisturbed forest to pasture. J. Hydrol. 380, 473–480. https://doi.org/10.1016/j.jhydrol.2009.11.022

Germer, S., Neill, C., Krusche, A.V., Neto, S.C.G., Elsenbeer, H., 2007. Seasonal and within-event dynamics of rainfall and throughfall chemistry in an open tropical rainforest in Rondônia, Brazil. Biogeochemistry 86, 155–174. https://doi.org/10.1007/s10533-007-9152-9

Giertz, S., Junge, B., Diekkrüger, B., 2005. Assessing the effects of land use change on soil physical properties and hydrological processes in the sub-humid tropical environment of West Africa. Phys. Chem. Earth 30, 485–496. https://doi.org/10.1016/j.pce.2005.07.003

Glendell, M., Brazier, R.E., 2014. Accelerated export of sediment and carbon from a landscape under intensive agriculture. Sci. Total Environ. 476–477, 643–656. https://doi.org/10.1016/j.scitotenv.2014.01.057

Goldsmith, G.R., Muñoz-Villers, L.E., Holwerda, F., McDonnell, J.J., Asbjornsen, H., Dawson, T.E., 2012. Stable isotopes reveal linkages among ecohydrological processes in a seasonally dry tropical montane cloud forest. Ecohydrology 5, 779–790. https://doi.org/10.1002/eco.268

Goller, R., Wilcke, W., Fleischbein, K., Valarezo, C., Zech, W., 2006. Dissolved nitrogen, phosphorus, and sulfur forms in the ecosystem fluxes of a montane forest in Ecuador. Biogeochemistry 77, 57–89. https://doi.org/10.1007/s10533-005-1061-1

Goodridge, B.M., Melack, J.M., 2012. Land use control of stream nitrate concentrations in mountainous coastal California watersheds. J. Geophys. Res. 117, G02005. https://doi.org/10.1029/2011JG001833

Government of Kenya, 2009. Rehabilitation of the Mau Forest Ecosystem. A project concept prepared by the Interim Coordinating Secretariat, Office of the Prime Minister, on behalf of the Government of Kenya.

Gradstein, S.R., Homeier, J., Gansert, D. (Eds.), 2008. The tropical mountain forest. Patterns and processes in a biodiversity hotspot, Biodiversity and Ecology Series. Göttingen Centre for Biodiversity and Ecology, Göttingen, Germany.

Graeber, D., Gelbrecht, J., Kronvang, B., Gücker, B., Pusch, M.T., Zwirnmann, E., 2012a. Technical Note: Comparison between a direct and the standard, indirect method for dissolved organic nitrogen determination in freshwater environments with high dissolved inorganic nitrogen concentrations. Biogeosciences 9, 4873–4884. https://doi.org/10.5194/bg-9-4873-2012

Graeber, D., Gelbrecht, J., Pusch, M.T., Anlanger, C., von Schiller, D., 2012b. Agriculture has changed the amount and composition of dissolved organic matter in Central European headwater streams. Sci. Total Environ. 438, 435–446. https://doi.org/10.1016/j.scitotenv.2012.08.087

Grayson, R.B., Gippel, C.J., Finlayson, B.L., Hart, B.T., 1997. Catchment-wide impacts on water quality: The use of "snapshot" sampling during stable flow. J. Hydrol. 199, 121–134. https://doi.org/10.1016/S0022-1694(96)03275-1

Gücker, B., Silva, R.C.S., Graeber, D., Monteiro, J.A.F., Boëchat, I.G., 2016a. Urbanization and agriculture increase exports and differentially alter elemental stoichiometry of dissolved organic matter (DOM) from tropical catchments. Sci. Total Environ. 550, 785–792. https://doi.org/10.1016/j.scitotenv.2016.01.158

Gücker, B., Silva, R.C.S., Graeber, D., Monteiro, J.A.F., Brookshire, E.N.J., Chaves, R.C., Boëchat, I.G., 2016b. Dissolved nutrient exports from natural and human-impacted Neotropical catchments. Global Ecol. Biogeogr. 25, 378–390. https://doi.org/10.1111/geb.12417

Gunawardena, J., Ziyath, A.M., Egodawatta, P., Ayoko, G.A., Goonetilleke, A., 2015. Sources and transport pathways of common heavy metals to urban road surfaces. Ecol. Eng. 77, 98–102. https://doi.org/10.1016/j.ecoleng.2015.01.023

Gundersen, P., Emmett, B.A., Kjønaas, O.J., Koopmans, C.J., Tietema, A., 1998. Impact of nitrogen deposition on nitrogen cycling in forests: A synthesis of NITREX data. Forest Ecol. Manag. 101, 37–55. https://doi.org/10.1016/S0378-1127(97)00124-2

Hagedorn, F., Schleppi, P., Waldner, P., Flühler, H., 2000. Export of dissolved organic carbon and nitrogen from Gleysol dominated catchments - The significance of

water flow paths. Biogeochemistry 50, 137–161. https://doi.org/10.1023/A:1006398105953

Halliday, S.J., Skeffington, R.A., Wade, A.J., Neal, C., Reynolds, B., Norris, D., Kirchner, J.W., 2013. Upland streamwater nitrate dynamics across decadal to sub-daily timescales: A case study of Plynlimon, Wales. Biogeosciences 10, 8013–8038. https://doi.org/10.5194/bg-10-8013-2013

Halliday, S.J., Wade, A.J., Skeffington, R.A., Neal, C., Reynolds, B., Rowland, P., Neal, M., Norris, D., 2012. An analysis of long-term trends, seasonality and short-term dynamics in water quality data from Plynlimon, Wales. Sci. Total Environ. 434, 186–200. https://doi.org/10.1016/j.scitotenv.2011.10.052

Harmand, J.-M., Ávilla, H., Oliver, R., Saint-André, L., Dambrine, E., 2010. The impact of kaolinite and oxi-hydroxides on nitrate adsorption in deep layers of a Costarican Acrisol under coffee cultivation. Geoderma 1158, 216–224. https://doi.org/10.1016/j.geoderma.2010.04.032

Heidbüchel, I., Troch, P.A., Lyon, S.W., 2013. Separating physical and meteorological controls of variable transit times in zero-order catchments. Water Resour. Res. 49, 7644–7657. https://doi.org/10.1002/2012WR013149

Homyak, P.M., Sickman, J.O., Miller, A.E., Melack, J.M., Meixner, T., Schimel, J.P., 2014. Assessing nitrogen-saturation in a seasonally dry chaparral watershed: Limitations of traditional indicators of N-saturation. Ecosystems 17, 1286–1305. https://doi.org/10.1007/s10021-014-9792-2

Hood, E.W., Williams, M.W., Caine, N., 2003. Landscape controls on organic and inorganic nitrogen leaching across an alpine/subalpine ecotone, Green Lakes Valley, Colorado Front Range. Ecosystems 6, 0031–0045. https://doi.org/10.1007/s10021-002-0175-8

Hooper, R.P., 2003. Diagnostic tools for mixing models of stream water chemistry. Water Resour. Res. 39, 1055. https://doi.org/10.1029/2002WR001528

Hope, D., Billett, M.F., Cresser, M.S., 1994. A review of the export of carbon in river water: Fluxes and processes. Environ. Pollut. 84, 301–324. https://doi.org/10.1016/0269-7491(94)90142-2

Hrachowitz, M., Soulsby, C., Tetzlaff, D., Dawson, J.J.C., Malcolm, I.A., 2009. Regionalization of transit time estimates in montane catchments by integrating landscape controls. Water Resour. Res. 45, W05421. https://doi.org/10.1029/2008WR007496

Hrachowitz, M., Soulsby, C., Tetzlaff, D., Malcolm, I.A., Schoups, G., 2010. Gamma distribution models for transit time estimation in catchments: Physical interpretation of parameters and implications for time-variant transit time assessment. Water Resour. Res. 46, W10536. https://doi.org/10.1029/2010WR009148, 2010.

Hunter, H.M., Walton, R.S., 2008. Land-use effects on fluxes of suspended sediment, nitrogen and phosphorus from a river catchment of the Great Barrier Reef, Australia. J. Hydrol. 356, 131–146. https://doi.org/10.1016/j.jhydrol.2008.04.003

ISRIC, 2007. Soil and terrain database for Kenya, version 2.0, at scale 1:1 million (KENSOTER).

Jacobs, S.R., Breuer, L., Butterbach-Bahl, K., Pelster, D.E., Rufino, M.C., 2017. Land use affects total dissolved nitrogen and nitrate concentrations in tropical montane

streams in Kenya. Sci. Total Environ. 603–604, 519–532. https://doi.org/10.1016/j.scitotenv.2017.06.100

Jacobs, S.R., Weeser, B., Guzha, A.C., Rufino, M.C., Butterbach-Bahl, K., Windhorst, D., Breuer, L., 2018. Using high-resolution data to assess land use impact on nitrate dynamics in East African tropical montane catchments. Water Resour. Res. https://doi.org/10.1002/2017WR021592.

James, A.L., Roulet, N.T., 2006. Investigating the applicability of end-member mixing analysis (EMMA) across scale: A study of eight small, nested catchments in a temperate forested watershed. Water Resour. Res. 42, W08434. https://doi.org/10.1029/2005WR004419

Jennings, D.J., 1971. Geology of the Molo area (No. 86). Ministry of Natural Resources, Geological Survey of Kenya.

Johnson, M.S., Lehmann, J., Couto, E.G., Filho, J.P.N., Riha, S.J., 2006a. DOC and DIC in flowpaths of Amazonian headwater catchments with hydrologically contrasting soils. Biogeochemistry 81, 45–57. https://doi.org/10.1007/s10533-006-9029-3

Johnson, M.S., Lehmann, J., Selva, E.C., Abdo, M., Riha, S., Couto, E.G., 2006b. Organic carbon fluxes within and streamwater exports from headwater catchments in the southern Amazon. Hydrol. Process. 20, 2599–2614. https://doi.org/10.1002/hyp.6218

Juma, D.W., Wang, H., Li, F., 2014. Impacts of population growth and economic development on water quality of a lake: Case study of Lake Victoria Kenya water. Environ. Sci. Pollut. Res. 21, 5737–5746. https://doi.org/10.1007/s11356-014-2524-5

Kalbitz, K., Solinger, S., Park, J.-H., Michalzik, B., Matzner, E., 2000. Controls on the dynamics of dissolved organic matter in soils: A review. Soil Sci. 165, 277–304.

Kang, S., Lin, H., 2007. Wavelet analysis of hydrological and water quality signals in an agricultural watershed. J. Hydrol. 338, 1–14. https://doi.org/10.1016/j.jhydrol.2007.01.047

Katsuyama, M., Kabeya, N., Ohte, N., 2009. Elucidation of the relationship between geographic and time sources of stream water using a tracer approach in a headwater catchment. Water Resour. Res. 45, W06414. https://doi.org/10.1029/2008WR007458

Kaushal, S.S., Lewis, W.M., 2003. Patterns in the chemical fractionation of organic nitrogen in Rocky Mountain streams. Ecosystems 6, 483–492. https://doi.org/10.1007/s10021-003-0175-3

Kayombo, S., Jorgensen, S.E., 2005. Lake Victoria. Experience and lessons learned brief. International Lake Environment Committee Foundation, Kusatsu, Japan.

Kemp, P., Sear, D., Collins, A., Naden, P., Jones, I., 2011. The impacts of fine sediment on riverine fish. Hydrol. Process. 25, 1800–1821. https://doi.org/10.1002/hyp.7940

Kenya Water Towers Agency, 2015. Kenya Water Towers status report. Kenya Water Towers Agency, Nairobi, Kenya.

Kiese, R., Hewlett, B., Graham, A., Butterbach-Bahl, K., 2003. Seasonal variability of N_2O emissions and CH_4 uptake by tropical rainforest soils of Queensland, Australia. Global Biogeochem. Cy. 17, 1043. https://doi.org/doi:10.1029/2002GB002014

Kilonzo, F., Masese, F.O., Van Griensven, A., Bauwens, W., Obando, J., Lens, P.N.L., 2014. Spatial–temporal variability in water quality and macro-invertebrate

assemblages in the Upper Mara River basin, Kenya. Phys. Chem. Earth 67–69, 93–104. https://doi.org/10.1016/j.pce.2013.10.006

Kinyanjui, M.J., 2011. NDVI-based vegetation monitoring in Mau Forest Complex, Kenya. Afr. J. Ecol. 49, 165–174. https://doi.org/10.1111/j.1365-2028.2010.01251.x

Kirchner, J.W., Feng, X., Neal, C., Robson, A.J., 2004. The fine structure of water-quality dynamics: The (high-frequency) wave of the future. Hydrol. Process. 18, 1353–1359. https://doi.org/10.1002/hyp.5537

Koirala, S.R., Gentry, R.W., Mulholland, P.J., Perfect, E., Schwartz, J.S., Sayler, G.S., 2011. Persistence of hydrologic variables and reactive stream solute concentrations in an east Tennessee watershed. J. Hydrol. 401, 221–230. https://doi.org/10.1016/j.jhydrol.2011.02.022

Krhoda, G.O., 1988. The impact of resource utilization on the hydrology of the Mau Hills Forest in Kenya. Mt. Res. Dev. 8, 193–200. https://doi.org/10.2307/3673447

Labat, D., Ronchail, J., Guyot, J.L., 2005. Recent advances in wavelet analyses: Part 2. Amazon, Parana, Orinoco and Congo discharges time scale variability. Journal of Hydrology 314, 289–311. https://doi.org/10.1016/j.jhydrol.2005.04.004

Landon, M.K., Delin, G.N., Komor, S.C., Regan, C.P., 1999. Comparison of the stable-isotopic composition of soil water collected from suction lysimeters, wick samplers, and cores in a sandy unsaturated zone. J. Hydrol. 224, 45–54. https://doi.org/10.1016/S0022-1694(99)00120-1

Lawrence, D., Vandecar, K., 2015. Effects of tropical deforestation on climate and agriculture. Nat. Clim. Change 5, 27–36. https://doi.org/10.1038/nclimate2430

Lesack, L.F.W., 1993. Export of nutrients and major ionic solutes from a rain forest catchment in the Central Amazon Basin. Water Resour. Res. 29, 743–758. https://doi.org/10.1029/92WR02372

Lewis, W.M., Melack, J.M., McDowell, W.H., McClain, M., Richey, J.E., 1999. Nitrogen yields from undisturbed watersheds in the Americas. Biogeochemistry 46, 149–162. https://doi.org/10.1007/BF01007577

Leys, C., Ley, C., Klein, O., Bernard, P., Licata, L., 2013. Detecting outliers: Do not use standard deviation around the mean, use absolute deviations around the median. J. Exp. Soc. Psychol. 49, 764–766. http://dx.doi.org/10.1016/j.jesp.2013.03.013

Li, H., Ma, Y., Liu, W., 2016. Land use and topography as predictors of nitrogen levels in tropical catchments in Xishuangbanna, SW China. Environ. Earth. Sci. 75, 539. https://doi.org/10.1007/s12665-015-5241-6

Lin, T.-C., Shaner, P.-J.L., Wang, L.-J., Shih, Y.-T., Wang, C.-P., Huang, G.-H., Huang, J.-C., 2015. Effects of mountain tea plantations on nutrient cycling at upstream watersheds. Hydrol. Earth Syst. Sci. 19, 4493–4504. https://doi.org/10.5194/hess-19-4493-2015

Littlewood, I.G., 1992. Estimating contaminant loads in rivers: A review (No. 117). Institute of Hydrology, Wallingford, UK.

Lloyd, C.E.M., Freer, J.E., Johnes, P.J., Collins, A.L., 2016a. Using hysteresis analysis of high-resolution water quality monitoring data, including uncertainty, to infer controls on nutrient and sediment transfer in catchments. Sci. Total Environ. 543, Part A, 388–404. https://doi.org/10.1016/j.scitotenv.2015.11.028

Lloyd, C.E.M., Freer, J.E., Johnes, P.J., Collins, A.L., 2016b. Technical Note: Testing an improved index for analysing storm discharge–concentration hysteresis. Hydrol. Earth Syst. Sci. 20, 625–632. https://doi.org/10.5194/hess-20-625-2016

Lohse, K.A., Matson, P., 2005. Consequences of nitrogen additions for soil losses from wet tropical forests. Ecol. Appl. 15, 1629–1648. https://doi.org/10.1890/03-5421

Maghanga, J.K., Kituyi, J.L., Kisinyo, P.O., Ng'etich, W.K., 2012. Impact of nitrogen fertilizer applications on surface water nitrate levels within a Kenyan tea plantation. J. Chem-NY 2013, e196516. https://doi.org/10.1155/2013/196516

Malhi, Y., Gardner, T.A., Goldsmith, G.R., Silman, M.R., Zelazowsky, P., 2014. Tropical forests in the anthropocene. Annu. Rev. Env. Resour. 39, 125–159.

Maloney, K.O., Weller, D.E., 2011. Anthropogenic disturbance and streams: Land use and land-use change affect stream ecosystems via multiple pathways. Freshwater Biol. 56, 611–626. https://doi.org/10.1111/j.1365-2427.2010.02522.x

Maloszewski, P., Zuber, A., 1982. Determining the turnover time of groundwater systems with the aid of environmental tracers. 1. Models and their applicability. J. Hydrol. 57, 207–231. https://doi.org/10.1016/0022-1694(82)90147-0

Mango, L.M., Melesse, A.M., McClain, M.E., Gann, D., Setegn, S.G., 2011. Land use and climate change impacts on the hydrology of the upper Mara River Basin, Kenya: Results of a modeling study to support better resource management. Hydrol. Earth Syst. Sci. 15, 2245–2258. https://doi.org/10.5194/hess-15-2245-2011

Martínez, M.L., Pérez-Maqueo, O., Vázquez, G., Castillo-Campos, G., García-Franco, J., Mehltreter, K., Equihua, M., Landgrave, R., 2009. Effects of land use change on biodiversity and ecosystem services in tropical montane cloud forests of Mexico. Forest Ecol. Manag. 258, 1856–1863. https://doi.org/10.1016/j.foreco.2009.02.023

Masese, F.O., Kitaka, N., Kipkemboi, J., Gettel, G.M., Irvine, K., McClain, M.E., 2014. Litter processing and shredder distribution as indicators of riparian and catchment influences on ecological health of tropical streams. Ecol. Indic. 46, 23–37. https://doi.org/10.1016/j.ecolind.2014.05.032

Masese, F.O., Salcedo-Borda, J.S., Gettel, G.M., Irvine, K., McClain, M.E., 2017. Influence of catchment land use and seasonality on dissolved organic matter composition and ecosystem metabolism in headwater streams of a Kenyan river. Biogeochemistry 132, 1–22. https://doi.org/10.1007/s10533-016-0269-6

Masso, C., Baijukya, F., Ebanyat, P., Bouaziz, S., Wendt, J., Bekunda, M., Vanlauwe, B., 2017. Dilemma of nitrogen management for future food security in sub-Saharan Africa – A review. Soil Res. 55, 425–434. https://doi.org/10.1071/SR16332

McClain, M.E., Boyer, E.W., Dent, C.L., Gergel, S.E., Grimm, N.B., Groffman, P.M., Hart, S.C., Harvey, J.W., Johnston, C.A., Mayorga, E., McDowell, W.H., Pinay, G., 2003. Biogeochemical hot spots and hot moments at the interface of terrestrial and aquatic ecosystems. Ecosystems 6, 301–312. https://doi.org/10.1007/s10021-003-0161-9

McDowell, W.H., Asbury, C.E., 1994. Export of carbon, nitrogen, and major ions from three tropical montane watersheds. Limnol. Oceanogr. 39, 111–125. https://doi.org/10.4319/lo.1994.39.1.0111

McGuire, K., McDonnell, J., 2007. Stable isotope tracers in watershed hydrology, in: Michener, R., Lajtha, K. (Eds.), Stable Isotopes in Ecology and Environmental Science. Blackwell Publishing Ltd, pp. 334–374.

McGuire, K.J., McDonnell, J.J., 2006. A review and evaluation of catchment transit time modeling. J. Hydrol. 330, 543–563. https://doi.org/10.1016/j.jhydrol.2006.04.020

McGuire, K.J., McDonnell, J.J., Weiler, M., Kendall, C., McGlynn, B.L., Welker, J.M., Seibert, J., 2005. The role of topography on catchment-scale water residence time. Water Resour. Res. 41, W05002. https://doi.org/10.1029/2004WR003657

Mckenzie, J.M., Mark, B.G., Thompson, L.G., Schotterer, U., Lin, P.-N., 2010. A hydrogeochemical survey of Kilimanjaro (Tanzania): implications for water sources and ages. Hydrogeol. J. 18, 985–995. https://doi.org/10.1007/s10040-009-0558-4

McMillan, H., Freer, J., Pappenberger, F., Krueger, T., Clark, M., 2010. Impacts of uncertain river flow data on rainfall-runoff model calibration and discharge predictions. Hydrol. Process. 24, 1270–1284. https://doi.org/10.1002/hyp.7587

Mitchell, A., Reghenzani, J., Faithful, J., Furnas, M., Brodie, J., 2009. Relationships between land use and nutrient concentrations in streams draining a 'wet-tropics' catchment in northern Australia. Mar. Freshwater Res. 60, 1097–1108. https://doi.org/10.1071/MF08330

Mitchell, M.J., 2001. Linkages of nitrate losses in watersheds to hydrological processes. Hydrol. Process. 15, 3305–3307. https://doi.org/10.1002/hyp.503

Moatar, F., Abbott, B.W., Minaudo, C., Curie, F., Pinay, G., 2017. Elemental properties, hydrology, and biology interact to shape concentration-discharge curves for carbon, nutrients, sediment, and major ions. Water Resour. Res. 53, 1270–1287. https://doi.org/10.1002/2016WR019635

Mokaya, S.K., Mathooko, J.M., Leichtfried, M., 2004. Influence of anthropogenic activities on water quality of a tropical stream ecosystem. Afr. J. Ecol. 42, 281–288. https://doi.org/10.1111/j.1365-2028.2004.00521.x

Monteith, D.T., Henrys, P.A., Evans, C.D., Malcolm, I., Shilland, E.M., Pereira, M.G., 2015. Spatial controls on dissolved organic carbon in upland waters inferred from a simple statistical model. Biogeochemistry 123, 363–377. https://doi.org/10.1007/s10533-015-0071-x

Moore, R.D., 2004. Introduction to salt dilution gauging for streamflow measurement: Part 1. Streamline Watershed Management Bulletin 7, 20–23.

Mosquera, G.M., Célleri, R., Lazo, P.X., Vaché, K.B., Perakis, S.S., Crespo, P., 2016a. Combined use of isotopic and hydrometric data to conceptualize ecohydrological processes in a high-elevation tropical ecosystem. Hydrol. Process. 30, 2930–2947. https://doi.org/10.1002/hyp.10927

Mosquera, G.M., Lazo, P.X., Célleri, R., Wilcox, B.P., Crespo, P., 2015. Runoff from tropical alpine grasslands increases with areal extent of wetlands. CATENA 125, 120–128. https://doi.org/10.1016/j.catena.2014.10.010

Mosquera, G.M., Segura, C., Vaché, K.B., Windhorst, D., Breuer, L., Crespo, P., 2016b. Insights into the water mean transit time in a high-elevation tropical ecosystem. Hydrol. Earth Syst. Sci. 20, 2987–3004. https://doi.org/10.5194/hess-20-2987-2016

Mueller, M.H., Weingartner, R., Alewell, C., 2013. Importance of vegetation, topography and flow paths for water transit times of base flow in alpine headwater catchments. Hydrol. Earth Syst. Sci. 17, 1661–1679. https://doi.org/10.5194/hess-17-1661-2013

Mukundan, R., Radcliffe, D.E., Ritchie, J.C., Risse, L.M., McKinley, R.A., 2010. Sediment fingerprinting to determine the source of suspended sediment in a southern Piedmont stream. J. Environ. Qual. 39, 1328–1337.

Mulholland, P.J., Wilson, G.V., Jardine, P.M., 1990. Hydrogeochemical response of a forested watershed to storms: Effects of preferential flow along shallow and deep pathways. Water Resour. Res. 26, 3021–3036. https://doi.org/10.1029/WR026i012p03021

Munishi, P.K.T., Shear, T.H., 2005. Rainfall interception and partitioning in Afromontane rain forests of the Eastern Arc Mountains, Tanzania: Implications for water conservation. J. Trop. For. Sci. 17, 355–365.

Muñoz-Villers, L.E., Geissert, D.R., Holwerda, F., McDonnell, J.J., 2016. Factors influencing stream baseflow transit times in tropical montane watersheds. Hydrol. Earth Syst. Sci. 20, 1621–1635. https://doi.org/10.5194/hess-20-1621-2016

Muñoz-Villers, L.E., McDonnell, J.J., 2013. Land use change effects on runoff generation in a humid tropical montane cloud forest region. Hydrol. Earth Syst. Sci. 17, 3543–3560. https://doi.org/10.5194/hess-17-3543-2013

Muñoz-Villers, L.E., McDonnell, J.J., 2012. Runoff generation in a steep, tropical montane cloud forest catchment on permeable volcanic substrate. Water Resour. Res. 48, W09528. https://doi.org/10.1029/2011WR011316

Musolff, A., Schmidt, C., Rode, M., Lischeid, G., Weise, S.M., Fleckenstein, J.H., 2016. Groundwater head controls nitrate export from an agricultural lowland catchment. Adv. Water Resour. 96, 95–107. https://doi.org/10.1016/j.advwatres.2016.07.003

Musolff, A., Schmidt, C., Selle, B., Fleckenstein, J.H., 2015. Catchment controls on solute export. Adv. Water Resour. 86, Part A, 133–146. https://doi.org/10.1016/j.advwatres.2015.09.026

Mwangi, H.M., Julich, S., Patil, S.D., McDonald, M.A., Feger, K.-H., 2016. Relative contribution of land use change and climate variability on discharge of upper Mara River, Kenya. J. Hydrol.: Regional Studies 5, 244–260. https://doi.org/10.1016/j.ejrh.2015.12.059

Neal, C., Reynolds, B., Rowland, P., Norris, D., Kirchner, J.W., Neal, M., Sleep, D., Lawlor, A., Woods, C., Thacker, S., Guyatt, H., Vincent, C., Hockenhull, K., Wickham, H., Harman, S., Armstrong, L., 2012. High-frequency water quality time series in precipitation and streamflow: From fragmentary signals to scientific challenge. Sci. Total Environ. 434, 3–12. https://doi.org/10.1016/j.scitotenv.2011.10.072

Neff, K.J., Schwartz, J.S., Moore, S.E., Kulp, M.A., 2013. Influence of basin characteristics on baseflow and stormflow chemistry in the Great Smoky Mountains National Park, USA. Hydrol. Process. 27, 2061–2074. https://doi.org/10.1002/hyp.9366

Neill, C., Chaves, J.E., Biggs, T., Deegan, L.A., Elsenbeer, H., Figueiredo, R.O., Germer, S., Johnson, M.S., Lehmann, J., Markewitz, D., Piccolo, M.C., 2011. Runoff sources and land cover change in the Amazon: An end-member mixing analysis from small watersheds. Biogeochemistry 105, 7–18. https://doi.org/10.1007/s10533-011-9597-8

Neill, C., Deegan, L.A., Thomas, S.M., Cerri, C.C., 2001. Deforestation for pasture alters nitrogen and phosphorus in small Amazonian streams. Ecol. Appl. 11, 1817–1828. https://doi.org/10.2307/3061098

Neill, C., Deegan, L.A., Thomas, S.M., Haupert, C.L., Krusche, A.V., Ballester, V.M., Victoria, R.L., 2006. Deforestation alters the hydraulic and biogeochemical characteristics of small lowland Amazonian streams. Hydrol. Process. 20, 2563–2580. https://doi.org/10.1002/hyp.6216

Newbold, J.D., Sweeney, B.W., Jackson, J.K., Kaplan, L.A., 1995. Concentrations and export of solutes from six mountain streams in northwestern Costa Rica. J. N. Am. Benthol. Soc. 14, 21–37. https://doi.org/10.2307/1467722

Nimick, D.A., Gammons, C.H., Parker, S.R., 2011. Diel biogeochemical processes and their effect on the aqueous chemistry of streams: A review. Chem. Geol. 283, 3–17. https://doi.org/10.1016/j.chemgeo.2010.08.017

Nosrati, K., Govers, G., Smolders, E., 2012. Dissolved organic carbon concentrations and fluxes correlate with land use and catchment characteristics in a semi-arid drainage basin of Iran. CATENA 95, 177–183. https://doi.org/10.1016/j.catena.2012.02.019

Nottingham, A.T., Turner, B.L., Whitaker, J., Ostle, N.J., McNamara, N.P., Bardgett, R.D., Salinas, N., Meir, P., 2015. Soil microbial constraints along a tropical forest elevation gradient: A belowground test of a biogeochemical paradigm. Biogeosciences 12, 6071–6083. https://doi.org/10.5194/bg-12-6071-2015

Nyairo, W.N., Owuor, P.O., Kengara, F.O., 2015. Effect of anthropogenic activities on the water quality of Amala and Nyangores tributaries of River Mara in Kenya. Environ. Monit. Assess. 187, 691. https://doi.org/10.1007/s10661-015-4913-8

Nyayo Tea Zones Development Corporation, 2016. Mau and Embobut Forest Tea Buffer Belt [WWW Document]. Nyayo Tea Zones Development Corporation Projects. URL http://www.teazones.co.ke/index.php/ntzdc-projects/mau-and-embobut-forest-tea-buffer-belt (accessed 7.3.17).

O'Brien, R.M., 2007. A caution regarding rules of thumb for Variance Inflation Factors. Qual. Quant. 41, 673–690. https://doi.org/10.1007/s11135-006-9018-6

Olang, L.O., Kundu, P.M., 2011. Land degradation of the Mau Forest Complex in Eastern Africa: A review for management and restoration planning, in: Ekundayo, E.O. (Ed.), Environmental Monitoring. InTech, Rijeka, Croatia, pp. 245–262.

Ometo, J.P.H.B., Martinelli, L.A., Ballester, M.V., Gessner, A., Krusche, A.V., Victoria, R.L., Williams, M., 2000. Effects of land use on water chemistry and macroinvertebrates in two streams of the Piracicaba river basin, south-east Brazil. Freshwater Biol. 44, 327–337. https://doi.org/10.1046/j.1365-2427.2000.00557.x

Ongoma, V., Chen, H., Gao, C., Nyongesa, A.M., Polong, F., 2018a. Future changes in climate extremes over Equatorial East Africa based on CMIP5 multimodel ensemble. Nat. Hazards 90, 901–920. https://doi.org/10.1007/s11069-017-3079-9

Ongoma, V., Chen, H., Omony, G.W., 2018b. Variability of extreme weather events over the equatorial East Africa, a case study of rainfall in Kenya and Uganda. Theor. Appl. Climatol. 131, 295–308. https://doi.org/10.1007/s00704-016-1973-9

Oni, S.K., Futter, M.N., Molot, L.A., Dillon, P.J., 2014. Adjacent catchments with similar patterns of land use and climate have markedly different dissolved organic carbon concentration and runoff dynamics. Hydrol. Process. 28, 1436–1449. https://doi.org/10.1002/hyp.9681

Otte, I., Detsch, F., Gütlein, A., Scholl, M., Kiese, R., Appelhans, T., Nauss, T., 2017. Seasonality of stable isotope composition of atmospheric water input at the southern slopes of Mt. Kilimanjaro, Tanzania. Hydrol. Process. 31, 3932–3947. https://doi.org/10.1002/hyp.11311

Owuor, S.O., Butterbach-Bahl, K., Guzha, A.C., Jacobs, S., Merbold, L., Rufino, M.C., Pelster, D., Díaz-Pinés, E., Breuer, L., 2018. Conversion of natural forest results in a significant degradation of soil hydraulic properties in the highlands of Kenya. Soil Till. Res. 176, 36–44. https://doi.org/10.1016/j.still.2017.10.003

Owuor, S.O., Butterbach-Bahl, K., Guzha, A.C., Rufino, M.C., Pelster, D.E., Díaz-Pinés, E., Breuer, L., 2016. Groundwater recharge rates and surface runoff response to land use and land cover changes in semi-arid environments. Ecol. Process. 5, 16. https://doi.org/10.1186/s13717-016-0060-6

Pellerin, B.A., Bergamaschi, B.A., Gilliom, R.J., Crawford, C.G., Saraceno, J.F., Frederick, C.P., Downing, B.D., Murphy, J.C., 2014. Mississippi River nitrate loads form high frequency sensor measurements and regression-based load estimation. Environ. Sci. Technol. 48, 12612–12619. https://doi.org/10.1021/es504029c

Pellerin, B.A., Downing, B.D., Kendall, C., Dahlgreen, R.A., Kraus, T.E.C., Saraceno, J., Spencer, R.G.M., Bergamaschi, B.A., 2009. Assessing the sources and magnitude of diurnal nitrate variability in the San Joaquin River (California) with an in situ optical nitrate sensor and dual nitrate isotopes. Freshwater Biol. 54, 376–387. https://doi.org/10.1111/j.1365-2427.2008.02111.x

Perakis, S.S., Hedin, L.O., 2002. Nitrogen loss from unpolluted South American forests mainly via dissolved organic compounds. Nature 415, 416–419. https://doi.org/10.1038/415416a

Ponette-González, A.G., Marín-Spiotta, E., Brauman, K.A., Farley, K.A., Weathers, K.C., Young, K.R., 2014. Hydrologic connectivity in the high-elevation tropics: Heterogeneous responses to land change. BioScience 64, 92–104. https://doi.org/10.1093/biosci/bit013

Poor, C.J., McDonnell, J.J., 2007. The effects of land use on stream nitrate dynamics. J. Hydrol. 332, 54–68. https://doi.org/10.1016/j.jhydrol.2006.06.022

Prechsl, U.E., Gilgen, A.K., Kahmen, A., Buchmann, N., 2014. Reliability and quality of water isotope data collected with a low-budget rain collector. Rapid Commun. Mass Sp. 28, 879–885. https://doi.org/10.1002/rcm.6852

R Core Team, 2015. R: A language and environment for statistical computing. R Foundation for Statistical Computing, Vienna, Austria.

Rasiah, V., Armour, J.D., Yamamoto, T., Mahendrarajah, S., Heiner, D.H., 2003. Nitrate dynamics in shallow groundwater and the potential for transport to off-site water bodies. Water Air Soil Poll. 147, 183–202. https://doi.org/10.1023/A:1024529017142

Raymond, P.A., Oh, N.-H., 2007. An empirical study of climatic controls on riverine C export from three major U.S. watersheds. Global Biogeochem. Cy. 21, GB2022. https://doi.org/10.1029/2006GB002783

Recha, J.W., Lehmann, J., Walter, M.T., Pell, A., Verchot, L., Johnson, M., 2013. Stream water nutrient and organic carbon exports from tropical headwater catchments at a soil degradation gradient. Nutr. Cycl. Agroecosyst. 95, 145–158. https://doi.org/10.1007/s10705-013-9554-0

Recha, J.W., Lehmann, J., Walter, M.T., Pell, A., Verchot, L., Johnson, M., 2012. Stream discharge in tropical headwater catchments as a result of forest clearing and soil degradation. Earth Interact. 16, 1–18. https://doi.org/10.1175/2012EI000439.1

Ribeiro, K.H., Favaretto, N., Dieckow, J., de Paula Souza, L.C., Minella, J.P.G., de Almeida, L., Ramos, M.R., 2014. Quality of surface water related to land use: A case study in a catchment with small farms and intensive vegetable crop production in southern Brazil. Rev. Bras. Cienc. Solo 38, 656–668. http://dx.doi.org/10.1590/S0100-06832014000200030

Riskin, S.H., Neill, C., Jankowski, K., Krusche, A.V., McHorney, R., Elsenbeer, H., Macedo, M.N., Nunes, D., Porder, S., 2017. Solute and sediment export from Amazon forest and soybean headwater streams. Ecol. Appl. 27, 193–207. https://doi.org/10.1002/eap.1428

Roa-García, M.C., Weiler, M., 2010. Integrated response and transit time distributions of watersheds by combining hydrograph separation and long-term transit time modeling. Hydrol. Earth Syst. Sci. 14, 1537–1549. https://doi.org/10.5194/hess-14-1537-2010

Rode, M., Wade, A.J., Cohen, M.J., Hensley, R.T., Bowes, M.J., Kirchner, J.W., Arhonditsis, G.B., Jordan, P., Kronvang, B., Halliday, S.J., Skeffington, R.A., Rozemeijer, J.C., Aubert, A.H., Rinke, K., Jomaa, S., 2016. Sensors in the stream: The high-frequency wave of the present. Environ. Sci. Technol. 50, 10297–10307. https://doi.org/10.1021/acs.est.6b02155

Rodgers, P., Soulsby, C., Waldron, S., 2005a. Stable isotope tracers as diagnostic tools in upscaling flow path understanding and residence time estimates in a mountainous mesoscale catchment. Hydrol. Process. 19, 2291–2307. https://doi.org/10.1002/hyp.5677

Rodgers, P., Soulsby, C., Waldron, S., Tetzlaff, D., 2005b. Using stable isotope tracers to assess hydrological flow paths, residence times and landscape influences in a nested mesoscale catchment. Hydrol. Earth Syst. Sci. 9, 139–155. https://doi.org/10.5194/hess-9-139-2005

Rodhe, A., Seibert, J., 1999. Wetland occurrence in relation to topography: A test of topographic indices as moisture indicators. Agr. Forest Meteorol. 98–99, 325–340. https://doi.org/10.1016/S0168-1923(99)00104-5

Rothwell, J.J., Dise, N.B., Taylor, K.G., Allott, T.E.H., Scholefield, P., Davies, H., Neal, C., 2010. A spatial and seasonal assessment of river water chemistry across North West England. Sci. Total Environ. 408, 841–855. https://doi.org/10.1016/j.scitotenv.2009.10.041

Rozemeijer, J.C., van der Velde, Y., van Geer, F.C., de Rooij, G.H., Torfs, P.J.J.F., Broers, H.P., 2010. Improving load estimates for NO_3 and P in surface waters by characterizing the concentration response to rainfall events. Environ. Sci. Technol. 44, 6305–6312. https://doi.org/10.1021/es101252e

Rufino, M.C., Brandt, P., Herrero, M., Butterbach-Bahl, K., 2014. Reducing uncertainty in nitrogen budgets for African livestock systems. Environ. Res. Lett. 9, 105008. https://doi.org/10.1088/1748-9326/9/10/105008

Rusjan, S., Mikoš, M., 2010. Seasonal variability of diurnal in-stream nitrate concentration oscillations under hydrologically stable conditions. Biogeochemistry 97, 123–140. https://doi.org/10.1007/s10533-009-9361-5

Sahin, V., Hall, M.J., 1996. The effects of afforestation and deforestation on water yields. J. Hydrol. 178, 293–309. https://doi.org/10.1016/0022-1694(95)02825-0

Saunders, T.J., McClain, M.E., Llerena, C.A., 2006. The biogeochemistry of dissolved nitrogen, phosphorus, and organic carbon along terrestrial-aquatic flowpaths of a montane headwater catchment in the Peruvian Amazon. Hydrol. Process. 20, 2549–2562. https://doi.org/10.1002/hyp.6215

Scheren, P.A.G.M., Zanting, H.A., Lemmens, A.M.C., 2000. Estimation of water pollution sources in Lake Victoria, East Africa: Application and elaboration of the rapid assessment methodology. J. Environ. Manage. 58, 235–248. https://doi.org/10.1006/jema.2000.0322

Schmocker, J., Liniger, H.P., Ngeru, J.N., Brugnara, Y., Auchmann, R., Brönnimann, S., 2016. Trends in mean and extreme precipitation in the Mount Kenya region from observations and reanalyses. Int. J. Climatol. 36, 1500–1514. https://doi.org/10.1002/joc.4438

Semb, G., Robinson, J.B.D., 1969. The natural nitrogen flush in different arable soils and climates in East Africa. E. Afr. Agr. Forestry J. 34, 350–370. https://doi.org/10.1080/00128325.1969.11662315

Sharpley, A.N., 1991. Effect of soil pH on cation and anion solubility. Commun. Soil Sci. Plan. 22, 827–841. https://doi.org/10.1080/00103629109368457

Sherson, L.R., Van Horn, D.J., Gomez-Velez, J.D., Crossey, L.J., Dahm, C.N., 2015. Nutrient dynamics in an alpine headwater stream: Use of continuous water quality sensors to examine responses to wildfire and precipitation events. Hydrol. Process. 29, 3193–3207. https://doi.org/10.1002/hyp.10426

Shongwe, M.E., van Oldenborgh, G.J., van den Hurk, B., van Aalst, M., 2010. Projected changes in mean and extreme precipitation in Africa under global warming. Part II: East Africa. J. Climate 24, 3718–3733. https://doi.org/10.1175/2010JCLI2883.1

Singh, S., Inamdar, S., Mitchell, M.J., 2015. Changes in dissolved organic matter (DOM) amount and composition along nested headwater stream locations during baseflow and stormflow. Hydrol. Process. 29, 1505–1520. https://doi.org/10.1002/hyp.10286

Singh, S., Mishra, A., 2014. Spatiotemporal analysis of the effects of forest covers on stream water quality in Western Ghats of peninsular India. J. Hydrol. 519, Part A, 214–224. https://doi.org/10.1016/j.jhydrol.2014.07.009

Soares, M.R., Alleoni, L.R.F., Vidal-Torrado, P., Cooper, M., 2005. Mineralogy and ion exchange properties of the particle size fractions of some Brazilian soils in tropical humid areas. Geoderma 125, 355–367. https://doi.org/10.1016/j.geoderma.2004.09.008

Soderberg, K., Good, S.P., O'Connor, M., Wang, L., Ryan, K., Caylor, K.K., 2013. Using atmospheric trajectories to model the isotopic composition of rainfall in central Kenya. Ecosphere 4, 1–18. https://doi.org/10.1890/ES12-00160.1

Soulsby, C., Rodgers, P., Smart, R., Dawson, J., Dunn, S., 2003. A tracer-based assessment of hydrological pathways at different spatial scales in a mesoscale Scottish catchment. Hydrol. Process. 17, 759–777. https://doi.org/10.1002/hyp.1163

Soulsby, C., Tetzlaff, D., Rodgers, P., Dunn, S., Waldron, S., 2006. Runoff processes, stream water residence times and controlling landscape characteristics in a

mesoscale catchment: An initial evaluation. J. Hydrol. 325, 197–221. https://doi.org/10.1016/j.jhydrol.2005.10.024

Spracklen, D.V., Arnold, S.R., Taylor, C.M., 2012. Observations of increased tropical rainfall preceded by air passage over forests. Nature 489, 282–285. https://doi.org/10.1038/nature11390

Spracklen, D.V., Righelato, R., 2014. Tropical montane forests are a larger than expected global carbon store. Biogeosciences 11, 2741–2754. https://doi.org/10.5194/bg-11-2741-2014

Stephens, W., Othieno, C.O., Carr, M.K.V., 1992. Climate and weather variability at the Tea Research Foundation of Kenya. Agr. Forest Meteorol. 61, 219–235. https://doi.org/10.1016/0168-1923(92)90051-5

Swart, R., 2016. Monitoring 40 years of land use change in the Mau Forest Complex, Kenya. A land use change driver analysis. (MSc thesis). Wageningen University, Wageningen, the Netherlands.

Tamooh, F., Van den Meersche, K., Meysman, F., Marwick, T.R., Borges, A.V., Merckx, R., Dehairs, F., Schmidt, S., Nyunja, J., Bouillon, S., 2012. Distribution and origin of suspended matter and organic carbon pools in the Tana River Basin, Kenya. Biogeosciences 9, 2905–2920. https://doi.org/10.5194/bg-9-2905-2012

Taylor, P.G., Wieder, W.R., Weintraub, S., Cohen, S., Cleveland, C.C., Townsend, A.R., 2015. Organic forms dominate hydrologic nitrogen export from a lowland tropical watershed. Ecology 96, 1229–1241. https://doi.org/10.1890/13-1418.1

Tetzlaff, D., Soulsby, C., Waldron, S., Malcolm, I.A., Bacon, P.J., Dunn, S.M., Lilly, A., Youngson, A.F., 2007. Conceptualization of runoff processes using a geographical information system and tracers in a nested mesoscale catchment. Hydrol. Process. 21, 1289–1307. https://doi.org/10.1002/hyp.6309

Timbe, E., Feyen, J., Timbe, L., Crespo, P., Célleri, R., Windhorst, D., Frede, H.-G., Breuer, L., 2017. Multicriteria assessment of water dynamics reveals subcatchment variability in a seemingly homogeneous tropical cloud forest catchment. Hydrol. Process. 31, 1456–1468. https://doi.org/10.1002/hyp.11146

Timbe, E., Windhorst, D., Crespo, P., Frede, H.-G., Feyen, J., Breuer, L., 2014. Understanding uncertainties when inferring mean transit times of water through tracer-based lumped-parameter models in Andean tropical montane cloud forest catchments. Hydrol. Earth Syst. Sci. 18, 1503–1523. https://doi.org/10.5194/hess-18-1503-2014

UNEP, Kenya Wildlife Service, Kenya Forest Working Group, Ewaso Ngiro South Development Authority, 2008. Mau Complex under siege. Values and threats.

USGS, 2000. Shuttle Radar Topography Mission (SRTM) 1 Arc-Second Global.

van Breemen, N., 2002. Nitrogen cycle: Natural organic tendency. Nature 415, 381–382. https://doi.org/10.1038/415381a

van der Ent, R.J., Coenders-Gerrits, A.M.J., Nikoli, R., Savenije, H.H.G., 2012. The importance of proper hydrology in the forest cover-water yield debate: Commentary on Ellison et al. (2012) Global Change Biology, 18, 806–820. Glob. Change Biol. 18, 2677–2680. https://doi.org/10.1111/j.1365-2486.2012.02703.x

Van Herpe, Y., Troch, P.A., 2000. Spatial and temporal variations in surface water nitrate concentrations in a mixed land use catchment under humid temperate climatic

conditions. Hydrol. Process. 14, 2439–2455. https://doi.org/10.1002/1099-1085(20001015)14:14<2439::AID-HYP105>3.0.CO;2-H

Varanka, S., Hjort, J., Luoto, M., 2015. Geomorphological factors predict water quality in boreal rivers. Earth Surf. Process. Landforms 40, 1989–1999. https://doi.org/10.1002/esp.3601

Verschuren, D., Johnson, T.C., Kling, H.J., Edgington, D.N., Leavitt, P.R., Brown, E.T., Talbot, M.R., Hecky, R.E., 2002. History and timing of human impact on Lake Victoria, East Africa. P. Roy. Soc. Lond. B. Bio. 269, 289–294. https://doi.org/10.1098/rspb.2001.1850

von Freyberg, J., Radny, D., Gall, H.E., Schirmer, M., 2014. Implications of hydrologic connectivity between hillslopes and riparian zones on streamflow composition. J. Contam. Hydrol. 169, 62–74. https://doi.org/10.1016/j.jconhyd.2014.07.005

Wanyama, I., Pelster, D.E., Arias-Navarro, C., Butterbach-Bahl, K., Verchot, L.V., Rufino, M.C., 2018. Management intensity controls soil N_2O fluxes in an Afromontane ecosystem. Sci. Total Environ. 624, 769–780. https://doi.org/10.1016/j.scitotenv.2017.12.081

Warwick, J.J., 1986. Diel variation of in-stream nitrification. Water Res. 20, 1325–1332. https://doi.org/10.1016/0043-1354(86)90165-X

Waterloo, M.J., Oliveira, S.M., Drucker, D.P., Nobre, A.D., Cuartas, L.A., Hodnett, M.G., Langedijk, I., Jans, W.W.P., Tomasella, J., de Araújo, A.C., Pimentel, T.P., Múnera Estrada, J.C., 2006. Export of organic carbon in run-off from an Amazonian rainforest blackwater catchment. Hydrol. Process. 20, 2581–2597. https://doi.org/10.1002/hyp.6217

Weeser, B., Stenfert-Kroese, J., Jacobs, S.R., Njue, N., Kemboi, Z., Ran, A.M., Rufino, M.C., Breuer, L., in review. Citizen science pioneers in Kenya - a crowdsourced approach for hydrological monitoring. Sci. Total Environ.

Weng, L., Boedhihartono, A.K., Dirks, P.H.G.M., Dixon, J., Lubis, M.I., Sayer, J.A., 2013. Mineral industries, growth corridors and agricultural development in Africa. Glob. Food Secur. 2, 195–202. https://doi.org/10.1016/j.gfs.2013.07.003

Were, K., Singh, B.R., Dick, O.B., 2016. Spatially distributed modelling and mapping of soil organic carbon and total nitrogen stocks in the Eastern Mau Forest Reserve, Kenya. J. Geogr. Sci. 26, 102–124. https://doi.org/10.1007/s11442-016-1257-4

Were, K.O., Dick, Ø.B., Singh, B.R., 2013. Remotely sensing the spatial and temporal land cover changes in Eastern Mau forest reserve and Lake Nakuru drainage basin, Kenya. Appl. Geogr. 41, 75–86. https://doi.org/10.1016/j.apgeog.2013.03.017

Wilcke, W., Leimer, S., Peters, T., Emck, P., Rollenbeck, R., Trachte, K., Valarezo, C., Bendix, J., 2013. The nitrogen cycle of tropical montane forest in Ecuador turns inorganic under environmental change. Global Biogeochem. Cy. 27, 2012GB004471. https://doi.org/10.1002/2012GB004471

Wilcke, W., Yasin, S., Valarezo, C., Zech, W., 2001. Change in water quality during the passage through a tropical montane rain forest in Ecuador. Biogeochemistry 55, 45–72. https://doi.org/10.1023/A:1010631407270

Willett, V.B., Reynolds, B.A., Stevens, P.A., Ormerod, S.J., Jones, D.L., 2004. Dissolved organic nitrogen regulation in freshwaters. J. Environ. Qual. 33, 201–209. https://doi.org/10.2134/jeq2004.2010

Williams, L.A.J., 1991. Geology of the Mau area (No. 96). Ministry of Environment and Natural Resources, Mines and Geological Department.

Williams, M.R., Fisher, T.R., Melack, J.M., 1997. Solute dynamics in soil water and groundwater in a Central Amazon catchment undergoing deforestation. Biogeochemistry 38, 303–335. https://doi.org/10.1023/A:1005801303639

Williams, M.R., Melack, J.M., 1997. Solute export from forested and partially deforested catchments in the Central Amazon. Biogeochemistry 38, 67–102. https://doi.org/10.1023/A:1005774431820

Wilson, H.F., Xenopoulos, M.A., 2008. Ecosystem and seasonal control of stream dissolved organic carbon along a gradient of land use. Ecosystems 11, 555–568. https://doi.org/10.1007/s10021-008-9142-3

Windhorst, D., Kraft, P., Timbe, E., Frede, H.-G., Breuer, L., 2014. Stable water isotope tracing through hydrological models for disentangling runoff generation processes at the hillslope scale. Hydrol. Earth Syst. Sci. 18, 4113–4127. https://doi.org/10.5194/hess-18-4113-2014

Windhorst, D., Waltz, T., Timbe, E., Frede, H.-G., Breuer, L., 2013. Impact of elevation and weather patterns on the isotopic composition of precipitation in a tropical montane rainforest. Hydrol. Earth Syst. Sci. 17, 409–419. https://doi.org/10.5194/hess-17-409-2013

Wohlfart, T., Exbrayat, J.-F., Schelde, K., Christen, B., Dalgaard, T., Frede, H.-G., Breuer, L., 2012. Spatial distribution of soils determines export of nitrogen and dissolved organic carbon from an intensively managed agricultural landscape. Biogeosciences 9, 4513–4525. https://doi.org/10.5194/bg-9-4513-2012

Wong, M.T.F., Nortcliff, S., 1995. Seasonal fluctuations of native available N and soil management implications. Fert. Res. 42, 13–26. https://doi.org/10.1007/BF00750496

Woolley, A.R., 2001. Alkaline rocks and carbonatites of the world - Part 3: Africa. The Geological Society, Bath, UK.

Yamashita, N., Sase, H., Kobayashi, R., Leong, K.-P., Hanapi, J.M., Uchiyama, S., Urban, S., Toh, Y.Y., Muhamad, M., Gidiman, J., Chappell, N.A., 2014. Atmospheric deposition versus rock weathering in the control of streamwater chemistry in a tropical rain-forest catchment in Malaysian Borneo. Journal of Tropical Ecology 30, 481–492. https://doi.org/10.1017/S0266467414000303

Yusop, Z., Douglas, I., Nik, A.R., 2006. Export of dissolved and undissolved nutrients from forested catchments in Peninsular Malaysia. Forest Ecol. Manag. 224, 26–44. https://doi.org/10.1016/j.foreco.2005.12.006

Zamyadi, A., Gallichand, J., Duchemin, M., 2007. Comparison of methods for estimating sediment and nitrogen loads from a small agricultural watershed. Canadian Biosystems Engineering 49, 27–36.

Zhang, J., Tian, P., Tang, J., Yuan, L., Ke, Y., Cai, Z., Zhu, B., Müller, C., 2016. The characteristics of soil N transformations regulate the composition of hydrologic N export from terrestrial ecosystem. J. Geophys. Res. Biogeosci. 121, 2016JG003398. https://doi.org/10.1002/2016JG003398

Zhou, M., Brandt, P., Pelster, D., Rufino, M.C., Robinson, T., Butterbach-Bahl, K., 2014. Regional nitrogen budget of the Lake Victoria Basin, East Africa: Syntheses,

uncertainties and perspectives. Environ. Res. Lett. 9, 105009. https://doi.org/10.1088/1748-9326/9/10/105009

Zimmermann, A., Wilcke, W., Elsenbeer, H., 2007. Spatial and temporal patterns of throughfall quantity and quality in a tropical montane forest in Ecuador. J. Hydrol. 343, 80–96. https://doi.org/10.1016/j.jhydrol.2007.06.012

Zimmermann, B., Elsenbeer, H., De Moraes, J.M., 2006. The influence of land-use changes on soil hydraulic properties: Implications for runoff generation. Forest Ecol. Manag. 222, 29–38. https://doi.org/10.1016/j.foreco.2005.10.070

Zuijdgeest, A., Baumgartner, S., Wehrli, B., 2016. Hysteresis effects in organic matter turnover in a tropical floodplain during a flood cycle. Biogeochemistry 131, 49–63. https://doi.org/10.1007/s10533-016-0263-z

Zuijdgeest, A.L., Zurbrügg, R., Blank, N., Fulcri, R., Senn, D.B., Wehrli, B., 2015. Seasonal dynamics of carbon and nutrients from two contrasting tropical floodplain systems in the Zambezi River basin. Biogeosciences 12, 7535–7547. https://doi.org/10.5194/bg-12-7535-2015

Acknowledgements

This dissertation was part of a joint research project of the Centre for International Forestry Research (CIFOR), the Institute of Meteorology and Climate Research, Atmospheric Environmental Research (IMK-IFU) of the Karlsruhe Institute of Technology (IMK-IFU) and the Justus Liebig University Giessen. The project was partially funded by the CGIAR programme on Forest, Trees and Agroforestry led by CIFOR. Additional funding was generously supplied by the Deutsche Forschungsgemeinschaft DFG and the Deutsche Gesellschaft für Internationale Zusammenarbeit GIZ. The assistance of the Kenya Forest Service (KFS), who provided permission to conduct this study in the South-West Mau and helped with field activities inside the forest, and the Water Resources Authority (WRA) was greatly appreciated. I would also like to express my gratitude to one of the tea estates near Kericho for supporting our work, with special thanks to the research manager for all his help and informative conversations.

My sincere thanks go to my advisors Prof. Dr. Klaus Butterbach-Bahl, Prof. Dr. Mariana Rufino and Prof. Dr. Lutz Breuer, who were always there for me to answer questions, give advice and, in general, provide all the support that I needed. I appreciate the freedom they gave me to work where and how I wanted, which allowed me to make the most of my time in Kenya for both personal and academic development. This project would not have been possible without the help of Dr. Alphonce Guzha, with whom I spent many hours traversing the South-West Mau, digging and dealing with dubious fundi's (and other interesting characters) to get our monitoring systems up and running. A very big thank you goes to Björn Weeser, who helped with a countless number of things, from installing wick samplers and solving database issues to sending sensors and sampling supplies across continents. I would also like to thank Naomi Njue for her substantial

support with field work and being a capable successor to take charge of the monitoring network, and Jaqueline Stenfert-Kroese for enjoyable days in the field and just being there when I needed to talk.

I am very grateful for the unconditional support I received from my parents Rik and Els and brother Daan when I decided to pack my stuff and move to Kenya, and during the years that followed. My gratitude extends to other family and friends and their enthusiastic responses to my African adventures. My time in Kericho would never have been as good without the presence of Ingrid De Loof, Anne Siema and Patrick Waringa, who generously offered me a place to work from, on whom I could count for laughter and good company, and from whom I got the opportunity to learn and experience so much. Special thanks, also, to Paul Karugu for the good times, experiences and continuous support in difficult times.

I am running out of space and ways to say thank you, but there are still many people that deserve a word of thanks, including (but not limited to): Maurice Otieno for always being ready to help and showing me how to use the 4WD; Vincent Ruto for his assistance during all the hours spent in the field and the many times the car had to be pulled out of the ditch; Steven Owuor for the good days in the field in sunshine and rain, introduction to 'Kuresoi life' and many interesting discussions – scientific and otherwise; all students and staff of Mazingira Centre, Nairobi, for the warm welcome every time I visited; and the people of Tealand Engineering for their technical support, practical advise and great hospitality. I am deeply grateful to all the friendly, warm and helpful people I met in the past four years, who made my time as PhD student a time to never forget!

Declaration

I declare that I have completed this dissertation single-handedly without the unauthorized help of a second party and only with the assistance acknowledged therein. I have appropriately acknowledged and cited all text passages that are derived verbatim from or are based on the content of published work of others, and all information relating to verbal communications. I consent to the use of an anti-plagiarism software to check my thesis. I have abided by the principles of good scientific conduct laid down in the charter of the Justus Liebig University Giessen "Satzung der Justus-Liebig-Universität Giessen zur Sicherung guter wissenschaftlicher Praxis" in carrying out the investigations described in the dissertation.

_____

Suzanne Robin Jacobs

Giessen, 28 February 2018